Molecular Imaging of Inflammation/Infection: Nuclear Medicine and Optical Imaging Agents and Methods

A. Signore,*[,†,‡] S. J. Mather,[§] G. Piaggio,[||] G. Malviya,[†,‡] and R. A. Dierckx[‡]

Nuclear Medicine Unit, II Faculty of Medicine and Surgery, "Sapienza" University of Rome, Rome, Italy, Department of Nuclear Medicine and Molecular Imaging, University Medical Centre Groningen, University of Groningen, Groningen, The Netherlands, Centre for Molecular Oncology and Imaging, Institute of Cancer, Barts and The London School of Medicine, John Vane Science Centre, London, UK, and Dipartimento di Oncologia Sperimentale, Istituto Nazionale Tumori Regina Elena IRCCS - IFO, Rome, Italy

Received October 23, 2009

Contents

* To whom correspondence should be addressed. Tel.: +39-06-33775471. Fax: +39-06-33776614. E-mail: alberto.signore@uniroma1.it.
† "Sapienza" University of Rome.
‡ University of Groningen.
§ The London School of Medicine.
|| Istituto Nazionale Tumori Regina Elena IRCCS - IFO.

1. Introduction

Inflammatory diseases are a heterogeneous class of diseases that may be divided into acute and chronic forms. They can affect multiple organs (systemic) or can be localized to one specific organ. Inflammatory diseases are often relapsing, invalidating, and may require life-long treatment. Acute and chronic forms of inflammation are characterized by a cluster of immunological and histopathological events. These events may occur years before the appearance of specific symptoms, on which the clinical diagnosis can be settled, and may last for years after the clinical diagnosis and the onset of treatment. The complex inflammatory response to these events can be classified in six different phases, a useful classification from the diagnostic point of view with molecular imaging techniques. These phases are not necessarily always consecutive in time and may also coexist in different parts of an affected organ, because most inflammatory conditions are asynchronous. Optical imaging with fluorescent probes has very promising and useful features for the study of inflammation and to develop new probes, proof of concept, and physiopathological studies. It can be considered a preliminary and complementary technique to studies with radiolabeled probes. Its use, however, should not be limited to animals, as it is now, but expanded to humans for the study of superficial areas such as imaging of cutaneous lesions, endoscopic, and intraoperative use. Few studies are ongoing in this direction.

10.1021/cr900351r
Published on Web 04/23/2010

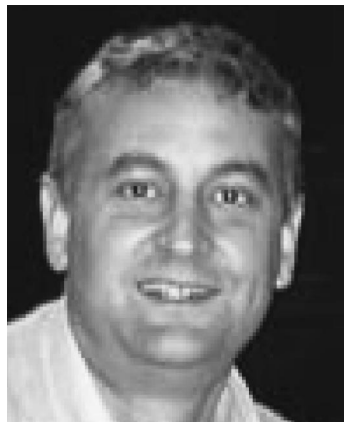

Alberto Signore graduated in Medicine & Surgery from the University of Rome "Sapienza", Italy, in 1984 and then obtained his diploma in Endocrinology in 1987 and in Nuclear Medicine in 1991. He obtained his Ph.D. in medicine in 2007. He is an Aggregated Professor in Nuclear Medicine at the second Faculty of Medicine of the University of Rome "Sapienza", Italy, and an Honorary Professor in Nuclear Medicine and Molecular Imaging at the University Medical Center, Groningen, The Netherlands. He is also a visiting Professor in Nuclear Medicine at the University of Ghent, Belgium; vice-director of the Specialization School in the Nuclear Medicine of University of Rome "Sapienza"; consultant of the International Atomic Energy Agency (IAEA), Vienna; consultant in Nuclear Medicine at the Mayo Clinic, Rochester, MN; and past-President of several international societies in the field. He coordinates the Task Group on "Inflammation-Infection-Imaging" of the European Association of Nuclear Medicine (EANM) and the Study Group on Inflammation-Infection of the Italian Association of Nuclear Medicine (AIMN). He is mainly involved in basic and clinical research in the field of inflammatory and infectious diseases, including autoimmune diseases and study of the host response to cancer. He is the author of over 160 scientific publications in national and international journals (with total Impact Factor of about 400) and the recipient of several national and international awards and research grants. He is the promoter of nine Ph.D. students.

Stephen Mather graduated in Pharmacy from the University of Nottingham in the UK in 1974 and obtained his M.Sc. in Biopharmacy in 1976 from King's College London. After briefly working as a hospital pharmacist, he specialized in Radiopharmacy and received his Ph.D. in 1986 from King's College. He was for many years head of the ICRF Nuclear Medicine Research Laboratory at St. Bartholomews Hospital where he ran a research and teaching program in Radiopharmaceutical Sciences and has about 150 publications in the field. He is currently Professor of Radiopharmacy and Head of the Cancer Imaging Group at Barts and the London School of Medicine and Dentistry in London and visiting Professor at King's College, London.

Giulia Piaggio received her degree in Biological Sciences and her postgraduate degree in Clinical Pathology at the University of Rome "Sapienza". From 1988 to 1990, she accomplished a 2-year postdoctoral fellowship at the Department of Gene Expression of European Molecular Biology Laboratory (EMBL) in Heidelberg. She joined in 1991 the "Regina Elena" Cancer Institute of Rome as a senior scientist, where she is still working as a team leader. In the last 10 years, she spent several periods as a visiting scientist in the laboratory of Molecular Growth Regulation, directed by Dr. Keiko Ozato, of the National Institute of Child Health and Human Development at NIH in Bethesda. She is interested in transcriptional regulation of gene expression during cell proliferation and has set up several techniques to follow transcriptional molecular mechanisms in living cells and tissues such as in vivo genomic footprinting, chromatin immunoprecipitation, and fluorescence recovery after photobleaching (FRAP). Recently, she was involved in the development of a transgenic mouse model to follow physiological and pathological proliferation events by BLI.

Gaurav Malviya received his graduate degree in Biological Sciences at Gorakhpur University, India, in 2001 and his postgraduate degree in Biochemistry at Bundelkhand University, India, in 2003. He obtained the Advance Postgraduate Diploma in Bioinformatics from Kanpur University, India, in 2005. He is presently finishing a Ph.D. course in the Department of Nuclear Medicine and Molecular Imaging, University Medical Center Groningen, University of Groningen, The Netherlands, in a collaborative project with the Department of Nuclear Medicine, "Sapienza" University of Rome, Italy. His main field of research concerns radiolabeling of monoclonal antibodies and cytokines for molecular imaging of inflammation and infection.

Radiological imaging procedures computed tomography (CT) and ultrasonography (US), with the exception of functional magnetic resonance imaging (MRI), have high sensitivity but lack in specificity. Nuclear medicine techniques, by contrast, allow the in vivo detection in humans and animals of different physiologic and pathologic phenomena. In the field of inflammation, it may offer noninvasive tools to detect early pathophysiological changes, before the development of anatomical changes, detectable by conventional radiographical techniques, and before the clinical onset of disease. Moreover, it offers a way to evaluate disease activity and efficacy of therapy. Here, we focus on targets in different phases of inflammation for which radiopharmaceuticals are used or will be used in nuclear medicine imaging particularly for drug discovery. Furthermore, an

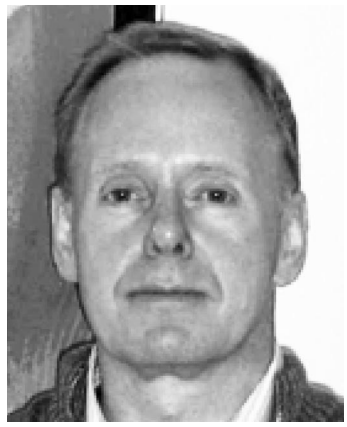

Rudi Dierckx obtained his medical degree at the Free University of Brussels, Belgium, in 1982. He was board certified in neuropsychiatry in 1987, and after a second specialization in Antwerp he was board certified in nuclear medicine in 1991. He obtained his Ph.D. in 1994 at the University of Antwerp, Belgium. Since 1994, he has been head of the Nuclear Medicine Department of the University Hospital of Gent and nominated Professor at the University of Gent in 1996, a position he still holds as he moved to become head of the Department of Nuclear Medicine and Molecular Imaging and Professor at the University Medical Centre Groningen, The Netherlands, in 2005. In 2004, he also obtained an international Masters in Business Administration (MBA) at the Vlerick Leuven Gent School for Management. He is the author and coauthor of over 330 scientific publications in international peer reviewed journals, the coeditor of 3 textbooks, and the promoter of more than 20 Ph.D. students.

overview of the current state of nuclear medicine and optical imaging techniques is given.

1.1. Acute and Chronic Inflammation

Inflammation is not synonymous of infection. An infection is caused by an exogenous pathogen, while inflammation is the response of the organism to the pathogen or tissue injury. Acute inflammation lasts hours or days and is usually resolved without residual lesions; chronic inflammation can last from a few weeks to many years and usually causes late complications. There are several clinical and histopathological differences between acute and chronic inflammation that are mainly determined by the cause of the inflammation and its duration. Furthermore, two main types of chronic inflammation can be recognized: primary and secondary chronic inflammation.

1.1.1. Acute Inflammation

Acute inflammation is a reaction of tissues to injuries, in a way that is independent of the different possible pathogenic exogenous noxae. The presence of nonself antigens or tissue degradation products activates mechanisms, like the release of histamine and serotonin, the increase of vascular permeability, hyperexpression of adhesion molecules on endothelial cells, and secretion of chemotactic factors. All of these phenomena induce leukocyte rolling along endothelium and migration of these leucocytes through the capillary wall. Complement and antibody production together with the release of mediators amplify the local response by the continuous recruitment of cells from the peripheral blood, such as granulocytes, lymphocytes, monocytes, as well as several plasma proteins. The inflammation persists until elimination of the pathogenic noxa. If the noxa persists, a chronic type of inflammation arises.

Imaging targets in this phase are neutrophils and pathogens but also activated endothelial cells.

1.1.2. Primary Chronic Inflammation

This immune response follows after infection from intracellular microorganisms or viruses, after generation of autoimmunity, and after cancer or transplantation. In this type of chronic inflammation, a distinctive chronic reaction is observed from the onset with little increased vascularity and permeability and little or no neutrophil infiltration. This is usually observed in cell-mediated immune responses against cells of the body that become the target of the immune system. Autoimmune diseases can give rise to different histological characteristics ranging from a typical lymphocytic infiltration, as in thyroiditis, to a mixed cell population consisting of T and B cells, plasma cells, and neutrophils, as in rheumatoid arthritis. Tumors also show infiltration by lymphomononuclear cells, and in graft rejection a typical infiltration by cytotoxic lymphocytes is observed.

Imaging targets in this phase are T- and B-lymphocytes but also monocyte/macrophages and apoptotic cells.

1.1.3. Secondary Chronic Inflammation

This type is due to the persistence of the stimulus that caused the acute inflammation. If an inflammatory agent persists, the character of the inflammatory lesion changes into chronic inflammation. Polymorphonuclear cells migrate out of the lesion; vasodilatation, vascular permeability, and endothelial activation tend to normalize. The infiltrate becomes predominantly mononuclear, consisting of lymphocytes and cells of the monocyte−macrophage series, and further progression of the process is mainly via proliferation of infiltrating cells. Examples of this type of inflammation are chronic infections such as tuberculosis, leading to the formation of chronic granulomas, sarcoidosis, and contact dermatitis.

Imaging targets in this phase are predominantly T-lymphocytes and monocytes.

2. Optical and Nuclear Medicine Imaging Instrumentation

2.1. Optical Imaging

In vivo optical imaging represents an interesting current and future new approach to molecular imaging. It allows imaging of internally generated light linked to specific biological functions, including pathogenic infections and inflammation in living small animals. This noninvasive technique, combined with pathogens engineered to express luciferase, allows quantification in the same animal of the spatial and temporal progression of the infection and identification of animal-to-animal variations in pathogen replication and dissemination. Very relevant are ongoing studies designed to develop imaging strategies to detect not only pathogen dissemination, but also cellular and tissue host reactions. Furthermore, this noninvasive imaging technique will potentially facilitate the discovery and development of new antimicrobial drugs.

One strategy to use optical imaging in living animals is the use of luciferase reporter genes as internal sources of light. This strategy, called bioluminescence imaging (BLI), enables real-time noninvasive imaging of infections and gene

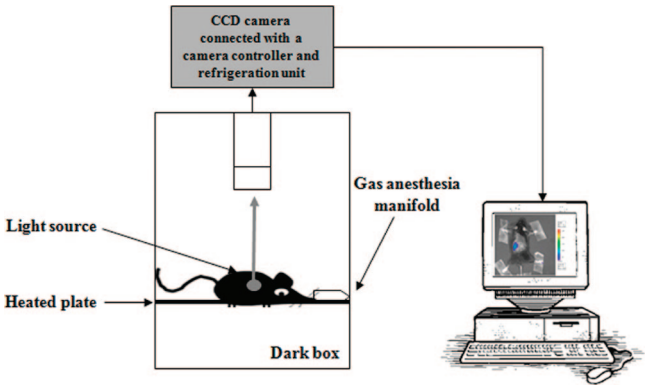

Figure 1. The instrument used for luminescence is based on an ultrasensitive cooled CCD camera connected with a dark box. In the box, there is a shelf heated at 37 °C where the mice are positioned and a manifold system to deliver isoflurane to sedate the mice during imaging. The CCD camera detects light coming from reporter cells or transgenic mice tagged with luciferase. The images are collected and quantified by advanced dedicated software.

expression in living organisms. The sensitivity of detecting internal light generated by luciferase in an intact animal is dependent upon many parameters. One crucial issue is the depth of the luciferase-labeled cells (host or pathogen) within the body. In other words, the distance that the photons must travel through tissues to exit the mouse's body surface strongly influences the sensitivity of the system. The light emitted by luciferase is able to penetrate tissue depths of the order of several millimeters to centimeters; however, photon intensity decreases 10-fold for each centimeter of tissue depth.[1] Experimental attenuations due to skin effects of a factor of 2−10 have been recently demonstrated. It seems that about 12% of the in situ luminescence appeared available for noninvasive imaging due to scattering and absorption in subcutaneous tissue and skin.[2,3] In addition to attenuation of light by overlying tissues, BLI is decreased by pigmentation of fur. Shaving mice with electric clippers or removing fur with a depilatory agent can minimize this problem. Alternatively, mice can be bred into an albino background, or mice without skin pigmentation can be employed.[4,5] Moreover, the limit of detection will vary between different strains of luciferase-expressing pathogens due to the varying strength of the promoter used to drive luciferase expression. It is reasonable to suppose that, because of the limitations in detecting light produced in deep tissues, BLI is unlikely to be used in humans in the near future, although it is possible to envision it could be used to image superficial biological processes such as dermatitis and skin infections. Another difficulty could be the necessity to alter the genetic code of human cells or tissues for luciferase expression.

The sensitivity of detection devices used is also an important variable that influences the sensitivity of this noninvasive optical imaging technique. To acquire images of small animals expressing luciferases, instruments have been developed equipped with cooled charge-coupled device (CCD) cameras (Figure 1). Varieties of charge coupled device (CCD) cameras have been used for BLI and are now commercially available. Supercooling the CCD camera reduces the thermal noise of the systems, increasing signal-to-noise ratio and preserving spectral sensitivity. Indeed, these cameras are sensitive to light across the entire visible spectrum and into the near-infrared. CCD cameras used for in vivo imaging of living mice are mounted inside a light-tight box in which the anesthetized mice are placed and imaged. Typically, the camera is accompanied with computer software for image data acquisition and analysis. The software converts electron signals into a two-dimensional image, quantifies the intensity of the emitted light (number of emitted photons striking the detectors), and converts these numerical values into a pseudocolor graphic. The actual data are measured in photons, but the pseudocolor graphic enables rapid visual interpretation. The data are quantified by region-of-interest (ROI) analysis, measuring photon flux from bioluminescence. For quantification purposes, it is important to bear in mind that there is a variable attenuation of light by different organs and tissues. For example, less light will be detected from the same number of molecules of luciferase in the liver as compared to the lung.[6] Most commercially available CCD cameras are equipped to generate an anatomical image, as well as the optical emission image, and the software superimposes these images for visualization and interpretation.[7] Several companies have developed systems specifically designed to measure light emission from small animals. Among these, the most commonly used is the IVIS imaging system, Xenogen Corp.[8] Other CCD-based imaging systems have been developed including devices from Berthold Technologies, Roper Scientific, Hamamatsu Photonics, and Biospace. The last has recently developed a new imaging device that permits studies with subsecond temporal resolution in nonanaesthetized and unrestrained mice expressing firefly luciferase or green fluorescent protein.[9] The system is based on an intensified CCD camera (ICCD) in a photon counting mode and includes a video monitoring function to track the animals. Unlike cooled CCDs, this technique enables fast kinetic imaging, which makes this method convenient for imaging moving animals. This new instrument would allow BLI where anesthetics are suspected to cause physiological interference, such as studies monitoring neurological process or calcium signaling.

Overall, BLI is a simple and rapid imaging technique as compared to others for preclinical studies, with accessible costs, making this technique relatively inexpensive and available for most research laboratories.

It is important to keep in mind that all conventional devices produce 2D images. The optical signals coming from a given ROI may therefore represent the summation of overlapping anatomic structures. Moreover, because the spatial resolution of BLI is 2−3 mm, the technique cannot differentiate between sources of light emanating from anatomical sites that are close together. Recently, a device has been developed that allows a 3D diffuse luminescence tomography (DLIT). DLIT is a method that takes into account the scattering and absorption of light in tissue and provides an estimate of the 3D location and brightness of the light-emitting sources (IVIS 200 Imaging System).

Another strategy for optical molecular imaging in living animals uses fluorescent proteins, endogenous fluorochromes, or injected optical contrast agents that incorporate visible light fluorophores, near-infrared fluorophores, or activatable fluorophores.[10,11] In this strategy, called fluorescence imaging (FLI), an external light of appropriate wavelength is used to excite a target fluorescent molecule, followed almost immediately by emission of longer-wavelength, lower-energy light for imaging. The use of fluorescent proteins as reporter genes such as green fluorescent protein (GFP) and related molecules, or fluorescent molecules such as optical contrast agents, allows noninvasive FLI.

Therefore, the use of fluorescent probes is conceptually similar to the use of radiolabeled probes in molecular nuclear medicine imaging.

In particular, FLI is accomplished by trans-illumination or reflection at single or multiple excitation wavelengths. Emission and excitation filters in the range from 450 to 800 nm enable fluorescent imaging from the visual region, such as of GFP, up to the near-infrared region. Image analysis software is able to distinguish different fluorescent reporters by using software for spectral unmixing, eliminating autofluorescence and reducing crosstalk between reporters.[12] In the IVIS system, an integrated fluorescence system (excitation filters from 400 to 900 nm are available) allows FLI of fluorescent proteins generated by pathogens. Similar to bioluminescence, tomographic optical imaging techniques have been developed, such as fluorescence molecular tomography (FMT), that overcome the 2D limitations and improve the accuracy of data analysis.[13,14] Quantitative tomography systems, based on VisEn's FMT technology, allow researchers to achieve a high quality and accurate quantification of images in vivo. VisEn has developed and optimized for use in the near-infrared spectral region a range of biocompatible fluorescence agents, which when working within the near-infrared spectral region (600−900 nm) minimize the background coming from tissue autofluorescence. An imaging system optimized for NIR fluorescence is the fluorescence time-domain (TD) imaging system produced by GE Healthcare to visualize, characterize, and quantitate biological processes in living animals.

Finally, fluorescence lifetime imaging microscopy (FLIM), which provides spatial variations in fluorescence lifetime of the probe, has become established as an extremely powerful technique in the physical and life sciences. The image is largely independent by concentration and intensity but is sensitive to the environmental surroundings of the fluorophore, for example, pH and/or viscosity.[15] While in cell biology FLIM is commonly used for measuring protein−protein interactions via Förster resonance energy transfer (FRET) in intact cells, this technique in living animals is not yet commonly used.

One caveat in the implementation of FLI is the natural autofluorescence of tissues. To partially resolve this problem, manufacturers have developed filter sets and algorithms for unmixing spectra of several different fluorescent signals, resulting in greater sensitivity for detecting multiple fluorescent reporters in vivo. Another crucial issue is the wavelength of emitted light that substantially affects transmission through tissues. Wavelengths from 650−900 nm preferentially transmit through tissues because absorption by hemoglobin, lipids, and water is lowest in this range.

2.2. Nuclear Medicine Imaging

Nuclear medicine imaging is characterized by the use of radiopharmaceuticals (radiolabeled probes) that, administered in pico- and nanomolar amounts, take part in biochemical and physiological processes and in this way allow assessment and visualization and quantitation of these processes in vivo. Radiopharmaceuticals will be discussed in detail in another section of this Review. Briefly, a radiopharmaceutical consists of a targeting compound (the drug or probe) labeled with a radionuclide (an unstable isotope). Depending on the radionuclides used, positron emitters or single photon emitters, the tomographic equipment specifically designed according to the intrinsic physical characteristics of these radionuclides is classified as positron emission tomography (PET) or single photon emission computed tomograpy (SPECT), respectively. Decay of SPECT isotopes by single photon emittion results in the production of γ rays, while PET isotopes emit $\beta+$ particles (positrons), which, upon collision with electrons, produce two colinear γ rays of 511 keV that are then detected. This signal is captured by external detectors, allowing in vivo assessment of the aforementioned processes.

2.2.1. PET

PET radionuclides are mostly produced by irradiation of target material with highly accelerated protons or deuterons using a cyclotron. Commonly used radionuclides in PET imaging are carbon-11, nitrogen-13, oxygen-15, and fluorine-18 with relatively short half-lives varying from 2 to 110 min. As these radionuclides resemble building blocks of biological life, they may be incorporated into relevant molecules using radiochemical methods. Radioactive decay takes place through emission of a positron. Following administration to a patient, the positron interacts after a short distance with an electron from surrounding tissues resulting in annihilation. During the annihilation, the masses of positron and electron are converted into energy according to Einstein's formula $E = mc^2$. The energy appears as two photons with energy of each 511 keV emitted under an angle of 180° from each other.[16] For the coincident detection of γ rays, the PET camera disposes of an annular configuration of crystals coupled to an electronic circuitry. This allows coincidence detection of two simultaneously emitted photons within 10 ns. As a result of the coincidence detection process, two fundamental physical limits can occur in PET imaging. The first is due to the small deviation from perfect colinearity ($180 \pm 0.25°$) that results from the residual momentum of the positron and electron before annihilation. The second results from the finite distance traveled by the positron before annihilation, commonly referred to as the positron range.[17] PET shows a higher spatial resolution (full width at half-maximum) of 4−5 mm as compared to conventional SPECT with a resolution of approximately 8−15 mm. So-called micro-PET cameras used for small animal imaging reach a resolution of 1−2 mm.[18] Challenges and limitations of small animal PET have to do among others with relative volumetric differences in organs and tissues between humans and small animals and herewith related the need for specific detector designs and adequate specific activity, allowing meaningful sensitivity and resolution.[19]

Over the past 30 years, detector technologies for PET have progressed from the simple photomultiplier scintillator assembly to advanced block and Anger readout schemes with solid-state detectors, such as avalanche photodiodes. The arrival of high-luminosity scintillators, such as LSO-like cerium-activated materials and LaBr3, and improved electronics have made time-of-flight (TOF) PET clinically realistic.[17] With conventional (non-TOF) data acquisition, the emission position between coincident detectors is not known, and all pixels along the line-of-response must be incremented by the same amount during image reconstruction. With TOF PET, the emission position can be approximated along the line-of-response, and each pixel on the line-of-response can be incremented accordingly by the probability that the source is located in a few pixels.[17] A trend in recent years has been toward the development of large axial aperture systems that can collect data in a full

3D geometry. Extending the axial field of view is more efficient rather than improving detector efficiency to increase sensitivity and reduce imaging time, especially for whole body imaging. Although the larger axial extent increases the number of detectors and electronic channels, it makes a more efficient use of the detector volume and, more importantly, of the injected dose to the patient.[17] After injection of the radiopharmaceutical, the distribution can be followed in time in a part of the body (dynamic scan) or by moving the bed into several positions (static whole-body scan).[16] A general approach to dynamic PET imaging consists of independently reconstructing tomographic data with each dynamic frame. Recent work has indicated that the availability of list-mode acquisition in modern PET scanners in which the time of detection of each event is also stored can be used to further improve temporal resolution.[20]

Human and small animal PET technologies, when properly calibrated, provide quantitative images of radionuclide concentrations. There are a number of methods to convert these quantitative image data sets into estimates of tissue biology (such as estimates of protein concentrations and ligand binding characteristics). Most of these techniques require the acquisition of a temporal sequence of images to characterize regional PET tracer kinetics. Knowledge of the time course of the PET tracer concentration in the arterial blood is often necessary as an input function for mathematical tracer kinetic models that are fit to regional tissue time activity curves providing estimates of biological parameters.[19] Molecular imaging agents coupled with advanced data analysis methods support the application of PET for the assessment of normal biological processes, the assessment of changes in biological processes associated with disease formation and progression, and the ability to monitor the response of healthy and diseased tissue to therapeutic intervention. PET imaging is also utilized in the drug discovery process to provide information about novel drug distribution, drug occupancy at specific biological targets, and biological responses to drug exposure.[19]

With this regard, although most PET radiopharmaceuticals are relatively short-lived, longer lived PET radionuclides such as copper-64, iodine-124, or even zirconium-89, with a half-life of 78.4 h, are now being explored for labeling antibodies to get the best of both worlds: PET resolution and sensitivity and an adequate half-life.[21]

2.2.2. SPECT

SPECT is similar to PET in its use of radiopharmaceuticals and detection of γ rays. Unlike PET, however, the radiopharmaceuticals used in SPECT emit γ radiation, which is measured directly. Also, the levels of energy of the emitters used in SPECT are lower than those used in PET. SPECT radionuclides are single photon emitters with a half-life in the order of magnitude of several hours. Technetium-99m with a half-life of 6 h is the most commonly used single photon emitter and is available as the product of a generator. The generator consists of a mother isotope molybdenum-99 attached onto a column and decaying to the aforementioned daughter isotope (Figure 2). The half-life of 66 h of the mother isotope produces a source of technetium-99m being continuously available on demand. Other frequently used SPECT tracers are the cyclotron products iodine-123 with a half-life of 13.1 h and indium-111 with a half-life of 2.8 days. Unlike the substitution and incorporation of the positron-emitters in PET, single photon emitters such as

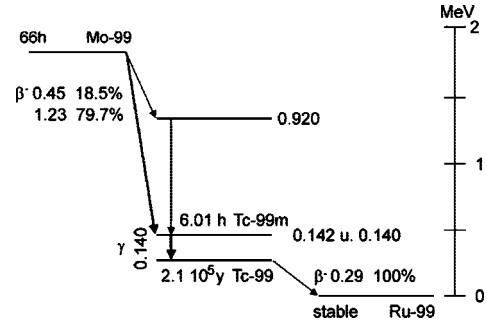

Figure 2. Decay scheme of technetium-99m.

technetium-99m are mostly attached with a radiochemical process using so-called spacers and chelators, while iodine-123, for example, can be directly bound to thyrosin residues of proteins. Because of the longer half-life of some single photon emitters, SPECT offers the possibility to widen the observational time window, thus allowing observation of biological processes in vivo several hours or days after administration of the labeled compound.[20,21] This may be relevant for the assessment of substances with a longer biological half-life such as antibodies and labeled cells.

SPECT imaging is performed using a γ camera to acquire multiple 2D images from multiple angles. Most commercially available SPECT systems nowadays consist of dual-head systems, using two opposite detectors. A computer then applies a tomographic reconstruction algorithm to the multiple projections, yielding a 3D data set. This data set may then be manipulated to show slices along any chosen axis of the body, similar to those obtained from any other tomographic techniques. To acquire SPECT images, the γ camera is rotated around the patient, and projections are acquired at defined points during the rotations.[18]

To obtain spatial resolution, single photon emitters also impose the need for a mechanical solution using collimators at the expense of sensitivity. Obviously, a trade-off between sensitivity and resolution has to be found for any given type of acquisition. The total performance of a collimator depends on the size of the collimator holes, the thickness and the length of the septa, and the source.[22] This results in a sensitivity that is 2 or 3 orders of magnitude lower than for PET. In SPECT, the use of specialized collimators, for example, slant-hole, is viewed as a technique for improving sensitivity without degrading image resolution. Furthermore, pinhole SPECT technology is seen as an area of interest, particularly due to its ability to enhance resolution capabilities in SPECT (to submillimeter range) and to offer the possibility of stationary small animal SPECT imaging.[20] There are several problems one has to deal with in an attempt to present a correct image. The reconstruction from the acquired data is based on a mathematical model for the acquisition process. Because of the complexity of that process (scatter, attenuation, depth-dependent resolution, partial volume, noise, etc.), some approximations have to be introduced. The resulting deviations between the mathematical model and the true acquisition process cause artifacts in the reconstructed image. Correction techniques can be applied to both filtered back projection (FBP) and iterative reconstructions. The reconstruction is always based on a mathematical model, and the main difference between both techniques lies in the calculation of inverse operator. In FBP, the inverse operator is analytically calculated assuming certain approximations; in iterative reconstruction, however, the inverse problem is calculated numerically. With the latter method, the model

can be incorporated in more accurate way.[22] While using SPECT FBP may still be the clinical reality, iterative reconstruction is considered the standard in PET reconstruction. Besides primary detected photons, the system will also detect photons, which have interacted with the object with resulting loss of energy. The scatter contribution will depend on the distribution of the scatter material in the field of view. Correction techniques should take into account these properties. In the dual and triple window techniques, windows are used to calculate scatter fraction under the main photopeak. It is also possible to use energy-based scatter corrections, while convolution−deconvolution techniques try to model the scatter component in the acquisition.[22] Incorporation of nonuniform attenuation in SPECT as well as collimator detector response and scatter modeling into statistical iterative image reconstruction algorithms is seen as an area of considerable potential toward artifact-free quantitative SPECT imaging. Finally, while simultaneous dual tracer imaging is impossible to perform using PET because all of its detected photons are of the same energy (511 keV), multiple energy windows can be used in SPECT for simultaneous imaging of radiotracers of different energies.[20]

2.3. Hybrid Imaging

Hybrid approaches have become popular in biomedical imaging because they provide complementary synergistic information, with the patient being in the same position.

2.3.1. Software

In addition to simple visual alignment or the use of stereotactic frames that are undesirable or inconvenient in a diagnostic setting, sophisticated image fusion software was developed from the eighties onward. For relatively rigid objects, such as the brain, software can successfully align images from MRI, CT, and PET, whereas in more flexible environments such as the rest of the body, accurate alignment is more difficult because of the large number of the possible degree of freedom. Software fusion is also dependent on matching common features that are extracted from the image or from markers placed on the patient. Functional imaging modalities such as PET and SPECT often lack reliable anatomic correlation and have coarser spatial resolution and greater noise levels than CT or MRI.[23] Various types of algorithms are available for the matching of medical images from the same or from different modalities; co-registration algorithms based on voxel properties consist of similarity or dissimilarity measures and an iterative or non iterative method minimizing the dissimilarity or maximizing the similarity between the two images by a transformation of one image relative to the other.[24]

2.3.2. PET-CT

A combined or multimodality scanner such as PET-CT can acquire coregistered structure and function in a single study. A further advantage is that the anatomical information of CT can be used to further improve quantitation of functional images through more accurate attenuation, scatter, and partial volume corrections. CT-based attenuation correction has become the de facto standard for PET-CT. Since the commercial introduction of the technology in PET-CT in 2001, adoption of the technology has been rapid, particularly in oncology. The improvement in accuracy of PET-CT as compared to PET or CT for staging and restaging is statistically significant and averages 10−15% over all cancers.[23] Although the benefits of CT-based attenuation are now well-known and documented, a number of challenges have emerged. There are two main concerns: The first is the presence of materials in the patient with Z_{eff} (effective atomic number) values that do not conform to the basic assumptions in the bilinear model, used to convert CT numbers (Hounsfield units) to linear attenuation coefficients (μ) at 511 keV. Examples include metallic objects, dental hardware, calcified lymph nodes, intravenous, and oral contrast. The second is mismatch between the CT caused by patient respiration, cardiac motion, and bowel movement. Regarding breathing, currently the simplest and most widely used protocol is shallow breathing for both CT and PET. With the incorporation of fast CT into PET-CT, the incidence of related artifacts has been greatly reduced.

Despite the aforementioned problems, the advantages of hybrid imaging, which include convenience and short acquisition times, largely outweigh the drawbacks. Finally, as with human PET imaging, there are ongoing efforts to integrate micro-PET with complementary imaging modalities, including optical and bioluminescence imaging, high resolution CT, and MRI.[19]

2.3.3. SPECT-CT

The advantages and disadvantages of SPECT-CT parallel those of PET-CT in many ways. Using a combined system, one can now sequentially acquire both anatomic and functional information that is accurately fused in a single examination. For imaging infection, early reports indicate that SPECT-CT increases specificity and may significantly affect disease management. A second important feature is the ability to correct the nuclear emission images for attenuation and scatter to obtain more accurate image data. The benefits of using CT for attenuation correction as opposed to a radionuclide transmission source include less noise, faster acquisition, no influence on CT data by the SPECT radionuclide, and no need to replace decayed transmission sources.

Unfortunately, a potential disadvantage is that there is a sequential acquisition of CT data and SPECT data; therefore, misregistration can occur with patient movement, leading to an artifact on the corrected scintigraphic images. This not only affects anatomic localization but also produces an incorrect attenuation map, causing defects on the attenuation corrected images. Furthermore, movement can result from respiratory and cardiac motion or sagging of the emission table. Other sources of error include CT truncation, metal artifacts, and beam hardening artifacts. Truncation, which occurs because the smaller CT field of view may not account for part of the patient beyond the field of view, can result in an incorrect attenuation correction map and reduce image quality, particularly in large patients. Quality control programs should ensure correct alignment, and patient motion should be corrected for.[25]

2.3.4. PET-MRI

PET-MRI adds the major advantage of combining biochemical information with the strength of MRI for defining soft tissue and providing additional biomedical parameters. As compared to other multimodality imaging approaches such as PET-CT and SPECT-CT, PET-MRI is still at an early

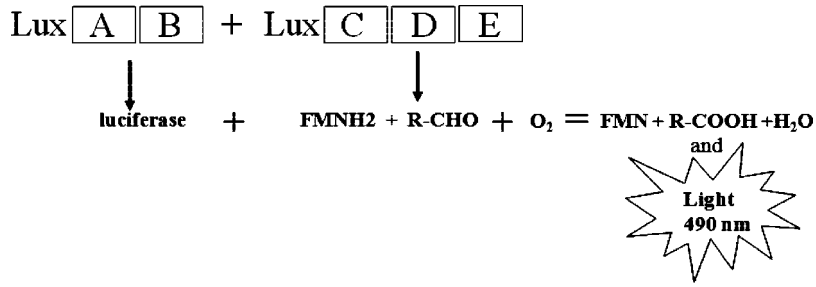

Figure 3. LuxAB form the α- and β-subunits of the luciferase enzyme that catalyzes the oxidation of reduced flavin mononucleotide (FMNH2) and a long-chain fatty aldehyde (R-CHO), generated by the LuxCDE proteins. This results in the emission of a blue-green light at 490 nm.

stage. The first prototype systems clearly show that, as compared to SPECT-CT and PET-CT, PET-MRI is engineered to allow simultaneous data collection, which is so far a unique feature and allows a temporal correlation of the measured data sets. It seems that the technical hurdles of engineering an MR compatible PET system that can be fully integrated into an MRI are understood. These include among others the influence of magnetic and radiofrequency (RF) fields on the imaging properties of both devices by using avalanche photo diodes (APD) and adding proper RF shielding. The next steps are to concentrate on the design of adequate PET inserts comparable to the commercial animal PET modules and in the development of software tools and imaging protocols.[26] Hence, the first commercially available whole-body PET-MRI systems are expected in 2011.

3. Probes and Animal Models for Optical Imaging of Inflammation/Infections

3.1. Molecular Reporter Probes for Optical Imaging

3.1.1. Bioluminescence Imaging

Recently, BLI has emerged as a powerful technique for monitoring microbial pathogenesis in living animals. BLI technology has been applied in studies to monitor dissemination and progression of viral and bacterial infections, chronic and acute inflammation, cell transplantation, tumor growth and metastasis, response to therapy, drug discovery, and gene expression.[1,27−29]

BLI detects light produced by the enzymatic reaction of a luciferase enzyme with its substrate in the context of living animals. This enzymatic production of visible light is a naturally occurring phenomenon in many nonmammalian species, and there are a variety of luciferase enzymes coming from different organisms. Many of these have been used to transfect both pathogens and host cells.[30]

Bioluminescence can be isolated from organisms like the firefly (*Photinus pyralis*) or the sea pansy (*Renilla reniliformis*) or can be aquired from bacterial lux operons (*Photorhabdus luminescens*, *Xenorhabdus luminescens*).[29] Interestingly, all identified species of naturally occurring marine and terrestrial bioluminescent bacteria are Gram-negative. Lux operons from bacteria, such as *Photorhabdus luminescens* and *Xenorhabdus luminescens*, have been used to image the pathogenesis of a plethora of Gram-negative bacteria strains, such as *Salmonella* and *Escherichia coli*.[6,31] While the lux operon of *P. luminescens* has been expressed successfully into a variety of Gram-negative bacteria to confer a bioluminescent phenotype, the transformation of Gram-positive bacteria to a light phenotype has been limited due to the different genetics of these Gram-positive bacterial groups. Indeed, the lux operon is expressed poorly in Gram-positive bacteria, and to be expressed the promoter of the operon has been modified and a redesigned lux operon containing Gram-positive transcriptional start sites has been used in Gram-positive bacteria such as *Staphylococcus aureus* and *Streptococcus pneumoniae*.[32,33] Bacterial lux operons contain all five genes required for bioluminescence, so bacteria do not require an exogenous substrate to produce blue light. In particular, luxAB operon, codify for the expression of the luciferase enzyme and the luxCDE operon, is responsible for biosynthesis of the polypeptides substrate for the luminescence reaction.[34] Bacterial luciferase catalyzes the oxidation of reduced flavin mononucleotide (FMNH2) and a long-chain fatty aldehyde (R-CHO), resulting in the emission of a blue-green light at 490 nm (Figure 3). Bioluminescent bacteria could be detected in vivo in murine models, and the bioluminescence is closely correlated with the number of viable bacteria. However, it has been observed that bioluminescence could be influenced by temperature as well as by the oxygen concentration during growth.[32] Indeed, luciferase is an oxygenase enzyme and requires oxygen to function as a reporter. Moreover, another important factor of bioimaging variability is the growth phase-dependent metabolic state of organisms that may result in differential expression of luciferase and luciferase substrates and light emission. A growth phase dependence of bacterial luminescence, showing a dramatic decrease in bioluminescence in the stationary phase, has been described.[33] Although there are efforts to use these operons in eukariotic cells, so far they have been successfully used in the yeast *Saccharomyces cerevisiae* and with limited success in mammalian cells.[35]

The most common reporter used in eukariotic cell molecular imaging is the firefly (*Photinus pyralis*) luciferase, normally a heat-unstable enzyme with a biological half-life of approximately 2 h. Heat-stable variants of firefly luciferase have been recently produced.[36] These mutant enzymes are very promising due to their greater light emission, but they are not yet used routinely. However, the short half-life of the wild type firefly luciferase allows studies of the dynamics of biological processes such as changes in pathogen replication, promoter activation, etc. Mammalian cells do not produce the substrate for the light producing process, the luciferine, and it must be delivered systemically. The substrate (luciferin) distributes throughout the animal rapidly after intraperitoneal (i.p.) or intravenous (i.v.) injection at saturating levels for the luciferase reaction (about 2.5 mg per 25 g in mice[38]). Moreover, it has been demonstrated that luciferase passes across blood−tissue barriers including placenta.[39] It can therefore be imaged in any organ. The enzyme oxidizes luciferin in a reaction that requires oxygen

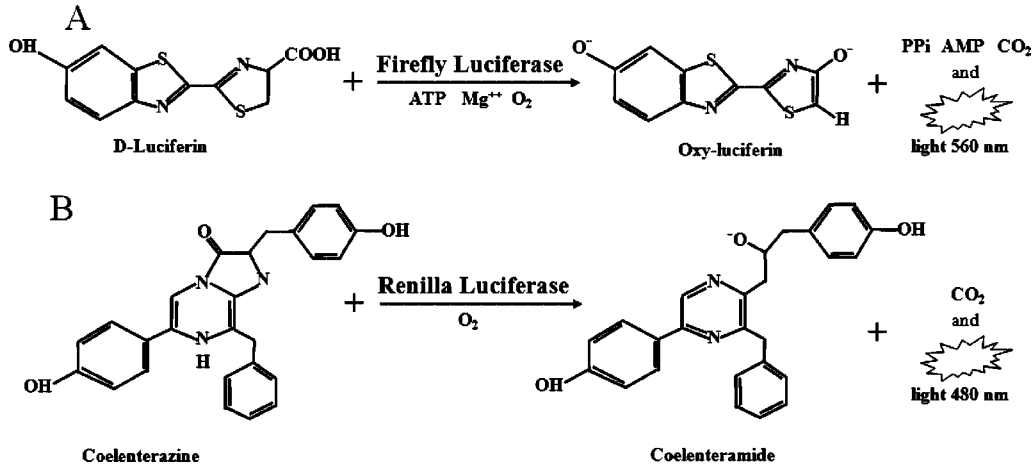

Figure 4. Bioluminescent reactions catalyzed by firefly and renilla luciferases. (A) Firefly luciferase, in the presence of oxygen and in an ATP-dependent manner, catalyzes the oxidation of luciferin to oxyluciferin, which yields light at 560 nm. (B) Renilla luciferase, in the presence of oxygen, catalyzes the oxidation of coelenterazine to coelenteramide, which yields light at 480 nm.

and adenosine triphosphate (ATP), emitting light with a broad emission spectrum with a peak at approximately 560 nm (Figure 4A). Because of tissue attenuation, only the red component of the emission spectra is useful for imaging. Studies of photon diffusion through tissues have indicated that as few as one hundred bioluminescent cells could be detectable at subcutaneous tissue sites.[4] Recently, the generation of red-shifted variants of these enzymes has been described.[37]

Light from firefly luciferase peaks 10−12 min after injection of luciferin and decreases slowly over the next 60 min,[38] providing a broad time window for image acquisition. Typically, imaging begins 8−10 min after injection.

Other luciferases such as *Renilla* from sea pansy[40] and luciferase from marine copepod react with a different substrate, coelenterazine, to produce blue light with an emission peak at approximately 480 nm (Figure 4B). They are ATP-independent and are smaller than firefly luciferase, giving them an advantage for integrating into host genomes to produce fusion proteins.[41] The substrate is injected into the vascular systemic by intravenous or intracardiac route, and imaging begins as soon as possible. Indeed, Renilla luciferase peaks at 1 min after injection of coelenterazine and then declines in 10 min. These enzymes have been used successfully for BLI studies; however, the high background due to the blue emission wavelength of these enzymes, the poor distribution, and the rapid kinetics of coelenterazine in small animals have limited their application.[40,42] The generation of red-shifted variants of these enzymes will probably improve their use in the future.[43] Although Renilla luciferase has begun to be used, so far the firefly luciferase is the most commonly used in experimental bioluminescent imaging applications.

Renilla luciferase and the bacterial lux operon luciferase have peak emissions at 480 and 490 nm, respectively, while firefly luciferase is at 560 nm. This raises the possibility of simultaneously imaging two different biological processes using spectral filters to distinguish light produced by each enzyme. Moreover, as described above, firefly and Renilla luciferase use different substrates, and the lux operon does not require a substrate allowing further discrimination of the light produced by these three enzymes. The use of two of these reporter genes to image two different biological processes is described in a very interesting study on *S. pneumoniae* where the authors have combined the two bioluminescent systems to simultaneously image bacterial replication and host response.[44] It is clear that this multicolor strategy to image both the pathogen and the host response will allow important comprehensive studies of the pathogen−host interaction biology in the future. However, it is important to note that the depth-dependent spectral shifts in the emitted light of the different luciferases could affect quantification of imaging data.

3.1.2. Fluorescence Imaging

In fluorescence imaging, in contrast to bioluminescence imaging, an excitation light illuminates the subject, and a camera detects the emitted fluorescence. Cells can be labeled with fluorescently labeled antibodies or express GFP. Like bioluminescence, the procedure generally involves transduction of the GFP gene into cells or tissues. To improve fluorescence imaging in deeper tissues, there are ongoing research efforts to develop fluorescent proteins in the far red or near-infrared spectrum.[45−47] Indeed, absorption and fluorescence of GFP in the visible region, coupled with increased light scattering, may hinder the use of GFP for high-resolution imaging of deep tissues in vivo. Nonetheless, varieties of microbes have been transformed with GFP variants and have shown significant promise for the study of pathogenesis.[48,49]

Because of the high tissue penetration of light as well as poor autofluorescence, there is significant interest in applications of exogenous optical contrast agents conjugated with fluorophores. Exogenous contrasts could be either organic fluorophores (NIR fluorophores) or inorganic fluorescent semiconductor nanocrystals, called quantum dots (QDs). Molecules that absorb in the near-infrared (NIR) region, 700−1000 nm, can be efficiently used to visualize in vivo molecular targets because most tissues generate little NIR fluorescence. The most common organic NIR fluorophores are polymethines, among which the indocyanines are the most widely used with a peak excitation at 760−800 nm and peak emission at 790−830 nm. Their applications for in vivo fluorescence imaging have been summarized in a recent review.[50]

Another approach with exogenous agents involves the use of activated optical probes. Upon proteolysis these fluorophores are released into the surrounding environment, enabling the generation of florescence signals. An example

of these agents is the ProSense 680 probe that is a composite polymer containing a poly-L-lysine backbone on which quenched NIR fluorophore and several polyethyleno-glycol side-chains are attached. ProSense 680 is preferentially hydrolyzed by cathepsin B. Recently, Gounaris et al. have reported that this cathepsin inducible fluorescent probe is useful to image the local density of pro-inflammatory cells, infiltrating the lesions in a mouse model of hereditary colon cancer.[51]

Organic fluorophores are highly susceptible to photobleaching, which limits the sensitivity of detection, while QDs are remarkably resistant to photobleaching. QDs are synthesized in organic solvents, and typically comprise an inorganic core and inorganic shell of metal; and, for in vivo imaging, they are additionally coated with an aqueous compatible organic layer. QD fluorescence emission can be tuned to virtually any discrete wavelength, and absorption is broadband. QDs that emit at several different wavelengths can be excited with a single wavelength, and thus are suitable for multiplex detection of multiple targets in a single experiment.[52]

A recent development of probes for molecular imaging is the construction of a triple fusion gene that codifies for a bioluminescent, fluorescent, and positron emission reporter fusion protein.[53,54] Although this strategy has not yet been used for pathogenic diseases, it is likely that it will become an important tool for determining location, magnitude, and time variation of infections in small animals in the future.

3.2. Cellular and Animal Models for BLI Infectious and Inflammatory Diseases

The imaging strategies used so far to monitor bacterial and/or viral infections are based on the possibility to engineer bacterial or viral strains to express luciferase genes.

As already described above, bacteria strains can be manipulated to express genes from bacterial lux operons. The lux operon encodes all proteins required for bioluminescence, including the luciferase and the substrate. Bacteria that express a lux operon constitutively produce bioluminescence without the need for an exogenous substrate.

Firefly and/or Renilla luciferase enzymes are widely used in BLI strategies to visualize infection, replication, and dissemination of recombinant viruses engineered to express them. Until today, there are few literature reports of the use of fluorescent reporter genes or molecules to image infections and/or inflammation by optical imaging. Recently, NIR fluorescent probes, having strong affinity for the surfaces of bacteria, were used to image infections of Gram-positive *Staphylococcus aureus* in living mice. In particular, the fluorescent imaging probe was composed of a bacterial affinity group conjugated to a near-infrared dye. The affinity group is a synthetic zinc(II) coordination complex that targets the anionic surfaces of bacterial cells. The probe allows detection of *S. aureus* infection in a mouse leg infection model using whole animal NIR fluorescence imaging.[55,56] Interestingly, the same group has also developed fluorescent quantum dots that can selectively stain a rough *Escherichia coli* mutant permitting optical detection in an infected mouse thigh.[57]

Here, we review the most relevant recent papers describing the use of BLI and luciferase enzymes for imaging infection and inflammation. For additional references, readers can refer also to other recent reviews.[28,29]

3.2.1. Bacterial Infections

The first example of BLI applied to bacterial infection is described in the paper by Contag and colleagues.[31] Using BLI, they were able to compare, in intact mice, the virulence of three strains of *Salmonella typhimurium*, which carried the lux genes of *P. luminescens* on a multicopy plasmid. A few years later, a different group, using the same lux operon, conferred bioluminescence on a clinically isolated *Escherichia coli* strain. They used this strain to quantitatively validate in vivo that BLI could be used to detect bacterial replication and to measure antibiotic efficacy.[6] The *P. luminescens* lux operon is not useful for Gram-positive bacteria, but Francis and colleagues modified the *P. luminescens* lux operon and used it to generate bioluminescent *Staphylococcus aureus* and clinically isolated *Streptococcus pneumoniae* strains capable of producing high levels of light.[32,33,58] With these studies, they opened the route for the development of in vivo imaging of antibiotic efficacy studies designed to monitor gram-positive infections in animal models. Later, bioluminescent *S. aureus* and *Pseudomonas aeruginosa* models were used for monitoring catheter-related chronic biofilm infections and to evaluate the therapeutic efficacies of antimicrobial agents as well as post antibiotic effects and regrowth of biofilm bacteria in living animals by bioluminescent imaging.[59,60] Bioluminescent *S. aureus* strains have also been used to evaluate the therapeutic efficacies of a single dose of daptomycin in live mice and to compare this bacterial killer with that of other commonly used antibiotics. The authors used methicillin-susceptible *S. aureus* (MSSA) and methicillin-resistant *S. aureus* (MRSA) strains genetically modified to express the lux operon in a model of peritonitis in healthy and neutropenic mice. The bactericidal activity of daptomycin was greater and more rapid than the comparative drugs in both healthy and neutropenic mice.[61] A study by Hardy et al.[62] emphasizes the ability of BLI to reveal unexpected microbial replication. The authors generated bioluminescent *Listeria monocytogenes* and showed that upon oral infection, it enters a latent period followed by reemergence some days later. They observed that the reemergence of the signal in orally infected mice can occur in various organs such as the gut, the liver, or the gallbladder. Interestingly, their results also support the hypothesis that during the latent period the bone marrow is a niche for *L. monocytogenes*. A recent study by Cronin and colleagues[63] reported the use of a Lux operon-based reporter system for *Bifidobacterium* species. They observed in intact mice the colonization potential and persistence of this probiotic species and identified the cecum as a niche environment for *Bifidobacterium* in mammalian hosts. The impact of the bioterrorism event in the U.S. after 2001 provided the impetus for researchers to study the early steps in establishment of pulmonary anthrax. For this purpose, they transformed *Bacillus anthracis* with the lux operon under control of the spore small acid-soluble protein B (sspB) promoter. After intranasal infection of mice with spores that harbored the germination reporter, they observed that the primary site of *B. anthracis* spore germination is the lung.[64]

A transgenic mouse model has been developed to study the host inflammatory response to infections in living animals by BLI. Glial fibrillary acidic protein (GFAP) is considered to be a biomarker for monitoring neuronal activity under development and pathological conditions. Transgenic mice carry the luciferase gene under the transcriptional control of the mouse GFAP promoter and have been used to monitor

the host response to *S. pneumoniae* infections. In this interesting study, the bacterial strain was engineered with the lux operon. On the basis of the different spectra of light emission and substrate requirements for bacterial and firefly luciferase, the authors were able to separately monitor both the pathogen and the host neuronal damage and recovery following antibiotic treatment. This study is one of the few that combines the use, as report genes, of two different luciferases.[44]

3.2.2. Viral Infections

Viruses can also be engineered to encode luciferase. Several reports of bioluminescent *herpes simplex virus* models have been reported by Luker and colleagues. First, they have engineered *herpes simplex virus type 1* (HSV-1) using both firefly and Renilla luciferases. Viral infection, replication, and spread in a mouse model were then evaluated. While firefly luciferase activity was detectable in the footpads, peritoneal cavity, brain, and eyes after systemic administration of the luciferase substrate, the Renilla luciferase activity was only detectable in the eyes, demonstrating the increased usefulness of firefly luciferase as compared to *Renilla*.[65] Indeed, it seems that the pharmacokinetics and bioavailability of the Renilla substrate, coelenterazine, after systemic administration limit the in vivo bioluminescent reaction. This limitation potentially could be overcome by increasing the dose of coelenterazine, but, from a practical perspective, the high cost of coelenterazine represents a disadvantage.

Next, using this model, they have dissected the effects of different interferons in limiting systemic dissemination of HSV-1, further validating the use of bioluminescence imaging for studies of viral pathogenesis.[66] Finally, as an alternative approach to facilitate BLI studies of HSV-1, they have developed a transgenic reporter mouse that expresses firefly luciferase in response to HSV-1.[67] The transgene comprises a fragment of the promoter from HSV-1 thymidine kinase linked to firefly luciferase. In these mice, the expression and the activity of the enzyme reproduce the spatial and temporal progression of HSV-1 infection observed using the luciferase engineered HSV-1 strain, indicating that this reporter mouse can be used to quantify HSV-1 viral infection in vivo without constructing reporter virus.

Antimicrobial compounds often progress into clinical trials based on demonstration of in vitro activity in cell-based assays. For evaluating antiviral compounds against hepatitis C virus (HCV) in living animals, Zhu and colleagues[68] have reported the development, validation, and application of a xenograft bioluminescent HCV mouse model. The model utilizes a hepatoma cell line expressing a luciferase reporter linked to the HCV subgenome. These cells are implanted subcutaneously or directly into the liver of gamma (γ)-irradiated SCID mice, and a significant reduction in the viral replication levels was observed by BLI after treatment with interferon. Bioluminescence imaging has also been successfully used for real-time monitoring of the dynamic interaction of different luciferase-expressing γ herpes viruses with their hosts.[69,70] These studies have identified the salivary glands as novel sites of viral replication as well as the nose as an entry point. Moreover, continuous monitoring of infection in individual mice allows the assessment of the dynamics of transition to different organs and the local clearance. A bioluminescent model for studying the infection and dissemination of a RNA virus has been developed by Cook and Griffin.[71] These authors have used a luciferase-expressing recombinant *Sindbis virus* for studies of viral entry into the central nervous system. They have demonstrated that the amount of light generated directly reflected the amount of infectious virus in the brain and that this imaging strategy can quantitatively substitute for traditional methods of assaying virus replication. Interestingly, they observed that after viremic spread the virus entries into the nervous system by retrograde axonal transport from neurons innervating the initial site of the virus replication. Recently, Zaitseva et al have employed whole-body bioimaging to follow the dissemination of vaccinia virus expressing luciferase in live animals. Interestingly, the measurements of photon fluxes have been shown to correlate in linear fashion with viral loads in internal organs in vaccinia virus-infected mice, suggesting that bioluminescence provides a direct measure of viral dissemination.[72]

3.2.3. Transgenic Mouse Models of Inflammation

Several transgenic mouse models have been developed to study inflammatory and/or immune processes in living animals by BLI. These mice are useful tools for tracking various inflammatory processes in vivo, and also for testing the efficacy of therapeutic compounds that target inflammatory and/or immune diseases. NF-kB is a transcription factor that is associated with inflammatory responses and immune disorders. To produce an early and sensitive detection marker of autoimmune disease in intact animals, transgenic mice that express luciferase driven by three NF-kB response elements (NF-kB-luc mice) have been developed. In these mice, in the absence of stimulation, strong, intrinsic luminescence is evident in lymph nodes, in the neck region, and in the thymus. Treating mice with stressors, such as TNF-α, IL-1α, or lipopolysaccharide (LPS), increases the luminescence in a tissue-specific manner.[73] Using this mouse model, the impact of inflammatory signaling in airway epithelial cells of host defenses against *P. aeruginosa*, a major cause of nosocomial pneumonia, has been studied. By BLI, the authors showed that airway instillation of *P. aeruginosa* resulted in NF-kB activation in the lungs.[74] In another study using these mice, it has been demonstrated that NF-kB plays a critical role in the early stages of the host immune response toward coliform intramammary infections, both at the local and at the systemic level.[75] Finally, NF-kB-luc mice crossed with autoimmune mouse models have provided a useful tool to demonstrate the role of NF-kB activation as an early in vivo marker for detection of autoimmune disease.[76] The inducible NO synthase gene (iNOS) plays a role in a number of chronic and acute conditions, including septic shock and contact hypersensitivity, and autoimmune diseases such as rheumatoid arthritis, gastrointestinal disorders, and myocardial ischemia. A transgenic mouse (iNos-luc) has been developed, providing a valuable tool for studying processes in which the iNOS gene is induced and for screening anti-inflammatory compounds in living animals.[77]

Acute phase serum amyloid A proteins (A-SAAs) are multifunctional apolipoproteins produced in large amounts during the acute phase of inflammation and during the development of chronic inflammatory diseases. A SAA1 promoter-driven luciferase expression transgenic mouse (Saa1-luc) has been developed. Using these Saa1-luc transgenic mice, a SAA induction in liver and other organs by many inflammatory agents has been shown, suggesting that

locally produced A-SAA may contribute to amyloid deposition in these organs and the pathogenesis of these inflammatory diseases.[78]

The expression of glial fibrillary acidic protein (GFAP) increases in acute autoimmune encephalomyelitis due to a rise in its transcription. A model for noninvasive imaging of autoimmune encephalomyelitis has been developed using a reporter mouse in which the injury-responsive GFAP promoter is fused to luciferase (GFAP-luc mice). In these mice, bioluminescence from the brain and spinal cord correlates strongly with the severity of clinical disease.[79] The cyclooxygenase-2 (Cox-2) gene plays a role in a variety of normal and pathophysiological conditions including both chronic and acute inflammation. The generation of two knock-in mice has been reported in which the firefly or the Renilla luciferase reporter enzyme is expressed at the start site of translation of the endogenous Cox-2 gene, providing tools to analyze Cox-2 expression in inflammation.[80,81]

3.2.4. Vaccines

A very interesting new field is the application of BLI in the study of the development and evaluation of DNA vaccination. DNA vaccines, encompassing a bacterial plasmid encoding a variety of viral, bacterial, and parasitic antigens, are emerging as a useful immunotherapy modality for small animals and humans. Immunization with the DNA vaccine results in effective humoral and cellular immune response that protect against disease in preclinical models of infectious disease and autoimmunity. In an interesting paper from Jeon and colleagues,[82] firefly luciferase has been used to determine the localization, intensity, and duration of gene expression of naked DNA vaccines in living animals. They demonstrated that, when a DNA encoding luciferase (pcDNA3.1-firefly luciferase) is injected into the bilateral posterior flanks, bioluminescence is present at the injection site and at inguinal lymph node from 10 to 24 h postinjection. However, when the same DNA is injected into the middorsum, bioluminescent signals are observed at the injection site for up to 14 days postinjection, but no bioluminescent signals are detected in inguinal lymph nodes, suggesting that optical reporter genes could be used to determine optimal injection sites for DNA vaccines. In another paper, Schweichel and colleagues[83] have used a recombinant adenovirus encoding an antigen-luciferase fusion protein and have compared the immune response after injection of recombinant adenovirus or recombinant adenovirus-transduced dendritic cells (DC). They observed that intravenous injection of adenovirus-transduced DC stimulates the strongest cytotoxic T-lymphocyte (CTL) responses, although it delivers 2 orders of magnitude less antigen in vivo when compared to direct injection of recombinant adenovirus. Finally, the distribution of two recombinant poxvirus vectors, potentially useful for preclinical and clinical vaccine development, has been reported by Gómez and colleagues[84] in a study employing BLI. They compared the virus dissemination in mice inoculated by the mucosal or systemic route with replication-competent (Ankara strain of vaccinia virus) and attenuated recombinant viruses (derived from Ankara and Copenaghen strains of vaccinia virus) expressing the luciferase gene. BLI experiments showed that, in contrast to the replication-competent, the attenuated recombinants express the reporter gene transiently for most of the routes assayed.

4. Radiopharmaceuticals for Molecular Imaging of Inflammation/Infection

Radiopharmaceuticals are designed to interact with a biological process, pathway, or target molecule in the body. They consist of two essential components, a nonradioactive "vector", which interacts with the desired target following administration to the subject, and a radionuclide "tag", which emits radiation that can be detected externally and provides noninvasive information on the distribution of the radiopharmaceutical in the body. The mechanisms by which the radiopharmaceuticals interact with their targets are very varied and include physical trapping in blood vessels or lymphatic vessels, passive diffusion into body cavities and compartments, active secretion or excretion by various organs, ion-exchange onto bone surfaces, and binding to receptors, transporters, or structural components on cells. External imaging of the emitted radiation therefore gives information on the distribution or the concentration of the biological target, which may be altered in diseased states. In the case of imaging of infection and inflammation, examples of target mechanisms include interactions with cytokine receptors on invading white cells, physical trapping in the increased extravascular volume that accompanies inflammation, binding to invading microorganisms, and others that are described elsewhere in this Review.

It follows that for each different biological target, the vector portion of the radiopharmaceutical must be different. Their chemical nature includes insoluble particles of various sizes, large and small proteins and peptides, sugars, simple ions, and metal chelates and complexes. The design of the vector will be tailored to optimize its interaction with the desired biological target and to minimize those with other undesired processes. So taking, for example, a radiopharmaceutical based on a biologically active peptide, the amino-acid sequence of the peptide will be optimized to increase its binding affinity for its complementary receptor and to minimize binding to other related or unrelated receptors that may be present in the body. However, the actual binding of the vector to the molecular target is actually a late step in the process of delivery of the radiopharmaceutical. The compound must be first administered to the subject. This is normally done by intravenous injection but may also be given by other routes such as oral, intradermal, or by inhalation. The tracer must then reach the tissues where the molecular targets are located. Most commonly it will travel via the bloodstream where it may bind to circulating proteins or cells or be degraded by enzymes. It may be rapidly excreted by organs, preventing its ultimate delivery to the tissue of interest. Once there, it must still be able to physically access its target. The most accessible of these are those located within the blood vessel itself, but normally the radiopharmaceutical will have to leave the vasculature, diffuse through surrounding tissues, and, in the case of intracellular targets, through the cell wall to arrive at its final destination. The design of the radiopharmaceutical must therefore take these factors into account. The compound must be sufficiently stable and its physicochemical parameters tailored to ensure maximum delivery at the final destination.

The radioactive portion of the radiopharmaceutical is that which enables its location in the body to be determined by external imaging. It follows therefore that the radionuclide must emit radiation of sufficient energy to pass through the overlying tissues and out of the body so they can interact with the detector. Because all radioactivity is ionizing and

Table 1. Desired Properties of Radionuclides for Diagnostic Imaging

(1) X-rays or γ-photons must be emitted in the range of 100−500 keV preferably with high abundance
(2) no particulate (α or β particles) should be emitted because these add to the radiation dose without providing any diagnostic information
(3) the half-life of the radionuclide should be long enough to enable the imaging procedure to be performed, but no longer, because radiation dose received thereafter provides no benefit
(4) the chemistry of the radioactive element should be versatile to allow it to be tagged to various targeting vectors of interest
(5) there must be a means of providing the radionuclide at the imaging site (typically a hospital) in sufficient quality and quantity at acceptable cost

Table 2. Radionuclides for SPECT Imaging[a]

radionuclide	type of decay	energy (MeV)		half-life
		$E_{\beta max}$	$E_{\gamma\ (abundance)}$	
^{123}I	EC		0.159 (84%)	13 h
^{131}I	β-,γ	0.61 (86%)	0.364 (80%)	8.04 days
		0.33 (13%)	0.284 (6%)	
^{111}In	EC		0.173 (91%)	2.8 days
			0.247 (94%)	
^{99m}Tc	IT		0.141 (89%)	6.02 h
^{67}Ga	EC		0.093 (35%)	78 h
			0.185 (21%)	
			0.300 (17%)	
^{201}Tl	EC		0.068−0.80 (95%)	73.1 h

[a] Abbreviations: EC = electron capture; IT = isomeric transition.

therefore potentially hazardous, a balance must be found between the benefits of the diagnostic information obtained from the diagnostic imaging procedure and the risk implied by the magnitude of the radiation dose received. The need for this balance is a major factor in the choice of radionuclide for diagnostic nuclear medicine. The properties required of radionuclides for incorporation into radiopharmaceuticals are summarized in Table 1.

Every radiopharmaceutical has its own advantages and disadvantages. Despite that we now have very accurate radiopharmaceuticals for imaging inflammation and infection, there is always a need for more specific and sensitive radiopharmaceuticals, which can specifically detect the levels of different activation markers, adhesion molecules, and receptors, as well as there is a need for more resolute imaging devices. The improvement of nuclear medicine images, indeed, stands on the progression of both aspects: radiopharmaceutical probes and devices. Nevertheless, the information provided by radiopharmaceuticals is already extremely useful not only for "receptor mapping" of the inflammatory/infectious lesions, but also for therapy decision making and follow-up of the treatment. This is further discussed below.

Radionuclide imaging can be divided into single photon (planar scintigraphy and SPECT) and positron (PET) imaging, and the radionuclides used for each of these modalities will differ.

4.1. Principles of SPECT Radiopharmaceuticals

A list of the most commonly used radionuclides for planar scintigraphy or SPECT imaging is shown in Table 2. These typically emit X- or γ-rays with energies in the range of 100−250 keV, although photons with energies lower and higher than these limits can be employed with lower efficiency because lower energy emissions are attenuated to a greater extent by body tissues, while higher energy γ rays interact less efficiently with γ cameras.

It can be seen that most of these radionuclides fulfill the requirement of a lack of particulate emissions and that they have half-lives ranging from a few hours to a few days. These relatively long half-lives mean that SPECT imaging can be employed to image processes, which are long-lived such as, for example, the biodistribution of a radiopharmaceutical with slow pharmacokinetics. The long half-life also facilitates distribution of the radionuclides to imaging centers because the logistics of reliable distribution of radionuclides with short half-lives from a central production site are difficult. However, the down-side of a long half-life is a higher radiation dose as described above. The preferred radionuclide for SPECT studies is, therefore, that with the shortest half-life in the table, technetium-99m.[85] The 6 h half-life is long enough for imaging procedures that can be completed within a working day, and the logistical problem of isotope supply is overcome by the fact that ^{99m}Tc can be obtained from a radionuclide generator.

^{99m}Tc is produced by the decay of its parent radionuclide ^{99}Mo as shown in the decay equation in Figure 2. A radionuclide generator consists essentially of a chromatographic column composed of alumina onto which the ^{99}Mo is loaded. As the ^{99}Mo decays, it produces ^{99m}Tc, which binds less strongly to the alumina, and it can therefore be separated from the parent isotope by passing a dilute salt solution down the column. The eluted ^{99m}Tc can be incorporated into the desired radiopharmaceutical, while the ^{99}Mo remains on the column and continues to decay to more ^{99m}Tc that can be eluted on a subsequent occasion.

Technetium-99m therefore complies with the requirements listed in Table 1 so far as physical decay characteristics and availability are concerned. It also has a highly versatile chemistry that allows it to be incorporated into a wide range of radiopharmaceuticals. This chemistry is highly redox dependent and involves reduction of the sodium pertechnetate provided by the generator into lower oxidation states, which may then be complexed by a variety of ligands for incorporation into radiopharmaceuticals.[85] Because radiopharmaceuticals are intended for immediate clinical use and will be administered to patients after preparation, this places high demands on their medicinal quality. Most medicines are manufactured by industrial processes and extensively tested and quality controlled before being released for use by patients. The short half-life of the radionuclides used in most radiopharmaceuticals means that this is not possible. The product must be prepared on site in the hospital and used within a few hours of preparation, which does not allow sufficient time for extensive testing to be undertaken. It is essential, therefore, that a means of preparation is developed, which ensures that the radiopharmaceutical can be reliably manufactured in such a way as to ensure that high pharmaceutical, chemical, and radionuclidic standards are maintained.

For routine use in the practice of nuclear medicine, such a requirement is provided by the use of radiopharmaceutical "kits". These kits are industrially developed and manufactured and essentially provide all of the nonradioactive components required for preparation of the desired radiopharmaceutical in a sterile (normally freeze-dried) formulation. A pharmaceutically acceptable supply of the radionuclide is also obtained either from a radionuclide generator or (in the case of longer-lived radionuclides) direct from a supplier, and the radiopharmaceutical is prepared by combining the two components together. Often the subsequent radiolabeling reaction occurs within a few minutes of incubation at room temperature, although sometimes heating is required. The aim of the process is a product of high quality, which is

Table 3. Radionuclides for PET Imaging[a]

		energy (MeV)		
radionuclide	type of decay	$E_{\beta^+\max}$	$E_{\gamma\ (\text{abundance})}$	half-life
^{15}O	$\beta+$	1.74	0.511 (100%)	2 min
^{14}N	$\beta+$	1.20	0.511 (97%)	10 min
^{11}C	$\beta+$	0.97	0.511 (99%)	20 min
^{18}F	$\beta+$	0.64	0.511 (97%)	110 min
^{68}Ga	$\beta+$	1.90	0.511 (89%)	68 min
^{64}Cu	EC, $\beta+$	0.65	0.511 (18%)	12.7 h
^{124}I	$\beta+$	2.14	0.511 (25%)	4.2 days

[a] Numerous other radionuclides such as yttrium-86, technetium-94m, and zirconium-57 have also been explored but are not in as widespread use as those listed above.

safe for administration to patients, and in the great majority of cases this will be achieved. However, to be absolutely sure that the radiopharmaceutical will function as desired, it is desirable to undertake a small number of simple tests to check the purity of the product before use. These checks should be simple and rapid so they can be performed within the time frame imposed by the decay of the radionuclide and the practical constraints of the operation of the imaging department.

"Kits" are only widely used when the labeling chemistry employed results in high labeling efficiencies so that no purification is needed before the resultant radiopharmaceutical is injected into the patient. This is often true of compounds labeled with technitium-99m as described above and also with indium-111, another widely used SPECT imaging agent (see "trivalent metals"). Other radionuclides, in particular, isotopes of iodine such as iodine-123 and iodine-131, have also been widely used (see "halogens"), but, in general the lower labeling efficiencies obtained using this chemistry means that postlabeling purification is required and a "kit" labeling approach cannot therefore be used.

While "kits" are available for many routinely undertaken nuclear medicine investigations, they are not available for developing and experimental procedures. For such preparations, it is normally necessary to combine varying quantities of several components to undertake the labeling procedure, and a purification step may be required before a sufficiently high purity can be obtained. It remains essential, however, that the final quality of such preparations is of the high standards required for clinical use, and this will normally require a more extensive quality control process before they can be administered.

4.2. Principles of PET Radiopharmaceuticals

The radionuclides most commonly used in PET imaging are listed in Table 3. With the exception of ^{124}I, these positron emitting radionuclides are characterized by short half-lives, in the order of hours at most or sometime just a few minutes.

This means that PET is most useful for monitoring process that are complete within a short time frame and are most commonly used for tracers that have rapid pharmacokinetics such as small molecules and small peptides but are less useful for imaging at later times when a significant proportion of the radioactivity will have decayed resulting in poor count statistics. Because of the higher sensitivity of PET detection systems, they are particularly useful for dynamic acquisitions of tracer distribution over the first few minutes after administration because the high count rates obtained provide the good statistics needed for modeling of pharmacokinetic parameters from this data. Using such approaches, it is possible to quantitatively determine the concentrations of PET radiopharmaceuticals in body compartments. However, the difficulties outlined above for the use of shorter half-life SPECT radionuclides are accentuated even more in the PET domain. For those with the shortest half-lives ^{15}O, ^{14}N, and ^{11}C, there is no alternative other than on-site production. Longer-lived radionuclides such as ^{18}F, ^{64}Cu, and ^{124}I can be distributed from a central producer, although the distribution radius for ^{18}F in particular is limited. ^{68}Ga is available from a radionuclide generator in an analogous manner to ^{99m}Tc, although the parent radionuclide in this case is ^{68}Ge that has a half-life of 271 days.[86]

With the exception of ^{68}Ge, all of these radionuclides must be produced with a cyclotron. Many hospitals with PET centers possess cyclotrons with limited production capacities but dedicated to the manufacture of ^{14}N, ^{11}C, and ^{18}F, while industrial suppliers and larger academic centers possess larger cyclotrons with a broader manufacturing capacity. The very short half-life of ^{15}O and ^{14}N means that the time available for their incorporation into radiopharmaceuticals is extremely limited and their use is essentially limited to two agents, $^{14}NH_3$, which is produced in situ within the cyclotron target itself, and $H_2{}^{15}O$, which is made in a dedicated online synthesizer. The 20 min half-life of ^{11}C also imposes severe restrictions on the preparation of radiopharmaceuticals, and its use is limited to relatively few specialized centers, while the 2 h half-life of ^{18}F provides greater time for labeling chemistry resulting in wider usage. A characteristic of all PET radionuclides is the 511 keV photon produced on annihilation of the emitted positron. This radiation is highly penetrating and represents a considerable radiation safety hazard to operators. The short half-lives and (sometimes) low yields from radiolabeling procedures means that very large starting amounts of radioactivity are sometimes required for the preparation of these radiopharmaceuticals, and this further exacerbates the radiation safety issue. For this reason, automated methods are generally employed for PET radiopharmaceuticals. For the most commonly used tracers (such ^{18}F-2-fluoro-2-deoxyglucose (FDG)), the process is fully automated and increasingly uses cartridge-based systems, which seek to emulate the "kit" approach for ^{99m}Tc radiopharmaceuticals. Apart from the radiation safety advantages, such methods reduce the effects of operator variability and human error and provide the reliability essential for compounds that will almost immediately be in clinical use. A restricted level of quality control (QC) testing can again be applied to such products. For less routinely used radiopharmaceuticals, the degree of automation employed ranges from complete to semiautomation, and cartridge-based systems are not available, resulting in the need for more extensive QC testing before use.

4.3. Radiochemistry of SPECT and PET Radiopharmaceuticals

A detailed description of radiopharmaceutical chemistry is outside the scope of this Review, and the intention is to give a brief overview of the methods used and to direct the reader to more detailed reviews where possible. The chemistry by which the vector portion of the radiopharmaceutical is tagged by the radionuclide will vary depending on the chemical properties of the element concerned. In general terms, the desire is to achieve a highly efficient radiolabeling method, which results in a bond that remains stable once administered into a biological environment. Four main

categories of labeling methods are employed: those used for labeling with C-11, for the halogens (iodine and fluorine), for trivalent metallic ions such as indium and gallium, and group VII elements such as technetium. As described above, SPECT imaging is most useful for monitoring relatively long-lived processes, and the vectors employed for such approaches are normally relatively large in molecular terms. They are often described as "biomolecules" of which the most commonly used type are polypeptides, either proteins or peptides. Methods for radiolabeling biomolecules are often classified as either "direct" or "indirect". In direct methods, the radioactive atom forms either covalent or coordinate bonds directly with the constituent atoms of the vector, while indirect methods rely on an intervening prosthetic moiety, which is first conjugated to the biomolecule.

4.3.1. Carbon-11

A major advantage of C-11 chemistry is the possibility to produce compounds that are chemically identical to their "cold" counterparts, whereas labeling with most other radioactive elements produces tracers that must be considered as analogues to the reference compounds. ^{11}C-based PET is a powerful research tool but (with few exceptions) is not employed in routine clinical practice. ^{11}C labeling can therefore be considered a much specialized area of radiopharmaceutical chemistry. Its use is based on the in situ generation in the cyclotron target of either $^{11}CO_2$ or $^{11}CH_4$ from which a small range of reactive labeled synthons, most commonly methyl iodide, hydrogen cyanide, and carbon monoxide, can be readily prepared for incorporation into small molecules.[87,88]

4.3.2. Halogens

Radioiodine has, in particular, been widely used for radiolabeling of proteins for which direct labeling by electrophilic substitution is by far the most widely practised method.[89] The labeling is mediated by oxidation of the iodide ion to the positively charged iodous ion (H_2OI^+), which labels the phenolic ring of the tyrosine amino acid side chain in the ortho- and para- positions. Many oxidizing systems have been used for this purpose, but the most popular are chloramine-T and Iodogen. Chloramine-T is a powerful oxidant and if exposed to the fragile proteins for long periods may oxidize the side chains of its constituent amino acids, while the Iodogen method provides milder oxidizing conditions, and other enzyme-based methods are gentler still. Radiolabeling is performed by the addition of the protein and the radioiodine to the oxidant and incubation for a few minutes. At the end of this time, a labeling efficiency typically ranging from 30−80% will be achieved, and the unreacted "free" iodine can be removed either by gel-filtration, ion-exchange, or reverse-phase chromatography.

Radioiodination is much less commonly used for peptides than for proteins.[90] One reason for this is that iodinated peptides are relatively hydrophobic and are excreted via the hepatobiliary tract (see below). Nevertheless, peptides containing tyrosine residues can also be labeled by the same methods. Peptides lacking tyrosine or larger proteins (in which electrophilic substitution results in a loss of biological activity) can also be labeled by indirect iodination methods, although these are rarely employed due to their low labeling yields.

Radioiodine is also used for labeling smaller molecules for which alternative methods are required. For compounds in which a high specific activity is not required, exchange methods, in which a nonradioactive atom is substituted by radioiodine, may be used, but the resulting product will necessarily contain many molecules still labeled with stable iodine. When high specific activity is required, demetalation approaches (followed by HPLC purification) are the methods of choice.

Fluorine-18 is the most widely used radionuclide for PET imaging. It is most commonly used for labeling small molecules, but, in recent years, has also been used for labeling biomolecules such as small peptide by the use of ^{18}F-labeled synthons. Small molecules and synthons may be labeled using either electrophilic or nucleophilic methods, but the former are less widely used due to the lower specific activity of the compounds generated and the fact that not all cyclotrons are set up to produce the electrophilic $^{18}F_2$ precursor. Nucleophilic methods based on ^{18}F-fluoride therefore dominate. These are performed mainly in anhydrous dipolar aprotic solvents such as acetonitrile and DMSO using a cryptand (most commonly Kryptofix 2.2.2.) in combination with an appropriate cation (normally K^+) to exclude water from the F^- sphere. ^{18}F can readily substitute a variety of leaving groups such as bromo, iodo, tosyl, nosyl, or sulfonate from aliphatic systems, less readily from heterocyclic ring systems, and only from aromatic rings that are activated by strong electron withdrawing substituents.[91,92]

4.3.3. Trivalent Metals

The radiochemistry of these elements is dominated by coordination chemistry, but such elements do not form stable complexes with amino-acid side chains. Accordingly, a chelating group is first inserted into the biomolecule to form a stable binding site for the radionuclide. This is normally achieved by the use of bifunctional chelating agents, which are compounds containing a chelating group capable of forming a strong complex with the metallic radionuclide plus a chemically reactive group that allows the chelator to be attached to a functional group on the biomolecule, typically an amino group.[93] Such bioconjugates can be prepared in two ways. For small peptides prepared by chemical synthesis, the preferred method is to attach the chelator while the peptide is on the resin; this improves reaction efficiency and simplifies purification, and it also allows the chelator to be placed at any desired point in the peptide sequence, which is essential to reduce the possibility of inhibition of receptor binding of the biomolecule by the chelate.[94] For proteins prepared by biosynthesis such as antibodies and cytokines, such a specific placement of the chelator is rarely possible. Conjugation is therefore performed after production of the protein, and the bifunctional chelator may react with any amino group present in the molecule such as at any lysine side chain or the N-terminus of the protein.[95] This results in a heterogeneous distribution of the chelating moieties throughout the bioconjugate with the result that it is very difficult to predict effects on the receptor binding properties of the molecule. It is, however, also possible to generate bifunctional chelating agents that react with other functionalities on amino acid side chains, in particular carboxylic acids (e.g., glutamic acid) and thiols (cysteine). This latter chemistry does often allow a more site-specific conjugation, especially if there is only a single free thiol group available in the molecule.

The most widely used chelating groups are those based on diethylenetriaminepentaacetic acid (DTPA) and tetraazacyclododecanetetraacetic acid (DOTA), for which a variety of bifunctional forms exist.[96] Although DOTA has the advantage of forming metal complexes with higher stability constants and therefore radiopharmaceuticals with higher stability in vivo, heating is normally required to prepare the chelate, and this limits its use for thermolabile biomolecules such as proteins. For thermostable compounds such as small peptides, however, it is the chelator of choice.

4.3.4. Group VIIA Elements: Technetium

Technetium-99m (Figure 2) is a useful radionuclide for labeling small peptides and proteins, and although it has a relatively short half-life, it does not match the long blood clearance times of large proteins such as intact immunoglobulins, and technetium-labeled antibodies have been used in clinical practice.[97]

Biomolecules can be labeled with technetium-99m using either direct or indirect approaches.[98] Technetium forms stable complexes with sulfur-containing compounds and can bind to free thiols in proteins. This method has been most widely exploited to label the thiol groups in the hinge region of immunoglobulins. Normally these thiol groups are in the oxidized, disulfide form and are unavailable for labeling. However, in the presence of mild reducing conditions, free thiols can be exposed to form a stable complex with technetium. The antibody is labeled by the addition of technetium, stannous ion, and a weak complexing agent such as methylene diphosphonate.[99] This ensures that any labeling of the protein occurs via the exposed thiol groups and not at other low-affinity binding sites in the protein. Labeling efficiencies of at least 95% can be routinely achieved without the need for any further purification of the radiopharmaceutical. Although this is a very simple and reliable method, its use is limited to disulfide-bridged proteins in which reduction of this bond does not compromise the biological function of the molecule. This is the case for very few types of protein because in many instances reduction of disulfide bridges results in a change in conformation that disturbs interaction with the receptor, and also many proteins lack disulfide bridges completely.

For most proteins and all small peptides, therefore this direct labeling method is unsuitable and an indirect labeling method based on the use of bifunctional complex agents must be used. Although similar in principle to the methods described above for trivalent metals, the chelating agents of choice for technetium will be different from those used for indium and gallium. The most widely used chelating agents are those based on amino- or amido-thiol chelators such as mercaptoacetyltriglycine (MAG3) and hydrazinonicotinic acid (HYNIC).

A further labeling method that falls somewhere between the categories of direct and indirect is that based on the tricarbonyl Tc(I) precursor.[100] In this complex, the technetium or rhenium is bonded to three stable carbonyl bonds and three unstable bonds with water. These later unstable bonds can be replaced by coordinate bonds with suitable donors in the peptide side chains. Pyridine nitrogen atoms in the side chains of histidine amino-acids have the potential to form strong complexes with this agent, and it has been used for labeling recombinant proteins containing the hexahistidine tag. However, the conformation of histidine as presented in a normal amino acid sequence does not provide the most ideal binding site, and "artificial" binding sites are normally inserted into the peptide sequence during synthesis.

4.4. The Effect of Labeling on in Vivo Performance

The in vivo characteristics of radiopharmaceuticals are influenced by their physicochemical properties, in particular, molecular size and hydro/lipophilicity.[101] Large molecules such as proteins with a size that exceeds the molecular weight cutoff of the renal glomerular filtration system (around 50 000 Da) have long circulation times in the blood. This includes intact antibodies and many larger antibody fragments. As a result of this, blood background activity remains high with such agents for many hours or even days after administration. There is often significant uptake into nontarget organs such as liver, and metabolism in these organs results in the formation of radiolabeled metabolites. The fate of these metabolites depends on the radiolabeling method employed. Metabolism of radioiodinated proteins results in the formation of iodotyrosine and free iodide, which are rapidly secreted out of the liver cells and then either excreted via the kidneys or (in the case of iodide) accumulated in thyroid and stomach. Metabolism of proteins labeled with metallic radionuclides results in labeled lysine adducts, which are trapped in the lysosomal compartments of the cells and are only slowly eliminated, while the metabolism of technetium-labeled antibodies follows a pattern somewhere between these two extremes. After administration of such large molecules, target uptake gradually increases, reaching a maximum (with intact antibodies) at about 24 h after injection, although maximal target to nontarget ratios may not be achieved until some time later. Unless it is located within the lumen of the blood vessel, target uptake in many tissues is limited by poor physical access of the labeled antibody to its cellular binding sites because such large proteins leave the vasculature with difficulty and diffuse only slowly into the surrounding tissues, although this may be increased in inflammation.

While antibody-based compounds show high stability in the blood, many naturally occurring neuropeptide hormones are unstable in the bloodstream and are rapidly degraded by serum proteases. This is a natural mechanism for limiting the duration of their normal pharmacological action. In addition, this pharmacological activity can lead to undesirable side effects even at very low doses. To improve the stability, the sequence of the natural peptide can be modified by insertion of unnatural amino acids or modification of peptide bonds, provided that this does not disrupt their interaction with the receptor. The pharmacological activity can be viewed from both negative and positive angles. The fate of most pharmacological agonists after binding to the receptor is that the receptor−ligand complex is internalized and packed in intracytoplasmic vesicles from which the receptor is recycled to the cell surface but in which the ligand is degraded. Depending on the radionuclide being used, this can result in it being trapped within the cell for the duration of its physical decay. This long retention time can greatly enhance the imaging or therapeutic performance of the radiopharmaceutical. The downside of the pharmacological activity is that receptor binding also results in transmission of a secondary intracellular message, which has some biological consequence. Depending on the nature of the biological effect, it may or may not be an acceptable side-effect of the nuclear medicine procedure. If it is considered

unacceptable, then either doses below the pharmacological limit must be used (if possible) or a peptide with antagonist actions be employed, even if these lack the desirable property of internalization.

Peptides and proteins with a molecular weight below around 50 000 Da can be filtered through the glomerulus and show a much more rapid blood clearance. The behavior of such conjugates is much more dependent on their relative hydro-/lipophilicity than their size. Lipophilic peptides, typically those labeled with radioiodine or F-18, show a mixed route of excretion, being eliminated by the hepatobiliary tract as well as the kidney.[102] As a result, there is generalized accumulation of radioactivity in the gastrointestinal tract, and this obscures any target tissue uptake in the abdomen. More hydrophilic peptides, typically those labeled with bifunctional chelates, show little excretion through the hepatobiliary tract and are excreted solely by the renal tract. However, they also show a variable degree of retention in the kidneys.[103] After filtration, many valuable substances in the primary urine such as vitamins, ions, and peptides are reabsorbed in the proximal tubules. They are catabolized in the lysosomes, and the constituent amino-acids are trafficked back to the blood where they are reabsorbed and recycled. Radiometabolites show a variable pattern of behavior depending on their characteristics. Radioiodinated compounds may be secreted out of the cells into the bloodstream, but radiometalated compounds are again trapped in the tubular cells, resulting in renal retention of radioactivity. The degree of renal retention varies considerably from compound to compound and can, to some extent, be reduced by coadministration of substances process such as positively charged amino-acids and gelofusine that compete for the renal reabsorption mechanisms.

4.5. Monoclonal Antibodies and Their Fragments

Radiolabeled monoclonal antibodies (mAbs) and their fragments have been successfully used for imaging inflammation and infection. Despite that the gold standard for imaging infections remains the use of radiolabeled white blood cells, mAbs have several advantages as compared to radiolabeled autologous leukocytes. These are easier to use, and there is no need to handle potentially hazardous biological specimens; moreover, labeled mAbs bind to their target with high specificity. Several mAbs and their fragments including anti-TNF-α, anti-CD25, anti-CD20, anti-DR, anti-CD3, anti-CD4, anti-MIF, antigranulocyte, and anti-E-selectin antibodies have been radiolabeled mainly with ^{99m}Tc, ^{111}In, or ^{123}I and used for imaging of inflammation/infection. A comprehensive list of radiopharmaceuticals with their clinical applications is provided (Table 4). Scintigraphic study with these radiolabeled mAb offers an exciting possibility for the detection of their specific target molecule on different cell populations including lymphocyte scintigraphy. This technique allows whole body imaging and detects inflammation or infection in an early stage of disease that might be difficult to assess clinically or by means of radiography. A long time interval is often required between the administration of labeled mAb and the acquisition of images (6−24 h) to have a good target/background ratio. Indeed, once injected, i.v. mAbs have a long plasmatic half-life and slow concentration in the affected site. Radiolabeled mAbs or their fragments are always injected in a tracer (nonpharmacological) dose for scintigraphic imaging, which rarely induce any clinical or side effects in patients. The only side effect that has been described in some cases of murine mAb administration is the induction of human antimurine antibodies (HAMA), a host response to foreign antigens. If mAbs are injected in patients with HAMA, they may affect mAb biodistribution, image quality, and clinical relevance of images.

A commercially available ^{99m}Tc-labeled antigranulocyte IgG1 murine antibody BW250/183 (Besilesomab, Scintimun) recognizes the nonspecific cross-reacting antigen 95 (NCA-95) expressed on human granulocytes, promyelocytes, and myelocytes.[271] This mAb has been used in the study of chronic inflammatory bowel disease,[130] bone infections,[131] lung abscesses,[131]diabetic foot infections,[132] and in infected pseudoaneurysm (Figure 5). Dominguez-Gadea et al. performed a study with a radiolabeled BW 250/183, for the diagnosis of pedal osteomyelitis in 25 diabetic patients.[132] In the study, the radiopharmaceutical demonstrated a sensitivity and specificity of 93% and 78%, respectively. A study performed by Becker et al. with ^{99m}Tc-antigranulocyte antibody in 34 fever of unknown origin (FUO) patients demonstrated that an overall specificity and sensitivity for infection of 92% and 40%, respectively.[272] The positive predictive value was 88%, and the negative predictive value was 52%; moreover, in 59% of the patients, an infectious cause for the fever was found, and no cause of the fever could be found in 11% patients. In another study, 51 patients with FUO underwent ^{99m}Tc-BW250/183 mAb immunoscintigraphy.[273] In this study, immunoscintigraphy was positive in 12 (out of 18) patients with infectious diseases and in 2 (out of 4) patients with malignant diseases. Therefore, only in 27% of patients, this radiopharmaceutical was found to be useful. Nevertheless, using this radiolabeled mAb, a HAMA production problem has been seen during studies that limits the use of this immunoscintigraphic technique.

Another commercially available SSEA-1 murine mAb, called ^{99m}Tc-fanolesomab (LeuTech), an IgM, has been developed that binds with high affinity to the CD15 antigen expressed on neutrophils. Scintigraphy with ^{99m}Tc-SSEA-1 has been proposed for diagnostic purposes in equivocal cases of appendicitis.[133] A study was performed in 25 diabetic patients for diagnosis of pedal ulcers.[274] The authors evaluated sensitivity, specificity, and accuracy of the radiolabeled mAb were 90%, 67%, and 76%, respectively. In another study, it shows a similar diagnostic accuracy when compared to the white blood cell (WBC) scan.[275] A transient neutropenia has been noted after the use of ^{99m}Tc-SSEA-1[275]; nevertheless, in most of these cases it does not represent a clinical problem and does not impair imaging quality. Unfortunately, as a consequence of serious and potentially fatal cardiopulmonary reactions associated with its use, ^{99m}Tc-SSEA-1 has been suspended from the market.

Controversial results have been obtained using the ^{99m}Tc-labeled sulesomab (Leukoscan, Immunomedics GmbH), an antigranulocyte, murine IgG1 antibody Fab' fragment of antibinding to NCA-90 on granulocytes. Immunoscintigraphy with ^{99m}Tc-sulesomab enables a rapid localization of osteomyelitis, a negligible HAMA response rate, and accuracy comparable to WBC scan.[134−136] Encouraging results have been obtained in the detection of suspected endocarditis[137] and appendicitis.[138] In a large study, 122 diabetic patients with foot ulcers were evaluated by radiolabeled sulesomab scintigraphy.[136] In the study, labeled mAb fragment showed a high sensitivity of 91% but

Table 4. Radiopharmaceuticals for Imaging Inflammation/Infection

radiopharmaceutical	target	isotopes	application in molecular imaging	ref
		Monoclonal Antibodies and Fab' Fragments		
Infliximab (Remicade) [Chimeric IgG1 mAb]	TNF-α	^{99m}Tc	Crohn's disease, rheumatoid arthritis imaging	104−106
Adalimumab (Humira) [Fully human IgG1 mAb]	TNF-α	^{99m}Tc	rheumatoid arthritis imaging	107, 108
1D09C3 [Humanised IgG4 mAb]	HLA-DR	^{99m}Tc	lymphoma imaging (experimental stage)	109, 110
Basiliximab (Simulect) [Chimeric IgG1 mAb]	CD25	^{211}At	T-cell leukemia imaging	111
Daclizumab (Zenapax) [humanized IgG1 mAb]	CD25	^{18}F, ^{99m}Tc, ^{111}In, ^{125}I, ^{212}Bi, ^{67}Ga	T-cell leukemia imaging	112−115
OKT-3 (Muromonab) [Murine IgG2a mAb]	CD3	^{99m}Tc	rheumatoid arthritis and renal transplant rejection imaging	116, 117
Visilizumab (Nuvion) [humanized IgG2 mAb]	CD3	^{99m}Tc	T-lymphocyte imaging in animal model	118
MAX.16H5 [Murine IgG1 mAb]	CD4	^{99m}Tc	rheumatoid arthritis imaging	119−121
anti-MIF mAb	MIF	^{125}I	inflammation imaging in animal model	122
anti E-Selectin [Murine IgG1 mAb]	E-Selectin	^{111}In	rheumatoid arthritis imaging	123−127
Rituximab (Mabthera) [Chimeric IgG1 mAb]	CD20	^{99m}Tc	sentinel lymph node (SLN) and rheumatoid arthritis	128, 129
BW250/183 (Antigranulocyte) [Murine IgG1 mAb]	nonspecific cross-reacting antigen 95 (NCA-95)	^{99m}Tc	bowel disease, bone infections,lung abscesses, and in diabetic foot infections	130−132
SSEA-1 (LeuTech) [Murine IgM]	CD15	^{99m}Tc	appendicitis imaging	133
antigranulocyte mAb (Sulesomab, Leukoscan) [Murine IgG1 mAb Fab' fragment]	human granulocytes	^{99m}Tc, ^{111}In	imaging of fever of unknown, acute inflammatory disorders, osteomyelitis, endocarditis, appendicitis	134−140
EP1645 [human anti-CD4 mAb fragment]	CD4	^{99m}Tc	imaging of rheumatoid arthritis	141
		Peptides, Cytokines, Chemokines, Interferons, and Growth factors		
IL-1 α/β	IL1RI[a] = B, Mo, N; IL1RII = En, Fi, He, Ke, T	^{123}I, ^{125}I	inflammatory process imaging in animal model	142−144
IL-1ra (receptor antagonist)	IL-1R	^{123}I, ^{125}I	rheumatoid arthritis, inflammatory process	145, 146
IL-2	T, B, NK	^{123}I, ^{125}I, ^{99m}Tc, ^{35}S, ^{18}F	Graves' ophthalmopathy, Type 1 diabetes, celiac disease, Crohn's disease, thyroid autoimmune disease, kidney graft rejection, cutaneous melanoma, kidney allograft, atherosclerosis	147−159
IL-8	N, Ba, T	^{99m}Tc, ^{123}I, ^{125}I, ^{131}I	infectious foci imaging, including osteomyelitis, liver abscess,joint prosthesis infection, and soft tissue infections imaging	160−165
IL-6, IL-10 G-CSF	T, B, Mϕ, He, HP, N, phagocytes	^{125}I	infectious foci imaging in animal model	166
IL-12	T, NK	^{125}I	T-lymphocytes and lymphocytic infiltrates imaging in animal models	167
MCP-1	Mo, Mϕ, Gr	^{99m}Tc	subacute inflammation imaging in animal model	168, 169
IFN-γ	many different cells	^{123}I	lung inflammatory diseases imaging	170
epidermal growth factor (EGF)	EGFR	^{123}I, ^{111}In, ^{125}I	metastatic lymph nodes in humans, imaging of breast cancer, study of skin wounds	171−173
tumour growth factor beta (TGF-β)	TGF-RI-V, many different cells	^{125}I	imaging study of angiogenesis	174
leukotriene (LTB_4) receptor antagonist (RP517; DPC 11870−11; MB88, fMLFK)	BLT1, BLT2	^{99m}Tc, ^{111}In	inflammation/infection imaging in animal model	175−183
platelet factor (PF4) (P482, P1827)	human leukocytes	^{99m}Tc	bacterial infections	184−186
IIa-IIIb receptor antagonist (DMP444)	IIa-IIIb	^{99m}Tc	imaging of infective experimental endocarditis	187
neutrophil elastase inhibitor (EPI-HNE-2/4)	neutrophil elastase	^{99m}Tc	inflammation/infection imaging in animal model	188−190
antimicrobial peptides (UBI 29−41, P483H, HNP1−3, hLF)	bacteria and fungi infection	^{99m}Tc	infection imaging	191−197
f-Met-Leu-Phe	formyl-peptide receptor on granulocytes and monocytes	^{99m}Tc, ^{111}In	bacterial infection imaging	142, 198, 199
complement factor 5a (C5a)	neutrophils, monocytes	^{99m}Tc	intramuscular infection imaging in animal model	200
bacteriophage	bacteria	^{99m}Tc	infection imaging in animal model	201
		Antibiotics		
ciprofloxacin (infecton)	prokaryotic topoisomerase IV and DNA gyrase	^{99m}Tc, ^{18}F	microbial infection imaging	196, 202−207
sparfloxacin	gram-positive and gram-negative bacteria	^{99m}Tc	bacterial infection imaging in animal model	208
ceftizoxime	bacterial wall	^{99m}Tc	bacterial infection imaging	209
isoniazid	mycobacteria	^{99m}Tc	*Mycobacterium tuberculosis* infection in animal model	210
ethambutol	mycobacteria	^{99m}Tc	mycobacterial infection imaging in animal model	211
fluconazole	microbial infections	^{99m}Tc	fungal infection imaging in animal model	212
enrofloxacin	bacterial infection	^{99m}Tc	infection imaging	213, 214
levofloxacin	bacterial infection	^{99m}Tc	infection imaging	215
norfloxacin	microbial infections	^{99m}Tc	infection imaging	216
ofloxacin	bacterial infection	^{99m}Tc	infection imaging	217
lomefloxacin	bacterial infection	^{99m}Tc, ^{18}F	infection imaging with PET	218
fleroxacin	bacterial infection	^{18}F	infection imaging in animal model	219
trovafloxacin	bacterial infection	^{18}F	infection imaging in animal model	220
		Other Radiopharmaceuticals		
human polyclonal immunoglobulin (HIG)	nonspecific	^{99m}Tc, ^{111}In	inflammation/infection imaging	221−225
fluorodeoxyglucose (FDG)	activated lymphocytes, monocytes, and granulocytes	^{18}F	imaging in animal model and humans for inflammatory disorders such as lymphoma, vasculitis, sarcoidosis, rheumatoid arthritis, Alzheimer's and Parkinson's disease, etc., and in infections such as osteomyelitis, spondylodicitis, prosthetic joint infection, etc.	226−230
^{67}Ga-citrate	transferrin receptors (CD71)	^{67}Ga	imaging in animal tumor model and imaging of fever of unknown origin in HIV patients	231−233
human autologous leukocytes	active migration in inflammatory lesion	^{99m}Tc-HMPAO, ^{111}In, ^{18}F	acute inflammation imaging	234−238
albumin nanocolloids	nonspecific extravasation	^{99m}Tc	rheumatoid arthritis, and other inflammatory lesion imaging	239−241

Table 4. Continued

radiopharmaceutical	target	isotopes	application in molecular imaging	ref
JOO1X	CD11b, CD14 (macrophages, monocytes)	^{99m}Tc	arthritis, chronic berilliosis, and other inflammatory lesions imaging in animal model	242−244
octreotide (octreoscan)	somatostatin receptor	^{111}In, ^{123}I, ^{99m}Tc	imaging of granulomatous and chronic inflammation	245−252
liposomes	cells of reticulo-endothelial system	^{111}In, ^{99m}Tc	small animal models of osteomyelitis, experimental colitis, and focal infection	253−259
biotin	nonspecific extravasation	^{111}In	osteomyelitis and endocarditis imaging	260−263
2′-fluoro-5-[^{124}I]iodo-1-β-D-arabinofuranosyluracil (^{124}I-FIAU)	herpes simplex virus thymidine kinase (HSVtk)	^{124}I	herpes virus infection imaging in animal model	264, 265
9-[(3-[^{18}F]fluoro-1-hydroxy-2-propoxy)methyl]guanine (^{18}F-FHPG)	herpes simplex virus (HSV)	^{18}F	herpes simplex encephalitis in animal model	266
9-[4-[^{18}F]fluoro-3-(hydroxymethyl)butyl] guanine (^{18}F-FHBG)	herpes simplex virus (HSV)	^{18}F	herpes simplex encephalitis in animal model	267
(*R*)-*N*-methyl-*N*-(1-methylpropyl)-1-(2-chlorophenyl)isoquinoline-3-carboxamide (^{11}C-PK11195)	peripheral benzodiazepine receptors (PBR)	^{11}C	imaging of HSV encephalitis, Rasmussen's encephalitis, AIDS patients	268−270

[a] IL1RI, IL1RII, TNF-R1, TNF-R2: receptor types I and II. Abbreviations: B = B lymphocytes; Ba = basophils; EGFR = epidermal growth factor receptor; Ep = epithelial cells; En = endothelial cells; Fi = fibroblast; Gr = granulocyte; He = haematopoietic cells; HP = haematopoietic precursor; Ke = keratinocyte; Lym = lymphocytes; Mo = monocytes; Mϕ = macrophage; T = T lymphocytes; N = neutrophil; NC = neoplastic cells; NK = natural killer cells; SMS = smooth cell muscle.

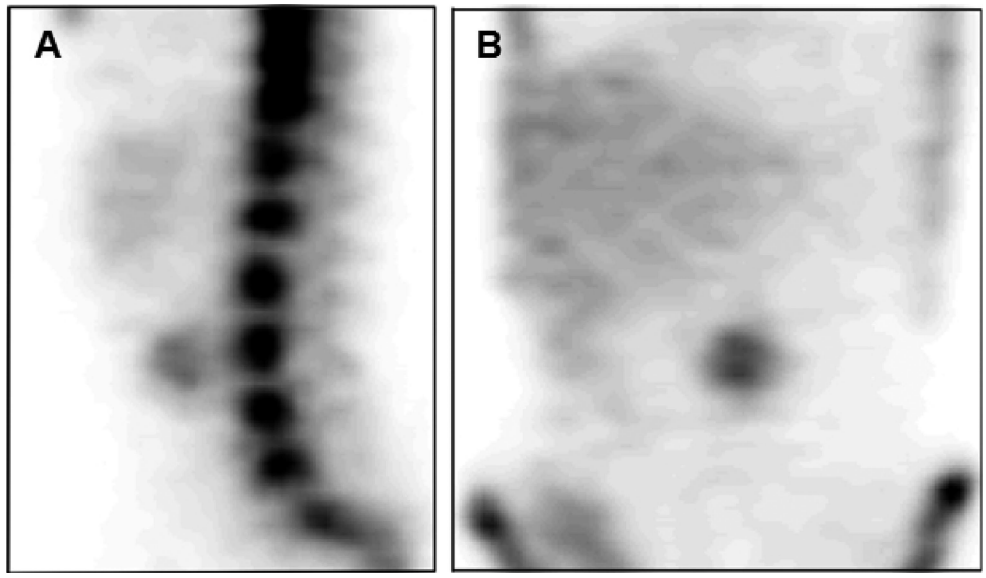

Figure 5. (A) Sagittal and (B) coronal views of the abdominal region in a patient with suspected vascular graft infection, 4 h after i.v. administration of ^{99m}Tc-scintimun (antigranulocyte antibody). Images show physiological uptake in the bone marrow and a site of pathological uptake in correspondence with an infected pseudoaneurysmal of the descending carotid (courtesy of Dr. J. Meller, Germany).

specificity of only 56% for reasons mentioned before. Another group performed an investigation in 25 diabetic patients with 31 sites of suspected pedal osteomyelitis to compare the utility of combined sulesomab/bone scan versus combined bone/gallium scan.[276] This study showed the sensitivity and specificity of sulesomab/bone scan were 67% and 85%, whereas the sensitivity and specificity of bone/gallium scan were 44% and 77%, respectively. Another study demonstrated the utility of ^{99m}Tc-labeled antigranulocyte mAb scintigraphy for the diagnosis of patients with infective endocarditis.[277] Scintigraphy was found to be 100% sensitive and 82% specific, when used in combination with echocardiography. However, in the study SPECT was more accurate than planar scans. Another study was performed in patients with infected endocarditis using SPECT with the radiolabeled antigranulocyte mAb.[137] Authors reported 71% sensitivity and 94% specificity for the detection, while, together with trans-esophageal echocardiography, it accurately identified all patients with infected endocarditis but missed the diagnosis in patients receiving long-term antibiotic therapy.

Radiolabeled anti-TNF-α mAbs infliximab (Remicade, Centocor) and adalimumab (Humira, Abbott) also demonstrated their prognostic value, to determine the benefit of anti-TNF-α therapy, in patients with Crohn's disease (CD) and arthritis patients. A recent study was performed on 10 patients with active Crohn's disease with ^{99m}Tc-labeled anti-TNF-α mAb (^{99m}Tc-infliximab), to detect the presence of TNF-α within the gut mucosa of patients.[106] In the study, radiolabeled mAb scintigraphy showed the presence of little TNF-α in the affected bowel of patients with active CD; therefore, authors concluded that the clinical benefit that patients have from anti-TNF-α mAb therapy is unlikely the consequence of a local reduction of TNF-α, and maybe the mechanism of action of anti-TNF-α mAb in therapeutic doses needs further investigation. This kind of scintigraphy also holds the promise for therapy decision making and disease follow-up, with a view to assessing whether the therapeutic target receptor/molecule is present in the lesion, before using the same unlabeled monoclonal antibody for therapeutic purposes. Another study with anti-TNF-α mAb (^{99m}Tc-infliximab) was performed by Conti et al., in patient with arthritis to assess the degree of TNF-α mediated inflammation in the affected joints.[104] Patients underwent scintigraphic examination with ^{99m}Tc-infliximab before and 4 months after the intra-articular Infliximab therapy. After the injection of ^{99m}Tc-infliximab (15 mCi), planar images of the inflamed

joint were acquired at 6 and 24 h. Scintigraphy showed intense accumulation of ^{99m}Tc-infliximab in the affected knee, probably reflecting the high levels of intralesional TNF-α. These preliminary studies in humans showed the specific targeting of this radiopharmaceutical in the inflamed joints. Moreover, these studies also demonstrate that the selection of the candidates for infliximab therapy and prediction of therapy response could be possible by using ^{99m}Tc-infliximab scintigraphy before initiating anti-TNF-α therapy. Also, another anti-TNF-α monoclonal antibody (adalimumab) was labeled with ^{99m}Tc and used for the molecular scintigraphic imaging in rheumatoid arthritis (RA) patients.[107,108] Preliminary published results with this radiolabeled mAb showed that arthritis patients with painful joints but negative (low target to background (T/B) ratio) at pretherapy scintigraphy with ^{99m}Tc-anti-TNF-α mAb do not benefit from unlabeled anti-TNF-α mAb therapy, whereas patients with positive (high T/B ratio) at pretherapy scintigraphy in joints showed most clinical benefit from therapy.[108] This kind of scintigraphy thereby offers the possibility to perform "evidence-based biological therapy" of autoimmune inflammatory diseases. The results obtained so far are highly encouraging and hold promise for therapy decision making and follow-up, with a view to assessing whether an antibody will accumulate in an inflamed joint before using the same unlabeled antibody for therapeutic purposes. This methodology is also known as the "pretherapy receptor mapping approach" for therapy decision making, and this approach may also provide a cost-effective solution for highly expensive biological therapies. A pharmaceutical company (Tecnonuclear, Argentina) has recently produced a good manufacturing practice (GMP) kit for radiolabeling anti-TNF-α mAb that will probably be commercialized.

As far as lymphocyte imaging, in the 1990s, Kinne et al. performed several studies with 99m-technetium-labeled anti-CD4 mAb and its Fab' fragments and demonstrated its specific imaging capability in comparison with radiolabeled nonspecific immunoglobulin and nonspecific mAb, for rheumatoid arthritis patients.[119−121] Yet, unfortunately, even after numerous studies that proved the sensitivity and specificity of this radiopharmaceutical for immunoscintigraphy, this useful technique is not commonly used in clinical practice and until now has remained a research tool inside selected laboratories. Recently, a phase I clinical trial has been performed by a commercial company (Biotectid GmbH, Germany) with a 99m-technetium-labeled anti-CD4 mAb fragment (EP 1645), showing very promising results for the immunoscintigraphy of rheumatoid arthritis patients.[141]

The use of a ^{99m}Tc-labeled mAb (OKT3) has been described in patients with rheumatoid arthritis;[116] in this study, the accumulation of the radiolabeled mAb correlated with the intensity of the inflammation, and also detected active joints that were clinically asymptomatic. The use of this antibody was, however, associated with side effects due to the release of cytokines following binding of the mAb to the CD3 molecule. In a recent study, ^{99m}Tc labeled anti-CD3 mAb has been successfully used for monitoring synovitis in 38 patients with RA, without causing any side-effect.[117]

Although radiolabeled mAbs are an interesting class of radiopharmaceuticals, they show some disadvantages, like any other radiopharmaceutical, that are mainly due to their high molecular weight.[101] Indeed, a radiopharmaceutical with low molecular weight may show nonspecific accumulation in inflammed sites just because of passive diffusion into perivascular space in inflamed tissues with increased blood flow, capillary exudate, and edema. On the other hand, if the molecular weight is too high (like most mAbs), sequestration by reticulo-endothelial cells and liver Kupfer cells may occur, and little mAb remains available for binding to the target. In both cases, we have a reduction in specificity and diagnostic accuracy. The diagnostic use of radiolabeled antibody fragments (e.g., Fab' or $F(ab')_2$) with intermediate molecular weight (40−80 kDa) could overcome these limitations; indeed, they show a lower immunogenicity, a more rapid blood clearance, a higher accumulation in inflamed tissues, and possibly a higher specificity, because of the absence of the Fc portion that nonspecifically binds the Fc receptor expressed on monocytes. However, often mAb fragments have an intrinsically lower affinity for the target antigen, and this may increase nonspecific accumulation due to nonspecific capillary extravasation.

4.6. Cytokines, Chemokines, Interferons, and Growth Factors

Radiolabeled cytokines, chemokines, interferons, and growth factors provide a novel mean for the characterization of different cell populations and their receptors in inflammatory and/or infectious lesions. Cytokines are proteins or glycoproteins and members of a family of overlapping and interdependent molecules with important roles in the homeostatic control of the immune system and other organs, in physiology and pathology. Most cytokines are between 6 and 25 kDa, and they are often similar in size, charge, and glycosylation.

The molecular weight is therefore lower than that of mAb and Fab fragments, but they do not show significant nonspecific accumulation in the inflamed site. The reason for this excellent performance as radiopharmaceuticals depends on their rapid blood clearance and high binding affinity to specific receptors.

The major sources of cytokines are T cells and macrophages, but their production varies depending on the individual cytokine. For example, Interleukin-2 (IL-2) is produced mainly by activated T cells, whereas Interleukin-1 (IL-1) can also be produced by macrophages, endothelial cells, large granular lymphocytes, fibroblasts, epithelial cells, astrocytes, keratinocytes, and osteoblasts. Cytokines act via the interaction with specific cell surface receptors expressed on known cell populations; cytokine receptors, usually of high affinity, are generally expressed at low levels on resting cells, but their expression can be up-regulated during activation. In summary, labeled cytokines have optimal characteristics as radiopharmaceuticals as they are characterized by (i) low molecular weight as compared to other proteins, (ii) rapid half-life and plasma clearance, (iii) high-affinity binding to specific receptors, (iv) ready availability by DNA recombinant technique, and (v) human recombinant origin and lack of immunogenicity.

IL-2 has a very high affinity for IL-2 receptors (hetero trimers of an α, β, and γ subunit, named CD25, CD122, and CD132, respectively) expressed by activated lymphocytes during inflammation. IL-2 is a growth-promoting factor of T-lymphocytes and has effects on a wide variety of cells such as CD4+ T cells, CD8+ T cells, B cells, and natural killer cells. Most prominently, it is important in T cell activation and inflammatory consequences thereof.[278] Both ^{99m}Tc- and ^{123}I-labeled IL-2 have been successfully used

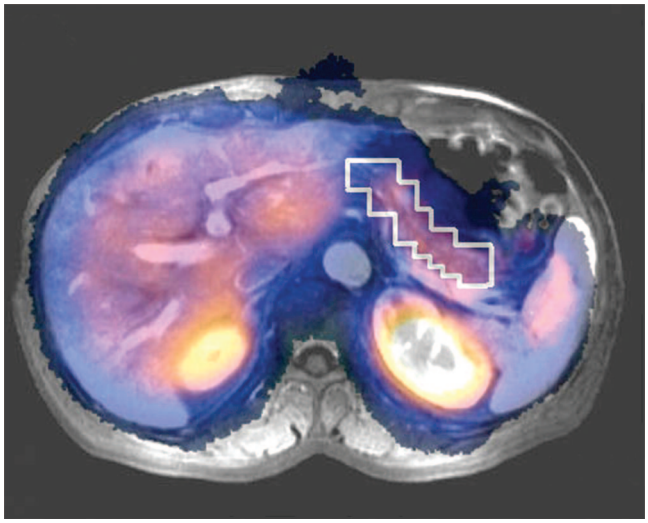

Figure 6. NMR and SPECT fusion images (transaxial view) of the pancreas in a patient with latent autoimmune diabetes in adults (LADA) 1 h after i.v. administration of ^{99m}Tc-IL-2. The image shows uptake in the pancreatic region, indicating the presence of activated T-lymphocytes in the endocrine pancreas (insulitis).

for imaging lymphocytes in several autoimmune and inflammatory diseases characterized by a chronic lymphocytic infiltration, such as Crohn's disease, celiac disease, type-1 diabetes, and autoimmune thyroid diseases.[147−159,279]

In a recent study, in patients with Hashimoto's thyroiditis, it was possible to highlight the presence of activated lymphocytes by γ-camera imaging using ^{99m}Tc-labeled IL-2. No correlation was detected between the degree of thyroid accumulation of ^{99m}Tc-IL-2 and the autoantibody titer. This interesting finding suggests that the humoral immunity and cell-mediated immunity are not directly related, and that both should be evaluated for the assessment of disease activity. Another study in asymptomatic sjogren syndrome patients, salivary gland scintigraphy by ^{99m}Tc-IL-2, showed clear pathological uptake in patients with biopsy proven infiltrated glands. Also, in this study, no correlation was found with anti SSA or anti SSB antibodies and the degree of IL-2 uptake in glands, indicating that t-cell mediated phenomena are not always coupled with B-cell mediated phenomena.[280]

Iodine-123-labeled IL-2 has also been tested in animal models of human autoimmune diabetes, in Bio Breeding Worcester (BB/W) rats and in Non Obese Diabetics (NOD) mice. These studies in prediabetic animals have shown that there was uptake and retention of ^{123}I-IL-2 in the pancreatic region between 5 and 15 min after injection. These data were confirmed by various experiments such as single organ counting after sacrifice of animals. Ex-vivo autoradiography confirmed that radioactivity was associated with infiltrating cells bearing IL-2R. Histological examination of pancreata revealed a positive correlation between radioactivity and the degree of lymphocytic infiltration. A preliminary study with radiolabeled IL-2 in high-risk subjects showed that this technique may be useful for early diagnosis of pancreatic infiltration and possibly for monitoring the efficacy of preventive treatments (Figure 8). A study performed in newly diagnosed type 1 diabetes using ^{99m}Tc-IL-2 showed that the imaging of inflammation in the pancreas at diagnosis (a sign of insulitis and an indirect sign of the presence of residual β-cell mass) can be detected and be a marker to identify

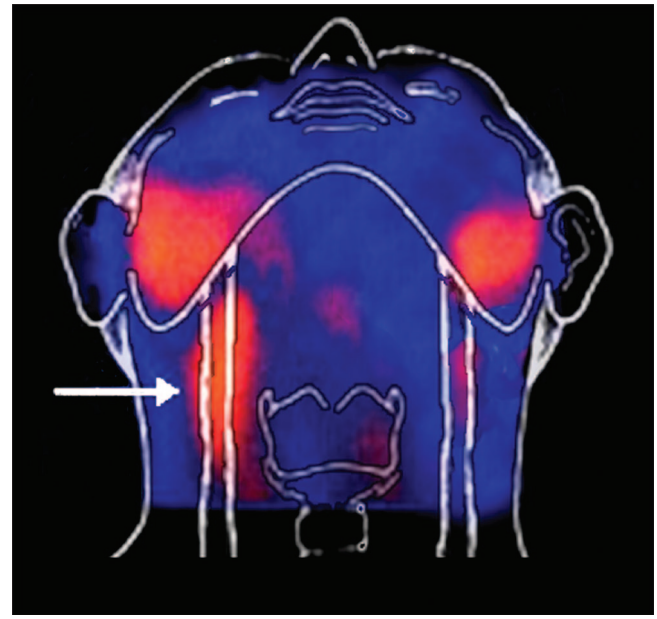

Figure 7. Antero-posterior images of the head and neck of a patient with bilateral carotid atherosclerotic plaques, 1 h after i.v. administration of ^{99m}Tc-IL-2. The image shows uptake of the radiopharmaceutical only in the right plaque (arrow), indicating the presence of active T-lymphocytes in the plaque, a sign of vulnerability. No significant uptake is detectable in the left plaque, indicating that this is at lower risk of rupture.

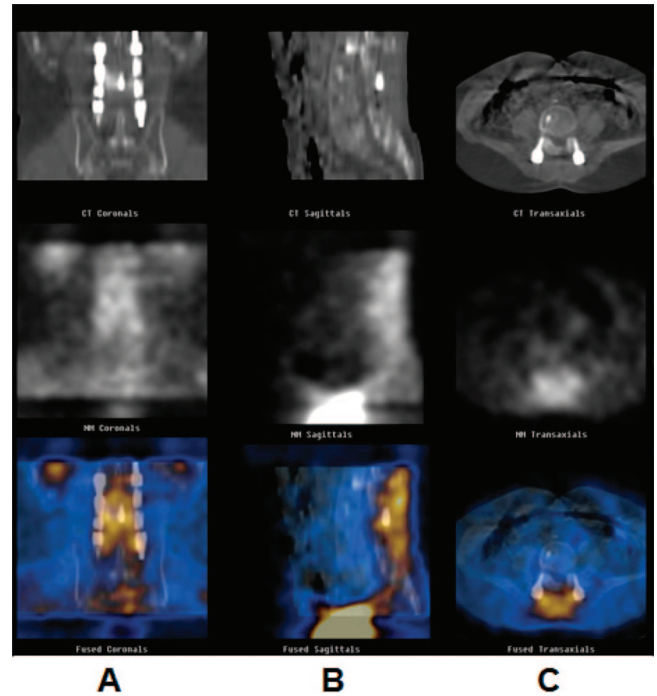

Figure 8. (A) Coronal, (B) sagittal, and (C) transaxial sections of the leg as detected by CT (upper panel), SPECT (middle panel), and fusion images (lower panel), in a patient with postsurgical spondylodiscitis after i.v. injection of ^{111}In-biotin. The images show intense pathological uptake by the vertebral body, as a sign of bacterial infection (courtesy of Dr. E. Lazzeri, Italy).

those patients to be treated with nicotinamide (50 mg/kg) to protect the residual β-cell mass present at diagnosis. Similar findings were previously reported using radiolabeled nonspecific human immunoglobulin-G (HIG) showing uptake in the pancreas of approximately 50% of newly diagnosed type 1 diabetic patients,[281] probably as a consequence of the

presence of immune complexes or secondary to increased vascular permeability. This may help identify patients who may benefit from adjuvant immunotherapy at the time of diagnosis, with an aim to induce clinical remission.

Radiolabeled IL-2 was successfully used also to detect inflamed atherosclerotic carotid plaques, those most vulnerable to rupture and prone to cause strokes.

Indeed, high serum IL-2 levels are associated with increased carotid artery thickness, a predictor of stroke and vascular disease.[282] ^{99m}Tc-IL-2 was therefore also used for imaging carotid atherosclerosis in humans (Figure 7). Fourteen patients (16 plaques) eligible for endarterectomy underwent ^{99m}Tc-IL-2 scintigraphy before surgery. Another nine patients (13 plaques) received atorvastatin or a standard hypocholesterolaemic diet, and scintigraphy was performed before and after 3 months treatment. ^{99m}Tc-IL-2 accumulated in vulnerable carotid plaques and the accumulation correlated with the amount of IL-2R+ cells within the plaque (measured ex vivo by histology). Also, the amount of ^{99m}Tc-IL-2 within the plaque was influenced by lipid-lowering treatment with a statin.[157] ^{99m}Tc-IL-2 is a very promising tracer that could provide useful information for the selection of infiltrated vulnerable plaques at risk of rupture. There are no significant biological side effects at the low dose used for imaging purposes. However, it is not yet commercially available, and a major drawback, of in house preparation, is the complexity of the labeling procedure, as it has been described.[279]

^{123}I-IL-12 was successfully tested in a mouse model of autoimmune colitis and could be a possible alternative to IL-2.[279] A pharmaceutical company (POLATOM, Poland), recently, prepared an IL-2 radiolabeling kit, which hopefully will soon be commercially available for the diagnosis of patients with inflammatory autoimmune diseases.

Other cytokines have been labeled with iodide, but the applications remain uncertain. ^{125}I-IL-3 has only been tried for in vitro binding studies without further application in humans. ^{123}I-IL-6 was compared to iodinated IL-1. The degree of IL-6 uptake in different animal models of acute inflammation was much lower than IL-1.[166] Therefore, the use of radioiodinated IL-6 was abandoned.

IL-1 is also a proinflammatory cytokine with a high affinity to a specific receptor expressed on monocytes and lymphocytes. It was one of the first cytokines developed for imaging acute inflammation.[142−146] Labeled with ^{123}I or ^{125}I, IL-1 was tested in different animal models of infection or sterile inflammation.[283] There was a highly specific uptake at the infection site, but due to side effects (hypotension, headache) even in low doses, the radioiodinated IL-1 has never been tried in humans.

Consequently, a radiolabeled IL-1 receptor antagonist (IL-1ra) was developed, with the same binding affinity for IL-1 receptors but without any biological activity. However, in mice the abscess uptake of IL-1ra was much lower than that of IL-1 because of interaction with serum proteins.[145] This was also seen in a rabbit infection model; however, the observation of radiolabeled IL-1ra in the infectious focus was important.[142] After these results, ^{123}I- IL-1ra has been studied in patients with rheumatoid arthritis and to assess whether it is suitable for scintigraphic visualization of synovitis. ^{123}I-IL-1ra was able to image inflamed joints, but autoradiographic studies did not indicate that the joint accumulation of radiolabeled IL-1ra was due to specific IL-1 receptor targeting.[146] The uptake behavior was similar to those of nonspecific labeled agents, so it seems that radiolabeled IL-1ra is not suitable for scintigraphic detection of inflammation.

Chemokine receptor ligands have also been labeled for in vivo imaging of inflammatory sites. Studies have extensively investigated IL-8 in the preclinical setting. IL-8 is a member of the CXC family of chemokines, which binds with high affinity to the type I and II CXC receptors abundantly expressed on neutrophils and monocytes. Radiolabeled IL-8 reveals high and specific accumulation at the focus of acute infection within a few hours after injection both in animals and in humans.[160−164,284−286] In a recent study, Bleeker-Rovers et al. evaluated ^{99m}Tc-labeled IL-8 in 20 patients with various suspected localized infections, including osteomyelitis, liver abscess, joint prosthesis infection, and soft tissue infections.[165] This study demonstrated a specific accumulation of this radiopharmaceutical in 10 of 12 patients with infection at 4 h after injection, without any significant side effects.

Monocytes and macrophages, predominant cell types in acute and chronic inflammation, are attracted to and activated by monocyte chemotactic peptide-1 (MCP-1). *^{125}I-MCP-1* has been tested in normal mice and in atheroma-rich rabbits, and the uptake was correlated with the number of macrophages per unit area.[287] In another study in rats, *^{99m}Tc-MCP-1* was found to localize only in zones of subacute inflammation, reflecting the density of macrophages and monocytes.[172] Radiolabeled MCP-1 may be a useful tracer for imaging monocyte/macrophage-rich atherosclerotic lesions in the stage of subacute inflammation.[168,169]

^{125}I-labeled tumor growth factor beta (TGF-β) has been used for the study of angiogenesis and radiolabeled epidermal growth factor (EGF) has been used for the study of metastatic lymph nodes, for imaging breast cancer and for the study of skin wounds.[171−174] ^{123}I-interferon-gamma has been proposed for investigation of lung disease.[170]

In conclusion, most of these labeled cytokines and chemokines have been tested only in preclinical setting. Radiolabeled IL-2 is the only cytokine that showed optimal characteristics and has been deeply investigated in several human diseases. The message that can be drawn from these studies is that small biologically active proteins (hormones, cytokines, chemokines, and growth factors) are good candidates as imaging probes for inflammation and infection because of their human recombinant origin, high receptor affinity, and fast blood half-life, which increase the target to background radioactivity ratio. However, most have pharmacological effects when administered i.v. and are not applicable to humans. They remain of pivotal interest for in vivo histological characterization of inflamed tissues but may have a commercial interest only if they can provide relevant diagnostic information and may guide physicians in therapy decision and follow-up.

4.7. Other Peptide Radiopharmaceuticals

As compared to larger molecules, such as mAbs, chemokines, and cytokines, small peptides are rapidly taken up and retained in target tissues, in accordance with the usually rapid plasma clearance due to the renal excretion. They also generally show high receptor binding affinity and are internalized into the cells. Other important features of small proteins include the possibility of modification of the excretion route, modifiable biologically activity, and lack of immunogenicity. Radiolabeling of peptides is usually performed using a bifunctional chelating agent. For both monoclonal antibodies and small peptides, the choice of

radioisotope and radiolabeling method can play a major role in the overall in vivo distribution and in the target to nontarget ratios achieved.

The somatostatin analogue ^{111}In-labeled octreotide (Octreoscan) was officially introduced in 1994, and its use to visualize various somatostatin receptor-positive tumors and tissues is widely accepted. Somatostatin receptors are expressed on normal and activated lymphocytes and macrophages. A study was performed with ^{111}In-octreotide in patients with sarcoidosis, aspergillosis, tuberculosis, and Wegener's granulomatosis. Whole body images were acquired after administration of ^{111}In-octreotide. In this study, granuloma localizations were clearly visualized in all patients studied. Binding of ^{111}In-octreotide at sites of granulomatous inflammation has also been verified by in vitro autoradiography.[246] In contrast to the potential of octreotide for detection of chronic inflammation, studies in animal models of *Staphylococcus aureus* induced foci in rats revealed that ^{111}In-octreotide is not suitable for the detection of experimental abscesses, as lower accumulation than control ^{111}In-HIG was noted with no retention with time.

A recent study has described the use of a new somatostatin analogue ^{99m}Tc-HYNIC-tyr(3)-octreotide for the diagnosis of the state of activity in patients with rheumatoid arthritis and secondary Sjogren syndrome before and after treatment with infliximab. Results showed that inflamed parotid glands could be diagnosed by this radiopharmaceutical. Inflamed joints were also detected in patients with active rheumatoid arthritis.[106] Interestingly, after treatment with infliximab, normalization of the uptake in most inflamed joints was noted but not in salivary glands, probably reflecting the different nature of the two diseases.

^{111}In-pentetreotide has been used in imaging of Graves' disease, obtaining different contrasting results: a few studies have reported that this radiopharmaceutical accumulates in the thyroid and in the retro-orbital space in patients with exophtalmos, and there is a positive correlation with the activity of disease,[288,289] in disagreement with other authors.[290,291] Further studies are required to help elucidate the potential value of this compound in Graves' disease.

A hypothesis has been formulated on mechanisms of accumulation of octreotide: uptake occurs in the early phases of Graves' ophthalmopathy when active infiltration is present; in the later stage of the disease, there is fibroblastic activity with subsequent fibrosis in the retro-orbital region without expression of somatostatin receptors.[292,293]

A study was performed with ^{111}In-pentetreotide orbital scintigraphy on patients with severe ophthalmopathy caused by Graves' disease. Authors concluded that ^{111}In-pentetreotide scintigraphy allows one to select patients for octreotide therapy, which seems to be adequate in active, moderately severe thyroid eye disease, especially when it involves soft tissues.[294,295]

Indeed, to date, octreotide scintigraphy in inflammatory diseases is only used for therapy follow-up in those patients treated with unlabeled somatostatin analogues.

4.8. Antibiotics and Other Bacteria Imaging Agents

Imaging agents that target cell receptors expressed on the cells infiltrating inflamed tissue, which are recruited during the inflammatory response, and accumulate in the focus due to a common feature of infection and inflammation, often cannot be used to differentiate between infection and inflammation. Agents that specifically target the infectious organism (e.g., bacteria, fungi, or viruses) have the potential to distinguish microbial from nonmicrobial inflammation. During the past decade, a number of agents have been proposed, which aim to specifically visualize infectious foci by targeting the infectious organism. In the search for an infection diagnostic agent, antibiotic radiolabeling was first introduced by Solanki et al. in the early 1990s.[296] Ideally, the radiolabeled antibiotic should be metabolized and specifically incorporated by the microorganisms present in the infection, so that accumulation of radioactivity is directly proportional to the number of microorganisms. Several antibiotics have been radiolabeled so far, such as ciprofloxacin (Infecton), sparfloxacin, ceftizoxime, isoniazid, ethambutol, fluconazole, enrofloxacin, levofloxacin, norfloxacin, and ofloxacin, and most of these are members of the quinolones class.

The most exhaustively studied radiopharmaceutical in this group is ^{99m}Tc-ciprofloxacin, a synthetic broad spectrum fluoroquinolone antibiotic that binds to prokaryotic topoisomerase IV and DNA gyrase, expressed in proliferating bacteria.[297,298] ^{99m}Tc-labeled ciprofloxacin has been particularly evaluated for the diagnosis of osteomyelitis. Several studies published, until now, showed a mixed overview for its appropriate use in such patients.[191,207,299−301] A large multicenter study was coordinated by the International Atomic Energy Agency (IAEA) to evaluate the efficacy of ^{99m}Tc-ciprofloxacin for imaging infections. The overall sensitivity and specificity for infection, in a total of 879 patients, were reported to be 85.5% and 81.6%, respectively.[196] The sensitivity and specificity varied according to the type of infection imaged; for example, the sensitivity and specificity in prosthetic joint infections were 96% and 91%. However, in an animal model of infected and uninfected knee prosthesis and in patients with osteomyelitis or with septic arthritis, specificity of ^{99m}Tc-ciprofloxacin for bacterial infection was much lower than that previously mentioned.[205,206] Other studies have also confirmed a low specificity for this radiopharmaceutical, and overall there is not convincing evidence of its efficacy. A new kit formulation for ^{99m}Tc-ciprofloxacin (Infecton) has been produced by Draximage Inc. (Kirkland, Canada), and this preparation is currently in phase II clinical trials.

Several antibiotics including ciprofloxacin, fleroxacin, lomefloxacin, and trovafloxacin have also been radiolabeled with ^{18}F for PET imaging.[207,218−220] Most of these antibiotics are members of the fluoroquinolones class that inhibit bacterial DNA gyrase and topoisomerase IV. However, only for ^{18}F-fleroxacin and ^{18}F-trovafloxacin, the evaluation of the tracer in an animal model of infection was published.[220,302] Both labeled antibiotics were investigated in rat and rabbit animal models that were injected with *E. coli* in a thigh muscle. ^{18}F-fleroxacin was administered at a dose of 10 mg/kg in both species, and tissue distribution was determined by ex-vivo biodistribution or PET imaging.[303] These studies showed that sufficiently high drug concentrations could be obtained in all extra-cranial tissues to achieve antimicrobial activity. The drug concentration in the brain was low, suggesting that CNS toxicity is unlikely. In both species, uptake of the radiolabeled drug in the infected muscle was not significantly different from uptake in the control muscle, although it should be emphasized that a pharmacological concentration of the labeled drug was used and not a tracer dose. Similar results were obtained in a comparable study

with ^{18}F-trovafloxacin.[220] Overall, these animal studies and also studies in humans suggest that PET imaging of radiolabeled antibiotic is a promising noninvasive tool for determining pharmacokinetic parameters of the drug; however, still more investigations are required to confirm its utility in clinical setting.

A cationic human antimicrobial protein fragment, ubiquicidin 29−41 (UBI 29−41) (MW 1.69 kDa) with the aminoacid sequence Thr-Gly-Arg-Ala-Lys-Arg-Arg-Met-Gln-Tyr-Asn-Arg-Arg, and 6 positively charged residues (5 Arg +1 Lys), has been labeled with 99m-technetium. In animal studies, ^{99m}Tc-UBI 29−41 showed rapid visualization of infection with gram-positive and gram-negative bacteria, but little accumulation was found in sterile inflammation processes. Furthermore, a very recent study described the quantitative uptake of ^{99m}Tc-UBI 29−41 in rabbits with *S. aureus* infections during treatment with ciprofloxacin. The results showed that the uptake of the radiotracer was significantly decreased after treatment and was proportional to the number of bacteria, suggesting that the tracer might be used for monitoring the efficacy and duration of treatment.[193] Meléndez-Alafort et al. evaluated this peptide in 6 children with suspected bone infection (confirmed by ^{67}Ga-citrate scan but not microbiologically). The agent cleared rapidly from the body (85% in 24 h); however, uptake in the infectious lesions was low, and target-to-background ratios were 2.18 ± 0.74.[195]

Avidins are a family of proteins present in the eggs of amphibians, reptiles, and avians; streptavidin, produced by *Streptomyces avinii*, is also part of the same family. Both avidin and streptavidin (MW 64−60 kDa) have four sites for the binding of biotin with very high affinity ($K_d = 10^{15}$). Biotin, also known as vitamin H, is a compound of low molecular weight that can be radiolabeled with a variety of different radiometals. The avidin−biotin system has been used for the in vivo labeling of mAbs for the radioimmunodiagnosis and therapy of tumors. Radiolabeled biotin readily accumulates in the inflamed tissue where it binds irreversibly to streptavidin, while nonbound biotin is rapidly cleared through the kidneys with minimal accumulation in normal tissues. Although they are of heterologous origin and can cause immune responses, there is no evidence to date that avidin or streptavidin are toxic. The use of the avidin−biotin system has been studied in animal models of acute infection where it accumulated in the infected focus more than ^{111}In-HIG; moreover, it was also found to be very specific in the patients with suspected vertebral osteomyelitis, vascular graft infection, and spondylodiscitis (Figure 6).[260−263] The major advantages of this approach are increased concentration of the radiotracer at the target tissue, a good target to background ratio, and early acquisition of images.

In conclusion, radiolabeled antibiotics opened a new and promising approach in the search of an infection specific imaging agent, but the published results are controversial, and still more studies are required to understand the efficacy of this radiopharmaceutical in differentiating infection foci from sterile inflammation.

4.9. Other Radiopharmaceuticals for Imaging Inflammation/Infection

4.9.1. ^{99m}Tc- or ^{111}In-Labeled HIG

Human polyclonal immunoglobulin-G (HIG) is a nonantigen specific IgG antibody that can be labeled with ^{99m}Tc or ^{111}In and has been proposed for the detection of acute and subacute inflammation/infections; because HIG are of human origin, they do not produce allergic reactions; furthermore, they are commercially available as kits. The mechanisms of HIG uptake in inflamed tissues are not yet completely elucidated. Among various hypotheses, the increase of vascular permeability seems to be the main mechanism of their accumulation. Nevertheless, alternative binding mechanisms such as to the Fc receptor expressed by infiltrating cells, to the extracellular matrix proteins, and to bacteria have been described. HIG have proven to be very useful in lung inflammation imaging, for the detection of joint and bone inflammations and infections, and the study of fever of unknown origin.[221−225] In a very interesting comparative study in patients with RA, ^{99m}Tc-HIG, ^{99m}Tc-nanocolloid, and ^{99m}Tc-HMPAO-labeled leucocytes showed a similar diagnostic accuracy.[242] In some countries, ^{99m}Tc-HIG are still routinely used as the radiopharmaceutical for imaging infections.

4.9.2. ^{67}Ga-Citrate and ^{68}Ga-Citrate

^{67}Ga-citrate was discovered in 1971, for imaging infection and inflammation. ^{67}Ga-citrate binds in ionic form to circulating transferrin as an analogue of iron. It uses transferrin receptors (CD71) to access the cell and then becomes highly stable within the cells. It is still the best sold radiopharmaceutical for imaging infections in the world despite its very low specificity. During acute inflammation, ^{67}Ga-citrate extravasates at the site of inflammation due to the locally enhanced vascular permeability, where it binds with high affinity to lactoferrin excreted by leukocyte or to siderophores, produced by microorganisms grown in a low-iron environment. Approximately, 25% of the total injected dose is excreted through the urinary system, and the rest is retained in bone, bone marrow, liver, and soft tissues. This radiopharmaceutical is mainly used for the study of chronic osteomyelitis, lung infection, and for FUO in HIV patients.[232] Indeed, this technique could be very helpful for scintigraphic imaging of FUO patients, due to its diagnostic potential for both chronic and acute inflammations,[304] albeit not so many well designed studies are performed. A study was performed with ^{67}Ga-citrate scintigraphy in 145 patients with FUO; final diagnosis was established in 68% of total patients.[305] In this study, 43% scans were normal, and 57% were abnormal; only 51% of abnormal scans (29% of total scans) were considered useful in the diagnosis. Thus, 49% of abnormal scans were considered noncontributory in the diagnosis. However, the radiopharmaceutical has a long physical half-life (78 h) and high energy γ radiation, which are unfavorable characteristics for scintigraphic imaging and cause an increased radiation absorbed dose.[306,307]

The same authors have therefore started using the PET equivalent for Ga-citrate, the ^{68}Ga-citrate, with excellent detection of inflammatory and infective sites. Despite that more studies are required to confirm preliminary finding, these results deserve a comment.[308] It was really unexpected that using ^{68}Ga-citrate-PET the optimal time for infection imaging was within few hours after injection and that target-to-background ratio was clearly much higher than using ^{67}Ga-citrate-SPECT. By contrast, using ^{67}Ga-citrate-SPECT, the best target-to-background ratio is normally achieved after 48−72 h. Therefore, the change of isotope in this radiopharmaceutical not only has improved image resolution and sensitivity (mainly because PET is more resolute than

Table 5. Results of Meta-analysis Performed on All Published Papers between 1990 and 2005 in the Field of Radiopharmaceutical for Imaging Infection[a]

	sensitivity (%)	specificity (%)	accuracy (%)
^{99m}Tc-WBCs			
occult infections ($n = 100$)	89.0	94.0	**92.0**
diabetic foot infection ($l = 283$)	85.8	84.5	85.9
infections of peripheric bone and prosthetic joint implants ($l = 1453$)	89.0	89.1	89.1
prosthetic graft infection ($s = 434$)	97.7	88.6	**94.6**
^{111}In-WBCs			
inflammatory bowel diseases ($n = 682$)	87.9	93.4	**91.7**
appendicitis ($s = 128$)	89.5	95.0	**92.9**
prosthetic graft infection ($s = 397$)	84.1	79.4	81.5
^{67}Ga-Citrate			
occult infection ($n = 310$)	87.0	81.0	85.0
infections of peripheric bone and prosthetic joint implants ($l = 569$)	70.1	81.8	78.2
^{18}F-FDG-PET			
fever of unknown origin ($n = 168$)	78.0	59.0	77.0
occult infection ($n = 112$)	95.0	88.0	**92.0**
infections of peripheric bone and prosthetic joint implants ($l = 413$)	94.1	87.3	**91.9**
^{99m}Tc-MDP Bone Scan			
diabetic foot infection ($l = 719$)	90.3	46.4	65
infections of peripheric bone and prosthetic joint implants ($l = 1527$)	85.4	75.2	75.5
^{99m}Tc/^{111}In-HIG			
infections of peripheric bone and prosthetic joint implants ($l = 537$)	95.2	78.7	86.0
^{99m}Tc-mAb BW 250/183			
fever of unknown origin ($n = 115$)	66.0	92.0	78.0
infective endocarditis ($l = 194$)	65.3	86.0	79.9
infections of peripheric bone and prosthetic joint implants ($l = 258$)	81.7	80.1	83.2
appendicitis ($s = 629$)	90.8	87.3	89.0

[a] Abbreviations: n = number of patients; l = number of lesions; s = number of scans. Accuracy >90% is shown in bold. Only results with more than 100 patients/lesions are mentioned in this table. Complete meta-analysis results are published in refs 330, 363−365.

SPECT) but has improved biodistribution and possibly affinity, and therefore specificity. A similar finding has been described for several other peptide radiopharmaceuticals but never for a small molecule such as citrate.

4.9.3. Radiolabeled Autologous Leukocytes

Radiolabeled leukocytes are considered as the "gold standard" method for imaging infections in nuclear medicine and can be labeled using ^{111}In-oxine or ^{99m}Tc-HMPAO (see Table 5). These autologous leukocytes are characterized by high specificity, because they only accumulate as a consequence of active migration into inflamed tissues.[234−238] After intravenous injection, radiolabeled leukocytes show rapid clearance from lungs and blood-pool, with progressive migration into spleen, liver, and bone marrow and, of course, in sites of infection where a neutrophilic infiltrate predominates. Radiolabeled leukocytes first adhere to vascular endothelium and then migrate toward the inflammatory focus through endothelium and basal membrane. Thus, this radiopharmaceutical is a specific indicator for leukocytic infiltration. There is only one major possibility of false positivity due to the fact that radiolabeled leukocytes also migrate in activated bone marrow, particularly after inplant of prostheses and in diabetic Charcot foot. In this case, however, a differential diagnosis between expanded bone marrow and infection can be made by using radiolabeled-WBC scintigraphy combined with a bone marrow scintigraphy using ^{99m}Tc-labeled nanocolloids. There is no major kidney, bladder, or bowel excretion shown by ^{111}In-leukocytes, so the whole abdomen presents an excellent field for localization of infections. In contrast, ^{99m}Tc-HMPAO is released from the leukocytes, which starts within a few minutes after administration and is excreted by kidneys up to 7% of the label per hour and mainly by the liver and gut, thus disturbing imaging of abdomen after 3 h. Indium-111 has a long half-life of 67 h and radiation energy of 173 and 247 keV that increases the radiation burden, whereas ^{99m}Tc has a short half-life of 6 h and ideal γ-radiation energy of 140 keV.

Leukocyte labeling must be performed in sterile conditions with a complicated and time-consuming procedure (about 3 h). First, leukocytes are separated from other blood cells before labeling, because ^{111}In/^{99m}Tc-HMPAO being lipophilic, it labels all cell types indiscriminantly, then leukocytes are incubated 15 min with the radiopharmaceutical, then cells are washed by gentle centifugation and finally reinjected into the patient. Recently, the availability of a sterile medical devise for leukocyte labeling in a closed system (Leukokit, GI Pharma, Italy) has highly improved the quality and easiness of the labeling procedure.

Both ^{111}In- or ^{99m}Tc-labeled autologous leukocytes have been successfully used in nuclear medicine for the study of several infectious processes including FUO. A study with ^{111}In-labeled leukocytes in 68 FUO patients demonstrated its 90.5% specificity, 85.1% sensitivity, with 86.8% accuracy.[309] The ^{111}In-leukocyte scintigraphy was helpful in reaching a final diagnosis in 28% of these patients. Another study by MacSweeney et al. in 25 FUO patients with ^{111}In-labeled leukocytes showed that the accuracy did not correlate with symptoms duration, leukocytosis, or clinical suspicion index.[310] The authors found an overall accuracy of 67%, whereas a subgroup of patients with "spontaneous" FUO showed only 52% accuracy; therefore, the authors concluded that ^{111}In-leukocyte scintigraphy "is not particularly useful" in these patients. A study performed by Kjaer et al. in 31 patients with FUO[311] demonstrated that the use of ^{111}In-labeled leukocytes was helpful in the diagnosis of 19% patients, whereas the probability of reaching a diagnosis was

relatively high (71%). Specificity was 83%, sensitivity 75%, positive predictive value 60%, and negative predictive value 90%. CRP (C-reactive protein) level was, however, elevated in all patients with positive scans, but in only one-half of the patients with true-negative scans. Another more recent study by the same authors in 19 FUO patients showed that ^{111}In-labeled leukocytes scintigraphy was 71% sensitive and 92% specific, which was significantly higher than ^{18}F-FDG-PET (50% and 46%, sensitivity and specificity, respectively).[139] In the study, authors concluded that ^{111}In-leukocytes scintigraphy has a superior diagnostic performance as compared to ^{18}F-FDG-PET for diagnosis of a localized infectious/inflammatory or neoplastic cause of FUO. Moreover, most of the data about FDG-PET are published after 2005 and therefore not present in meta-analysis articles until now, and are consequently also not shown in Table 5. If these recent data are added to statistics, the diagnostic accuracy of FDG-PET for prostheses infection and osteomyelitis detection declines far below 90%. Therefore, the only radiopharmaceutical with more than 90% diagnostic accuracy for bone infections, evidence based, is ^{99m}Tc-labeled or ^{111}In-labeled WBC. Also, for the diagnosis of diabetic foot infection, radiolabeled autologous leukocytes could be considered as a "gold standard" for scintigraphic imaging. For diagnosing diabetic pedal osteomyelitis, ^{111}In-labeled autologous leukocytes demonstrated a sensitivity ranging from 72% to 100%, and specificity ranging from 67% to 100%,[312−316] whereas the ^{99m}Tc-HMPAO-labeled autologous leukocyte showed sensitivity ranging from 86% to 93%, and specificity ranging from 80% to 98%,[274,317−319] in a number of investigations mentioned below. In a large prospective study performed by Newman et al., 35 diabetic patients (41 foot ulcers) underwent 4 and 24 h radiolabeled leukocyte imaging.[319] In this study, an increased activity of the focal site with approximately the same intensity on the dorsal and planar views was the norm for osteomyelitis. Out of a total 41 diabetic foot ulcers, 28 (68%) showed the presence of osteomyelitis. The sensitivity of 4 and 24 h leukocyte imaging was 77% and 89%, respectively, whereas specificity was 77% and 69%, respectively. In comparison with bone scan, authors found 24 h leukocyte imaging was more sensitive (89% versus 69%) and more specific (69% versus 39%). Using the same criteria as Newman et al.,[319] a recent study performed by Palestro et al. for the evaluation of pedal ulcers in 25 diabetic patient demonstrated 80% specificity and 67% sensitivity for the diagnosis.[274] Several other studies, to evaluate ^{111}In-labeled autologous leukocytes scans in diabetic patients with suspected pedal osteomyelitis, demonstrated a high sensitivity of 79% to 100% and specificity of 70−78%.[312−314] ^{99m}Tc-HMPAO-labeled leukocytes scintigraphy, however, was also evaluated at 4 h p.i. in 42 diabetic patients with 56 foot ulcers.[317] In this study, authors evaluated the labeled leukocytes scintigraphy together with bone scan, and those studies in which the distribution of abnormal uptake was spatially similar on both studies were considered positive for osteomyelitis. This study demonstrated a sensitivity of 88% and specificity of 97% for ^{99m}Tc-HMPAO-labeled leukocyte scintigraphy. Using the similar criteria, Poirer et al. examined 83 sites of suspected diabetic pedal osteomyelitis with ^{99m}Tc-HMPAO-labeled leukocytes scintigraphy.[316] The 4−5 h p.i. scans were interpreted in conjunction with bone scans. This study showed a sensitivity of 92.6% and a specificity of 97.6% of labeled leukocytes for diagnosis of diabetic pedal osteomyelitis. In another study, Blume et al. investigated the potential of ^{99m}Tc-HMPAO-labeled leukocytes scans for diagnosing pedal osteomyelitis in 27 patients, including 20 patients with diabetes.[318] Scans were acquired at 3−4 h p.i. and were considered as positive for osteomyelitis when focally increased bony uptake at the site of suspected infection was greater than surrounding soft tissue uptake. Using this criterion, authors concluded a sensitivity of 90% and a specificity of 80%. Another study, in 52 diabetic patients, concluded a sensitivity of 86% and a specificity of 90% for the diagnosis of suspected pedal osteomyelitis; however, any specific criteria for scan evaluation and scan acquisition time were not mentioned.[314]

Several studies also demonstrated the use of ^{111}In-labeled leukocytes for the detection of myocardial abscess in infective endocarditis patients.[320,321] Recently, Erba et al. evaluated 78 patients with suspected endocarditis or infection of cardiac devices, with ^{99m}Tc-HMPAO-labeled autologous leukocytes SPECT/CT, and this study concluded that the SPECT/CT allows an accurate diagnosis of cardiac and additional unsuspected extra-cardiac infection sites.[322]

The radiolabeled autologous leukocytes scan demonstrated its high sensitivity (ranged from 82% to 100%) and specificity (ranged from 75% to 100%) for the diagnosis of vascular graft infection.[323] A study performed in 82 patients with suspected infection including 24 patients related to vascular graft demonstrated very promising results for diagnosis and localization of infection in suspected vascular graft infection by using ^{111}In-labeled leukocytes SPECT/CT.[324] ^{99m}Tc-HMPAO-labeled leukocytes, nowadays, are preferred for scintigraphy due to its short half-life, low radiation dose to the patient, and easy availability properties. Recently, leukocytes have been labeled also with ^{18}F-FDG and with ^{64}Cu for PET imaging. The ^{64}Cu seems to be retained inside the cells with no evident toxicity and allowing imaging up to 18−24 h after reinjection in patients, thus overcoming one of the major limitations of ^{18}F-FDG-labeled WBC that can be imaged only up to 3−4 h after injection. This is possible because of the longer physical half-life of ^{64}Cu (12.7 h) as compared to ^{18}F (2 h). Indeed, in most clinical situations, imaging at late time points (24 h postinjection) is mandatory because of the slow leukocyte accumulation in infected sites as compared to bone marrow.

4.9.4. ^{99m}Tc-Albumin Nanocolloids

As the name indicates, these are albumin-derived small particles of 30−80 nm diameter. Nonspecific extravasation due to increased vascular permeability causes the leakage of ^{99m}Tc-nanocolloid into inflamed tissue followed by accumulation through phagocytosis by macrophages in the reticulo-endothelial system.[239−241] They are characterized by rapid blood clearance and a satisfactory target-to-background ratio early after administration, which allows completion of study usually within 1 h. This technique is easy to perform and inexpensive.

^{99m}Tc-labeled nanocolloid demonstrated a high sensitivity (100%) but very low specificity (<60%) for diagnosis of osteomyelitis in diabetic patients with neuropathic foot disease. This radiopharmaceutical, nowadays, is not used for diagnosis of infection but rather to exclude infection.[325] It has recently reported, and confirmed by several authors, that radiolabeled colloids (sulfur colloids in particular) are trapped by reticulo-endothelial cells in bone marrow, and they can, therefore, be useful to differentiated infection from active

bone marrow in all suspected osteomyelitis in patients with implants or prostheses that may cause bone marrow displacement and activation. In these patients, a dual scan with radiolabeled WBC or antigranulocyte antibodies and with labeled colloids allows one to make a differential diagnosis. A mismatch of the two scans with lower uptake of colloids is indicative of infection, whereas a match of the two scans or a higher uptake of colloids is indicative of bone marrow activation.

4.9.5. ^{99m}Tc- or ^{111}In-Labeled Liposomes

Liposomes are microscopic lipid vesicles that are usually used as drug carriers to increase their solubility and to achieve selective deposition or to reduce toxicity. These are rapidly taken by reticuloendothelial (RES) cells. Liposomes can be radiolabeled with ^{99m}Tc and have been used for the detection of infection and inflammation. Sterically stabilized liposomes have been formulated, which show decreased uptake by the RES, a longer half-life, and enhanced localization in tumors and site of infection. Several studies with ^{111}In- or ^{99m}Tc-labeled liposomes in different small animal models have demonstrated their ability for the scintigraphic detection of infection and inflammation, such as focal infection in rats and experimental colitis in rabbits.[253−259]

4.9.6. ^{18}F-FDG

The FDG accumulation in activated lymphocytes, monocytes, and granulocytes is based on the fact that these cells use glucose as an energy source only after activation during the metabolic burst. Transport of FDG across the cellular membrane is mediated by the GLUT glucose transporter proteins. ^{18}F is a positron emitter with a physical half-life of 110 min. Intracellular FDG is subsequently phosphorylated to ^{18}F-FDG-6 phosphate by the enzyme hexokinase, and the phosphorylated molecule remains trapped inside the cell in contrast to phosphorylated glucose that enters the glycolysis cycle. ^{18}F-FDG is, however, an unspecific tracer for imaging inflammation/infection and can show uptake in any kind of cell with high glycolytic activity and may provide a false-positive result. Other disadvantages are the relatively high cost and the currently limited availability.

Several recent studies with ^{18}F-FDG-PET (^{18}F-fluorodeoxyglucose positron emission tomography) have demonstrated very promising results for imaging in different inflammation/infection, including vasculitis, CD, sarcoidosis and RA, and infections such as osteomyelitis, spondylodicitis, and prosthetic joint infection, etc. Recently, Beckers et al. performed a study using ^{18}F-FDG PET on 16 patients with active RA.[226] They found PET was positive in 69% of the knees, while MRI and US were positive in 69% and 75%, respectively. A study demonstrated that visual identification of RA knee synovitis by ^{18}F-FDG PET is related to its visual identification with MRI and US. The standardized uptake values also correlated with serum CRP and MMP-3 (matrix metalloproteinase-3) levels.

Studies in patients with spondylodiscitis proved FDG PET to be superior to MRI, ^{67}Ga-citrate scintigraphy, and three-phase bone scan for visualization.[227,228] Moreover, FDG PET is also able to differentiate between mild infection and degenerative changes.[229] These studies conclude that FDG PET is a highly sensitive tool to detect suspected osteomyelitis of the central skeleton, spondylodiscitis, or chronic low-grade infections of the peripheral skeleton.

Although FDG PET is a useful tool for detection of inflammation and infection in many disorders, it also has some limitations. FDG PET does not seem suitable for detection of every inflammation such as insulitis in the pancreas of diabetic patients. Although ex-vivo studies in NOD mice demonstrated enhanced FDG uptake in islets of Langerhans that were affected by insulitis, the relatively small difference between diseased and healthy islets and the small size of the islets combined with the limited resolution of the PET camera will most likely prevent successful application in patients.[326] Besides FDG, no validated PET tracers for imaging of peripheral inflammation are available, and thus more sensitive tracers for PET imaging of insulitis are urgently awaited.

For the diagnosis of FUO, nowadays, ^{18}F-FDG-PET and PET/CT is the most promising technique, and more than 300 patients with FUO have been already evaluated in different studies by using FDG-PET scans.[327−335] A study was performed in 10 patients with FUO, to evaluate the usefulness of FDG-PET/CT.[327] In the study, FDG-PET/CT was found to be useful in 50% of patients, in the final diagnosis. FDG-PET/CT was considered essential in 23% patients, because no other diagnostic examinations, such as abdominal and chest CT, were helpful. Furthermore, Meller et al.[328] compare the diagnostic potential of FDG-PET with ^{67}Ga-citrate scintigraphy in patients with FUO. In 18 patients, who were investigated both with ^{67}Ga citrate and FDG, the sensitivity and specificity were 81% and 86% for FDG, whereas ^{67}Ga citrate SPECT yielded a sensitivity of 67% and a specificity of 78%. This study and one other study performed on 40 patients with the same objective[329] both concluded that, in ^{67}Ga-citrate and FDG-PET, the diagnostic yields were at least comparable; however, FDG-PET has a significant advantage in terms of rapidity over ^{67}Ga-citrate scintigraphy; therefore, FDG-PET can substitute ^{67}Ga-citrate scintigraphy for the diagnosis of patients with FUO, in hospitals, where this technique is available. Cascini et al. performed a meta-analysis of peer-reviewed articles published between 1981 and 2005, related to the use of nuclear medicine imaging of FUO.[330] Authors evaluate a total of 33 series of patients, in which 14 examined series classified as occult infection and 19 were defined as FUO. Analysis demonstrated, however, all of the radiopharmaceuticals used in these studies have an overall good diagnostic accuracy (Table 5), although specific agents like ^{99m}Tc- or ^{111}In-labeled leukocytes and ^{99m}Tc-labeled mAbs showed a higher specificity than ^{67}Ga and ^{18}F-FDG-PET. This study, interestingly, showed an overall increase in the accuracy with both specific and nonspecific agents in patients with occult infections. Therefore, ^{18}F-FDG-PET could be considered the technique of choice for the diagnosis of FUO patients, due to their high negative predictive value, although we still need to stabilize a final diagnosis to calculate the specificity and sensitivity for the patients with FUO.

For the use of ^{18}F-FDG-PET and PET/CT in the diagnosis of diabetic foot infection, not much data are presented until now, and, at present, it is too early to predict its imaging potential. Keidar et al. published their initial data on the use of ^{18}F-FDG-PET/CT in patients with diabetic foot infection.[336] They performed this study in 18 suspected sites of 14 patients (ranging from 29 to 70 years). Authors made their final diagnosis on the basis of histopathologic findings and bacteriologic assays obtained at surgery or at clinical and imaging follow-up. This study demonstrated increased

Table 6. Summary of Results from Published Studies Using ^{18}F-FDG-PET for Detection of Infected Vascular Grafts[a]

study	year	no. of patients (*grafts)	18F-FDG dose (MBq)	acquisition time (min after injection)	interpretation criteria	TP	TN	FP	FN
Stumpe et al.[340]	2000	7	300−400	30−40	qualitative	2	5	0	0
Krupnick et al.[341]	2003	1	187	50	qualitative	1	0	0	0
Chacko et al.[342]	2003	3	2.55/kg	60	qualitative	2	1	0	0
Keidar et al.[343]	2003	1	370	60	qualitative	1	0	0	0
Stàdler et al.[344]	2004	1	375	90	qualitative	1	0	0	0
Fukuchi et al.[345]	2005	33	185	60	semiquantitative	10	14	8	1
Jaruskova et al.[346]	2006	7	279−717	40−165 (mean, 70)	qualitative	6	0	1	0
Tsunekawa et al.[347]	2007	1	185	60	qualitative	1	0	0	0
Tegler et al.[348]	2007	1			qualitative	1	0	0	0
Keidar et al.[349]	2007	39	185−370	90	qualitative	14	22	2	1
Lauwers et al.[350]	2008	5	259	90	qualitative	3	2	0	0
Wasselius et al.[351]	2008	16	4/kg	60	semiquantitative	1	5	10	0
Marion et al.[352]	2009	1			qualitative	1	0	0	0
Spacek et al.[353]	2009	96*	256−565	85	qualitative	43	38	3	12
Gardet et al.[354]	2010	1			qualitative	1	0	0	0

[a] Abbreviations: TP = true positive; TN = true negative; FP = false positive; FN = false negative. (Reprinted with permission from ref 355. Copyright 2007 Society of Nuclear Medicine.)

FDG uptake in 14 of the 18 sites, but found that PET alone could not differentiate soft tissue from bone uptake. PET/CT localized uptake to bone in 9 out of the 14 sites, including 8 sites of osteomyelitis. PET/CT correctly localized FDG uptake to the soft tissues in five cases, and one site of mildly increased uptake occurred at a focus of diabetic osteoarthropathy. Moreover, the overall accuracy of FDG-PET/CT in this study was 94.4%.

A recent study was performed by Schwegler et al. in 20 diabetic patients with a chronic foot ulcer, to compare the value of MRI, ^{18}F-FDG PET, and ^{99m}Tc-labeled monoclonal antigranulocyte antibody scintigraphy.[337] Ulcers were present for at least 8 weeks in all patients, and no patient had received antibiotic treatment before imaging. Osteomyelitis was confirmed by biopsy in 7 patients of the 20 clinically unsuspected foot ulcers. In the study, authors found MRI superior to ^{18}F-FDG PET and ^{99m}Tc-labeled antibody scan in the diagnosis of foot ulcer-associated osteomyelitis, being positive for 6 of the 7 patients with proven osteomyelitis. ^{18}F-FDG PET and ^{99m}Tc-labeled antibody scans were positive in only 2 of the 7 patients. Two recent studies, however, demonstrated that FDG-PET had a high negative predictive value for excluding osteomyelitis in the setting of the neuropathic joint, and, therefore, it can reliably differentiate osteomyelitis from neuropathic lesions.[338,339]

Studies demonstrated that ^{18}F-FDG-PET allows precise localization of abnormal uptake in the vascular graft infection.[340−354] Therefore, the possibility of exact anatomic localization of pathologic uptake seems as important as the choice of radiopharmaceutical. A prospective study was performed, by Fukuchi et al., on 33 consecutive patients with suspected arterial prosthetic graft infection to compare the effectiveness of ^{18}F-FDG-PET for the diagnosis of vascular graft infection relative to CT.[345] PET images were assessed visually as per uptake density. In this study, authors reported a higher sensitivity of PET than CT (91% versus 64%, respectively), whereas specificity was found lower in PET than CT (64% versus 86%, respectively), for the diagnosis of aortic graft infection. However, considering focal uptake as a criterion for positivity in PET, the specificity and positive predictive value significantly increased to 95%. A recent study was performed by Keidar et al. to evaluate the role of ^{18}F-FDG-PET for the detection of suspected vascular graft infections in 39 patients.[349] This study demonstrated 93% sensitivity and 91% specificity for the diagnosis; moreover, positive and negative predictive values were 88% and 96%, respectively.

In a recent publication, Burroni et al. analyze all published data on the use of ^{18}F-FDG-PET in vascular graft infections (Table 6); in this investigation, authors concluded that the combined use of PET and CT improves diagnostic accuracy by allowing image interpretation based on morphologic criteria and also reducing the rate of false-positive cases.[355] In conclusion, radiolabeled autologous leukocytes are still considered a "gold standard", because of their sensitivity and specificity, for such infections; however, ^{18}F-FDG-PET and PET/CT may provide a valid substitute for leukocyte scan.

The brain is another organ in which the application of FDG PET for detection of inflammation or infection is limited. Because the brain uses glucose as its source of energy, basal FDG uptake in healthy brain is high, and consequently increased FDG uptake as a result of inflammation can be hard to detect. Moreover, changes in FDG uptake are not specific for inflammation, but can also be induced by other physiological causes, such as activation of a specific brain region by an external stimulus or a specific task.[356] In addition, the inflammation-induced increase in FDG uptake can be obscured by neurodegeneration, which leads to a reduction in glucose consumption. Consequently, neurodegenerative diseases that are associated with chronic inflammation, such as Alzheimer's disease and Parkinson's disease, show characteristic patterns of glucose hypometabolism on PET scans due to destruction of brain tissue,[230] whereas acute encephalitic disorders usually exhibit distinct areas of glucose hypermetabolism, sometimes accompanied by hypometabolism in atrophic brain regions.[357]

4.9.7. ^{124}I-FIAU, ^{18}F-FHPG, ^{18}F-FHBG, and ^{11}C-PK11195

Viral thymidine kinase is an attractive target for imaging of herpes virus infections, because this enzyme is only expressed in replicating viruses. Several tracers are currently available for imaging of herpes simplex virus thymidine kinase (HSVtk) activity,[264] which are specifically phosphorylated by the viral thymidine kinase. Bennett et al. have shown that imaging of replication-competent herpes simplex virus type 1 viruses is possible by PET using 2′-fluoro-5-^{124}I-iodo-1-β-D-arabinofuranosyluracil (^{124}I-FIAU) tracer.[265] The authors injected virus particles into subcutaneous tumors

in the flanks of rats and could clearly visualize the HSV-infected tumors with ^{124}I-FIAU-PET, whereas control tumors could not be discerned. Moreover, in the study, tracer uptake also correlated with the HSV-1 dose and with the interval between virus infection and PET imaging. These results indicate that ^{124}I-FIAU-PET is a competent technique for diagnosis of virus infection and for monitoring oncolytic viral treatment of cancer.

The acyclic guanosine derivatives 9-[(3-^{18}F-fluoro-1-hydroxy-2-propoxy)methyl]guanine (^{18}F-FHPG) and 9-[4-^{18}F-fluoro-3-(hydroxymethyl)butyl]guanine (^{18}F-FHBG) are radiolabeled analogues of the antiviral agents ganciclovir and penciclovir, respectively. ^{18}F-FHPG and ^{18}F-FHBG have been investigated in animal models of herpes simplex encephalitis as potential PET tracers for detection of replicating herpes simplex virus (HSV) in the brain.[266,267] Ex-vivo autoradiography and consecutive metabolite analysis demonstrated that ^{18}F-FHPG selectively accumulated in infected brain regions, where it was phosphorylated by the virus.[266] In the same animal model, comparable selective accumulation of ^{18}F-FHBG was observed in ex-vivo biodistribution and PET imaging studies, although uptake was very low, even in infected brain regions.[267] ^{18}F-FHPG and ^{18}F-FHBG are both hydrophilic tracers that poorly penetrate the intact blood-brain barrier, but might enter the brain when the blood−brain barrier is disrupted during infection and inflammation. However, ^{18}F-FHBG-PET imaging studies could not demonstrate any enhanced tracer uptake in the HSV-infected brain by visual analysis, which is possibly due to a combination of low brain uptake and technical limitation of the imaging method, such as partial volume and spillover effects.

^{11}C-PK11195 is a validated PET tracer, for imaging peripheral benzodiazepine receptors (PBR, also called translocator protein) on the outer mitochondrial membrane of the microglia cells, for the measurement of inflammation-induced microglia activation. The expression of the PBR is low in the healthy brain, but is highly upregulated in neuroinflammation.

PET with ^{11}C-PK11195 ((*R*)-*N*-methyl-*N*-(1-methylpropyl)-1-(2-chlorophenyl)isoquinoline-3-carboxamide) has been successfully applied in a variety of neurological disorders. In patients with viral encephalitis, for example, HSV encephalitis, Rasmussen's encephalitis, and AIDS, ^{11}C-PK11195-PET could clearly identify brain areas with activated microglia.[268−270] Indeed, increased uptake was also detected in brain areas that appeared normal on MRI at the time of investigation, but which developed marked atrophy several months later. ^{11}C-PK11195-PET could also be applied successfully in dementia. In a PET study on patients with Alzheimer's disease, including patients with mild disease, increased ^{11}C-PK11195 binding was observed in affected brain regions.[358] Brain regions with high ^{11}C-PK11195 uptake exhibited signs of atrophy on follow-up MRI and FDG PET scans. ^{11}C-PK11195-PET could also demonstrate microglia activation in other forms of dementia, like frontotemporal dementia.[359] In drug-naive patients with early Parkinson's disease, ^{11}C-PK11195-PET revealed enhanced microglia activation in midbrain, as compared to healthy controls.[268] The uptake of ^{11}C-PK11195 in midbrain positively correlated with the severity of motor deficits. An inverse correlation was found between midbrain ^{11}C-PK11195 uptake and nerve terminal loss in striatum. In patients suffering from multiple sclerosis, enhanced ^{11}C-PK11195 uptake seems to correlate with new lesions, whereas old lesions show little tracer uptake.[360] Focal ^{11}C-PK11195 binding in structures that appeared normal by MRI and asymmetric increased tracer uptake in thalamus and brain stem were also observed. T2-weighted MRI lesions with elevated ^{11}C-PK11195 binding showed an increase in tracer uptake during relapse.[361] In stroke patients, areas with enhanced ^{11}C-PK11195 uptake overlap areas with abnormalities on MRI, but tend to be bigger. Several months after the stroke, the area of ^{11}C-PK11195 binding has extended from the primary infarction site into connected areas in the same hemisphere and the contralateral thalamus, whereas atrophy has developed in the areas that originally exhibited the highest tracer uptake.[362] As follows from above, ^{11}C-PK11195-PET can reveal early inflammatory responses, before abnormalities are visible by MRI. Increased ^{11}C-PK11195 binding in areas that appear normal on MRI was shown to develop atrophy afterward, suggesting that microglial activation precedes neurodegeneration.

5. Conclusions

In the last decades, increasing interest and research efforts have been invested in search of specific probes (fluorescinated or radiolabeled) for imaging different molecular events in inflammation and infection. This has led to early detection of diseases, deeper understanding of pathogenetic mechanisms, therapy decision making, and therapy follow-up.

Optical imaging and fluorescence imaging are the methods of choice for preclinical studies and proof of concept in the development of new imaging probes. They have been proved to be also very useful in drug development to test the efficacy of new antibiotics or biological drugs on bacterial and viral growth and dissemination. By contrast, nuclear medicine imaging offers the possibility to study in vivo different aspects of inflammatory process by the use of radiolabeled molecules that bind to specific recetor targets on cells and tissues. We have now a wide panel of fluorescinated and radiolabeled probes for studying bacteria and virus replication and spread, neutrophyl and lymphocyte trafficking, as well as their homing in inflamed tissues as signs of infection and inflammation, respectively. Molecular imaging in this field goes beyond diagnosis of infection or inflammation. It allows us to histologically characterize pathological processes, highlight the cell type and subtypes that are involved in the process, quantify the presence of bacteria and biologically active molecules, such as cytokines and chemokines, and detect the presence of apoptotic cells and autoreactive cells. All of this information is more and more useful to clinicians for defining a personalized tailored therapy and to follow up its efficacy.

These probes can also be used for early diagnosis of diseases, in susceptible subjects, for detection of disease relapse and radioguided surgery. In some cases, diagnostic probes have also been tested for therapeutic use in larger amounts or labeled with appropriate isotopes. This is the proof of concept that a good diagnostic probe can open new perspectives for therapeutic purposes.

6. Acknowledgments

We wish to thank Drs. Marco Chianelli and Andor Glaudemans for help in the preparation of the manuscript, Dr. Anne Paans for constructive advice, and Mrs. Loreta Antonietta Camillo Sforza for English proof editing and assistance.

7. References

(1) Sato, A.; Klaunberg, B.; Tolwani, R. *Comp. Med.* **2004**, *54*, 631.
(2) Engelsman, A. F.; Van der Mei, H. C.; Francis, K. P.; Busscher, H. J.; Ploeg, R. J.; Van Dam, G. M. *J. Biomed. Mater. Res., Part B* **2009**, *1*, 123.
(3) Sharma, P. K.; Engels, E.; Van Oeveren, W.; Ploeg, R. J.; Van der Mei, H. C.; Busscher, H. J.; Van Dam, G. M.; Rakhorst, G. *Surgery* **2009**, *147*, 89.
(4) O'Neill, K.; Lyons, S. K.; Gallagher, W. M.; Curran, K. M.; Byrne, A. T. *J. Pathol.* **2010**, *220*, 317.
(5) Rocchetta, H. L.; Boylan, C. J.; Foley, J. W.; Iversen, P. W.; LeTourneau, D. L.; McMillian, C. L.; Contag, P. R.; Jenkins, D. E.; Parr, T. R., Jr. *Antimicrob. Agents Chemother.* **2001**, *45*, 129.
(6) Luker, K. E.; Hutchens, M.; Schultz, T.; Pekosz, A.; Luker, G. D. *Virology* **2005**, *341*, 284.
(7) Troy, T.; Jekic-McMullen, D.; Sambucetti, L.; Rice, B. *Mol. Imaging* **2004**, *3*, 9.
(8) Rice, B. W.; Cable, M. D.; Nelson, M. B. *J. Biomed. Opt.* **2001**, *6*, 432.
(9) Roncali, E.; Savinaud, M.; Levrey, O.; Rogers, K. L.; Maitrejean, S.; Tavitian, B. *J. Biomed. Opt.* **2008**, *13*, 054035.
(10) Gross, S.; Piwnica-Worms, D. *Curr. Opin. Chem. Biol.* **2006**, *10*, 334.
(11) Dothager, R. S.; Piwnica-Worms, D. *Proc. Am. Thorac. Soc.* **2009**, *6*, 403.
(12) Sjollema, J.; Sharma, P. K.; Dijkstra, R. J.; van Dam, G. M.; van der Mei, H. C.; Engelsman, A. F.; Busscher, H. J. *Biomaterials* **2010**, *31*, 1984.
(13) Graves, E. E.; Ripoll, J.; Weissleder, R.; Ntziachristos, V. *Phys.* **2003**, *30*, 901.
(14) Garofalakis, A.; Zachanbmrakis, G.; Meyer, H.; Economou, E. N.; Mamalaki, C.; Papamatheakis, J.; Kioussis, D.; Ntziachristos, V.; Ripoll, J. *Mol. Imaging* **2007**, *2*, 96.
(15) Chang, C. W.; Sud, D.; Mycek, M. A. *Methods Cell Biol.* **2007**, *81*, 495.
(16) Neels, O. C. Tracer development for detection and characterization of neuroendocrine tumors with PET. Ph.D. Thesis, Rijksuniversiteit Groningen, Groningen, The Netherlands, 2008.
(17) Lecomte, R. *Eur. J. Nucl. Med. Mol. Imaging* **2009**, *36*, S69.
(18) Eshuis, S. A. Radiotracer imaging in PD. Ph.D. Thesis, Rijksuniversiteit Groningen, Groningen, The Netherlands, 2009.
(19) Hutchins, G. D.; Miller, M. A.; Soon, V. C.; Receveur, T. *ILAR J.* **2008**, *49*, 54.
(20) Rahmin, A.; Zaidi, H. *Nucl. Med. Commun.* **2008**, *29*, 193.
(21) Hohn, A.; Zimmerman, K.; Schaub, E.; Hirzel, W.; Schubiger, P. A.; Schibli, R. Q. J. *Nucl. Med. Mol. Imaging* **2008**, *52*, 145.
(22) Bouwens, L.; Van de Walle, R.; Nuyts, J.; Koole, M.; D'Asseler, Y.; Vandenberghe, S. *Comput. Med. Imaging Graph.* **2001**, *25*, 117.
(23) Townsend, D. W. *Semin. Nucl. Med.* **2008**, *38*, 152.
(24) D'Asseler, Y.; Koole, M.; Van Laere, K.; Vandenberghe, S.; Bouwens, L.; Van de Walle, R. *Technol. Health Care* **2000**, *8*, 35.
(25) Bybel, B.; Brunken, R. C.; DiFilippo, F. P.; Neumann, D. R.; Wu, G.; Cerqueira, M. D. *Radio. Graphics* **2008**, *28*, 1097.
(26) Wehrl, H.; Judenhofer, M. S.; Wiehr, S.; Pichler, B. J. *Eur. J. Nucl. Med. Mol. Imaging* **2009**, *36*, S56.
(27) Contag, P. R. *Methods Mol. Biol.* **2008**, *415*, 101.
(28) Doyle, T. C.; Burns, S. M.; Contag, C. H. *Cell Microbiol.* **2004**, *4*, 303.
(29) Hutchens, M.; Luker, G. D. *Cell Microbiol.* **2007**, *9*, 2315.
(30) Luker, G. D.; Luker, K. E. *J. Nucl. Med.* **2008**, *49*, 1.
(31) Contag, C. H.; Contag, P. R.; Mullins, J. I.; Spilman, S. D.; Stevenson, D. K.; Benaron, D. A. *Mol. Microbiol.* **1995**, *18*, 593.
(32) Francis, K. P.; Joh, D.; Bellinger-Kawahara, C.; Hawkinson, M. J.; Purchio, T. F.; Contag, P. R. *Infect. Immun.* **2000**, *68*, 3594.
(33) Francis, K. P.; Yu, J.; Bellinger-Kawahara, C.; Joh, D.; Hawkinson, M. J.; Xiao, G.; Purchio, T. F.; Caparon, M. G.; Lipsitch, M.; Contag, P. R. *Infect. Immun.* **2001**, *69*, 3350.
(34) Galluzzi, L.; Karp, M. *J. Biotechnol.* **2007**, *127*, 188.
(35) Gupta, R. K.; Patterson, S. S.; Ripp, S.; Simpson, M. L.; Sayler, G. S. *FEMS Yeast Res.* **2003**, *4*, 305.
(36) Law, G. H.; Gandelman, O. A.; Tisi, L. C.; Lowe, C. R.; Murray, J. A. *Biochem. J.* **2006**, *397*, 305.
(37) Tafreshi, N. Kh.; Sadeghizadeh, M.; Emamzadeh, R.; Ranjbar, B.; Naderi-Manesh, H.; Hosseinkhani, S. *Biochem. J.* **2008**, *412*, 27.
(38) Ciana, P.; Raviscioni, M.; Mussi, P.; Vegeto, E.; Que, I.; Parker, M. G.; Lowik, C.; Maggi, A. *Nat. Med.* **2003**, *9*, 82.
(39) Lipshutz, G. S.; Gruber, C. A.; Cao, Y.; Hardy, J.; Contag, C. H.; Gaensler, K. M. *Mol. Ther.* **2001**, *3*, 284.
(40) Bhaumik, S.; Gambhir, S. *Proc. Natl. Acad. Sci. U.S.A.* **2002**, *99*, 377.
(41) Venisnik, K. M.; Olafsen, T.; Gambhir, S. S.; Wu, A. M. *Mol. Imaging Biol.* **2007**, *9*, 267.
(42) Tannous, B. A.; Kim, D. E.; Fernandex, J. L.; Weissleder, R.; Breakefiled, X. O. *Mol. Ther.* **2005**, *11*, 435.
(43) Loening, A. M.; Wu, A. M.; Gambhir, S. S. *Nat. Methods* **2007**, *4*, 641.
(44) Kadurugamuwa, J. L.; Modi, K.; Coquoz, O.; Rice, B.; Smith, S.; Contag, P. R. *Infect. Immun.* **2005**, *73*, 7836.
(45) Shaner, N. C.; Lin, M. Z.; McKeown, M. R.; Steinbach, P. A.; Hazelwood, K. L.; Davidson, M. W.; Tsien, R. Y. *Nat. Methods* **2008**, *5*, 545.
(46) Nienhaus, G. U.; Wiedenmann, J. *ChemPhysChem* **2009**, *10*, 1369.
(47) Shu, X.; Royant, A.; Lin, M. Z.; Aguilera, T. A.; Lev-Ram, V.; Steinbach, P. A.; Tsien, R. Y. *Science* **2009**, *324*, 804.
(48) Bongaerts, R.; Hautefort, I.; Sidebotham, J.; Hinton, J. *Methods Enzymol.* **2002**, *358*, 43.
(49) Southward, C.; Surette, M. *Mol. Microbiol.* **2002**, *45*, 1191.
(50) Rao, J.; Dragulescu-Andrasi, A.; Yao, H. *Curr. Opin. Biotechnol.* **2007**, *18*, 17.
(51) Gounaris, E.; Tung, C. H.; Restaino, C.; Maehr, R.; Kohler, R.; Joyce, J. A.; Plough, H. L.; Barrett, T. A.; Weissleder, R.; Khazaie, K. *PloS ONE* **2008**, *3*, e2916.
(52) Xing, Y.; Rao, J. *Cancer Biomarkers* **2008**, *4*, 307.
(53) Ray, P.; Tsien, R.; Gambhir, S. S. *Cancer Res.* **2007**, *67*, 3085.
(54) Wunder, A.; Klohs, J.; Dirnagl, U. *Neuroscience* **2009**, *158*, 1161.
(55) Leevy, W. M.; Gammon, S. T.; Jiang, H.; Johnson, J. R.; Maxwell, D. J.; Jackson, E. N.; Marquez, M.; Piwnica-Worms, D.; Smith, B. D. *J. Am. Chem. Soc.* **2006**, *128*, 16476.
(56) Leevy, W. M.; Gammon, S. T.; Johnson, J. R.; Lampkins, A. J.; Jiang, H.; Marquez, M.; Piwnica-Worms, D.; Suckow, M. A.; Smith, B. D. *Bioconjugate Chem.* **2008**, *19*, 686.
(57) Leevy, W. M.; Lambert, T. N.; Johnson, J. R.; Morris, J.; Smith, B. D. *Chem. Commun.* **2008**, *28*, 2331.
(58) Qazi, S. N.; Harrison, S. E.; Self, T.; Williams, P.; Hill, P. J. *J. Bacteriol.* **2004**, *186*, 1065.
(59) Engelsman, A. F.; van der Mei, H. C.; Francis, K. P.; Busscher, H. J.; Ploeg, R. J.; van Dam, G. M. *J. Biomed. Mater. Res., Part B* **2009**, *88*, 123.
(60) Kadurugamuwa, J. L.; Sin, L. V.; Yu, J.; Francis, K. P.; Kimura, R.; Purchio, T.; Contag, P. R. *Antimicrob. Agents Chemother.* **2003**, *47*, 3130.
(61) Mortin, L. I.; Li, T.; Van Praagh, A. D.; Zhang, S.; Zhang, X. X.; Alder, J. D. *Antimicrob. Agents Chemother.* **2007**, *51*, 1787.
(62) Hardy, J.; Chu, P.; Contag, C. H. *Dis. Models Mech.* **2009**, *2*, 39.
(63) Cronin, M.; Sleator, R. D.; Hill, C.; Fitzgerald, G. F.; van Sinderen, D. *BMC Microbiol.* **2008**, *8*, 161.
(64) Sanz, P.; Teel, L. D.; Alem, F.; Carvalho, H. M.; Darnell, S. C.; O'Brien, A. D. *Infect. Immun.* **2008**, *76*, 1036.
(65) Luker, G. D.; Bardill, J. P.; Prior, J. L.; Pica, C. M.; Piwnica-Worms, D.; Leib, D. A. *J. Virol.* **2002**, *76*, 2149.
(66) Luker, G. D.; Prior, J. L.; Song, J.; Pica, C. M.; Leib, D. A. *J. Virol.* **2003**, *77*, 11082.
(67) Luker, K. E.; Schultz, T.; Romine, J.; Leib, D. A.; Luker, G. D. *Virology* **2006**, *347*, 286.
(68) Zhu, Q.; Oei, Y.; Mendel, D. B.; Garrett, E. N.; Patawaran, M. B.; Hollenbach, P. W.; Aukerman, S. L.; Weiner, A. J. *Antimicrob. Agents Chemother.* **2006**, *50*, 3260.
(69) Hwang, S.; Wu, T. T.; Tong, L. M.; Kim, K. S.; Martinez-Guzman, D.; Colantonio, A. D.; Uittenbogaart, C. H.; Sun, R. *J. Virol.* **2008**, *82*, 12498.
(70) Milho, R.; Smith, C. M.; Marques, S.; Alenquer, M.; May, J. S.; Gillet, L.; Gaspar, M.; Efstathiou, S.; Simas, J. P.; Stevenson, P. G. *J. Gen. Virol.* **2009**, *90*, 21.
(71) Cook, S. H.; Griffin, D. E. *J. Virol.* **2003**, *77*, 5333.
(72) Zaitseva, M.; Kapnick, S. M.; Scott, J.; King, L. R.; Manischewitz, J.; Sirota, L.; Kodihalli, S.; Golding, H. *J. Virol.* **2009**, *83*, 10437.
(73) Carlsen, H.; Moskaug, J. Ø.; Fromm, S. H.; Blomhoff, R. *J. Immunol.* **2002**, *168*, 144.
(74) Sadikot, R. T.; Zeng, H.; Joo, M.; Everhart, M. B.; Sherrill, T. P.; Li, B.; Cheng, D. S.; Yull, F. E.; Christman, J. W.; Blackwell, T. S. *J. Immunol.* **2006**, *176*, 4923.
(75) Notebaert, S.; Carlsen, H.; Janssen, D.; Vandenabeele, P.; Blomhoff, R.; Meyer, E. *Cell Microbiol.* **2008**, *10*, 1249.
(76) Zangani, M.; Carlsen, H.; Kielland, A.; Os, A.; Hauglin, H.; Blomhoff, R.; Munthe, L. A.; Bogen, B. *Am. J. Pathol.* **2009**, *174*, 1358.
(77) Zhang, N.; Weber, A.; Li, B.; Lyons, R.; Contag, P. R.; Purchio, A. F.; West, D. B. *J. Immunol.* **2003**, *170*, 6307.
(78) Zhang, N.; Ahsan, M. H.; Purchio, A. F.; West, D. B. *J. Immunol.* **2005**, *174*, 8125.
(79) Luo, J.; Ho, P.; Steinman, L.; Wyss-Coray, T. *J. Neuroinflammation* **2008**, *5*, 6.
(80) Ishikawa, T. O.; Jain, N. K.; Taketo, M. M.; Herschman, H. R. *Mol. Imaging Biol.* **2006**, *8*, 171.
(81) Kamei, K.; Ishikawa, T. O.; Herschman, H. R. *Genesis* **2006**, *44*, 177–82.

(82) Jeon, Y. H.; Choi, Y.; Kang, J. H.; Chung, J. K.; Lee, Y. J.; Kim, C. W.; Jeong, J. M.; Lee, D. S.; Lee, M. C. *Vaccine* **2006**, *24*, 3057.
(83) Schweichel, D.; Steitz, J.; Tormo, D.; Gaffal, E.; Ferrer, A.; Büchs, S.; Speuser, P.; Limmer, A.; Tüting, T. *J. Gene Med.* **2006**, *8*, 1243.
(84) Gómez, C. E.; Nájera, J. L.; Domingo-Gil, E.; Ochoa-Callejero, L.; González-Aseguinolaza, G.; Esteban, M. *J. Gen. Virol.* **2007**, *88*, 2473.
(85) Jurisson, S.; Berning, D.; Jia, W.; Ma, D. *Chem. Rev.* **1993**, *93*, 1137.
(86) Maecke, H. R.; Andre, J. P. *Ernst Schering Research Foundation Workshop* **2007**, *62*, 215.
(87) Allard, M.; Fouquet, E.; James, D.; Szlosek-Pinaud, M. *Curr. Med. Chem.* **2008**, *15*, 235.
(88) Wuest, F.; Berndt, M.; Kniess, T. *Ernst Schering Research Foundation Workshop* **2007**, *62*, 183.
(89) Mather, S. J. *Int. J. Biochem.* **1988**, *20*, 759.
(90) Sosabowsky, J.; Melendez-Alafort, L.; Mather, S. Q. J. *Nucl. Med.* **2003**, *47*, 223.
(91) Wester, H. J.; Schottelius, M. *Ernst Schering Research Foundation Workshop* **2007**, *62*, 79.
(92) Wuest, F. *Ernst Schering Research Foundation Workshop* **2007**, *62*, 51.
(93) Liu, S. *Adv. Drug Delivery Rev.* **2008**, *60*, 1347.
(94) Sosabowski, J. K.; Mather, S. J. *Nat. Protoc.* **2006**, *1*, 972.
(95) Cooper, M. S.; Sabbah, E.; Mather, S. J. *Nat. Protoc.* **2006**, *1*, 314.
(96) Ginj, M.; Maecke, H. R. *Met. Ions Biol. Syst.* **2004**, *42*, 109.
(97) Granowska, M.; Mather, S. J.; Britton, K. E. *Int. J. Appl. Radiat. Isot.* **1991**, *18*, 413.
(98) Liu, S.; Edwards, D. S.; Barrett, J. A. *Bioconjugate Chem.* **1997**, *8*, 621.
(99) Mather, S. J.; Ellison, D. *J. Nucl. Med.* **1990**, *31*, 692.
(100) Schibli, R.; Schwarzbach, R.; Alberto, R. *Bioconjugate Chem.* **2002**, *13*, 750.
(101) Mather, S. J. *Mol. Biosyst.* **2007**, *3*, 30.
(102) Decristoforo, C.; Mather, S. J. Q. *J. Nucl. Med.* **2002**, *46*, 195.
(103) Melis, M.; Krenning, E. P.; Bernard, B. F.; de Visser, M.; Rolleman, E.; de Jong, M. *Nucl. Med. Biol.* **2007**, *34*, 633.
(104) Conti, F.; Priori, R.; Chimenti, M. S.; Coari, G.; Annovazzi, A.; Valesini, G. *Arthritis Rheum.* **2005**, *52*, 1224.
(105) Tsopelas, C.; Penglis, S.; Ruskiewicz, A.; Bartholomeusz, D. L. *J. Nucl. Med.* **2006**, *9*, 85.
(106) D'Alessandria, C.; Malviya, G.; Viscido, A.; Aratari, A.; Maccioni, F.; Amato, A. Q. J. *Eur. J. Nucl. Med. Mol. Imaging* **2007**, *51*, 1.
(107) Barrera, P.; Oyen, W. J. G.; Boerman, O. C.; van Riel, P. L. C. M. *Ann. Rheum. Dis.* **2003**, *62*, 825.
(108) Malviya, G.; D'Alessandria, C.; Lanzolla, T.; Lenza, A.; Conti, F.; Valesini, G.; Scopinaro, F.; Dierckx, R. A.; Signore, A. Q. J. *Eur. J. Nucl. Med. Mol. Imaging* **2008**, *52*, 13.
(109) Malviya, G.; Lagàna, B.; Signore, A.; Dierckx, R. A. *Curr. Pharm. Des.* **2008**, *14*, 2401.
(110) Malviya, G.; Dierckx, R. A.; Signore, A. *Eur. J. Nucl. Med. Mol. Imaging* **2009**, *36*, S404.
(111) Zhang, M.; Yao, Z.; Zhang, Z.; Garmestani, K.; Talanov, V. S.; Plascjak, P. S. *Cancer Res.* **2006**, *66*, 8227.
(112) Choi, C. W.; Lang, L.; Lee, J. T.; Webber, K. O.; Yoo, T. M.; Chang, H. K. *Cancer Res.* **1995**, *55*, 5323.
(113) Wu, C.; Jagoda, E.; Brechbiel, M.; Webber, K. O.; Pastan, I.; Gansow, O. *Bioconjugate Chem.* **1997**, *8*, 365.
(114) Kobayashi, H.; Yoo, T. M.; Drumm, D.; Kim, M. K.; Sun, B. F.; Le, N. *Cancer Res.* **1997**, *57*, 1955.
(115) Hartmann, F.; Horak, E. M.; Garmestani, K.; Wu, C.; Brechbiel, M. W.; Kozak, R. W. *Cancer Res.* **1994**, *54*, 4362.
(116) Marcus, C.; Thakur, M. L.; Huynh, T. V.; Louie, J. S.; Leibling, M.; Minami, C. *Nucl. Med. Commun.* **1994**, *15*, 824.
(117) Martins, F. P. P.; Gutfilen, B.; De Souza, S. A. L.; De Azevedo, M. N. L.; Cardoso, L. R.; Fraga, R. *Br. J. Radiol.* **2008**, *81*, 25.
(118) Malviya, G.; D'Alessandria, C.; Bonanno, E.; Vexler, V.; Massari, R.; Trotta, C.; Scopinaro, F.; Dierckx, R. A.; Signore, A. *J. Nucl. Med.* **2009**, *50*, 1683.
(119) Kinne, R. W.; Becker, W.; Schwab, J.; Horneff, G.; Schwarz, A.; Kalden, J. R. *Nucl. Med. Commun.* **1993**, *14*, 667.
(120) Kinne, R. W.; Becker, W.; Simon, G. *J. Nucl. Med.* **1993**, *34*, 92.
(121) Kinne, R. W.; Becker, W.; Schwab, J. *Eur. J. Nucl. Med.* **1994**, *21*, 176.
(122) Zhang, C.; Hou, G.; Han, J.; Song, J.; Liang, T. *Mediators Inflammation* **2007**, *2007*, 50180.
(123) Jamar, F.; Chapman, P. T.; Manicourt, D.-H.; Glass, D. M.; Haskard, D. O.; Peters, A. M. *Br. J. Radiol.* **1997**, *70*, 473.
(124) Jamar, F.; Chapman, P. T.; Harrison, A. A.; Binns, R. M.; Haskard, D. O.; Peters, A. M. *Radiology* **1995**, *194*, 843.
(125) Chapman, P. T.; Jamar, F.; Keelan, E. T.; Peters, A. M.; Haskard, D. O. *Arthritis Rheum.* **1996**, *39*, 1371.
(126) Jamar, F.; Houssiau, F. A.; Devogelaer, J. P.; Chapman, P. T.; Haskard, D. O.; Beaujean, V. *Rheumatology* **2002**, *41*, 53.
(127) Keelan, E. T. M.; Harrison, A. A.; Chapman, P. T.; Binns, R. M.; Peters, A. M.; Haskard, D. O. *J. Nucl. Med.* **1994**, *35*, 276.
(128) Stopar, T. G.; Mlinaric-Rascan, I.; Fettich, J.; Hojker, S.; Mather, S. J. *Eur. J. Nucl. Med.* **2006**, *33*, 53.
(129) Malviya, G.; Laganà, B.; Milanetti, F.; Del Mastro, C.; Familiari, D.; Dierckx, R. A.; Scopinaro, F.; D'Amelio, R.; Signore, A. *Eur. J. Nucl. Med. Mol. Imaging* **2008**, *35*, S142.
(130) Mahida, Y. R.; Perkins, A. C.; Frier, M.; Wastie, M. L.; Hawkey, C. J. *Nucl. Med. Commun.* **1992**, *13*, 330.
(131) Peltier, P.; Potel, G.; Lovat, E.; Baron, D.; Chatal, J. F. *Nucl. Med. Commun.* **1993**, *14*, 766.
(132) Dominguez-Gadea, L.; Martin-Curto, L. M.; de la Calle, H.; Crespo, A. *Nucl. Med. Commun.* **1993**, *14*, 212.
(133) Rypins, E. B.; Kipper, S. L. *Am. Surg.* **2000**, *66*, 891.
(134) Boerman, O. C.; Rennen, H.; Oyen, W. J.; Corstens, F. H. *Semin. Nucl. Med.* **2001**, *31*, 286.
(135) Becker, W.; Bair, J.; Behr, T.; Repp, R.; Streckenbach, H.; Beck, H. *J. Nucl. Med.* **1994**, *35*, 1436.
(136) Harwood, S. J.; Valdivia, S.; Hung, G. L.; Quenzer, R. W. *Clin. Infect. Dis.* **1999**, *28*, 1200.
(137) Gratz, S.; Raddatz, D.; Hagenah, G.; Behr, T.; Behe, M.; Becker, W. *Int. J. Cardiol.* **2000**, 75.
(138) Barron, B.; Hanna, C.; Passalaqua, A. M.; Lamki, L.; Wegener, W. A.; Goldenberg, D. M. *Surgery* **1999**, *125*, 288.
(139) Kjaer, A.; Lebech, A. M.; Eigtved, A.; Hojgaard, L. *Eur. J. Nucl. Med. Mol. Imaging* **2004**, *31*, 622.
(140) Vicente, A. G.; Almoguera, M.; Alonso, J. C.; Heffernan, A. J.; Gomez, A.; Contreras, P. I.; Martin-Comin, J. *Recent Adv. Clin. Nucl. Med.* **2004**, *29*, 781.
(141) Pierer, M.; Hesse, S.; Baerwald, C.; Linke, T.; Aringer, M.; Seidel, W. American College of Rheumatology, Annual Scientific Meeting 2008, P-1434. http://acr.confex.com/acr/2008/webprogram/Paper3179.html (accessed on 10/01/2010).
(142) van der Laken, C. J.; Boerman, O. C.; Oyen, W. J. G.; van de Ven, M. T.; van der Meer, J. W.; Corstens, F. H. *Eur. J. Nucl. Med.* **1998**, *25*, 347.
(143) Van der Laken, C. J.; Boerman, O. C.; Oyen, W. J. G.; Laverman, P.; Van de Ven, M. T. P.; Corstens, F. H. M. *J. Infect. Dis.* **1998**, *177*, 1398.
(144) Van der Laken, C. J.; Boerman, O. C.; Oyen, W. J. G.; Van de Ven, M. T. P.; Chizzonite, R.; Corstens, F. H. M. *J. Clin. Invest.* **1997**, *100*, 2970.
(145) Van der Laken, C. J.; Boerman, O. C.; Oyen, W. J. G.; Van der Ven, M. T. P.; Claessens, R. A. M. J.; Van der Meer, J. W. M.; Corstens, F. H. M. *Eur. J. Nucl. Med.* **1996**, *23*, 1531.
(146) Barrera, P.; van der Laken, C. J.; Boerman, O. C.; Oyen, W. J. G.; van de Ven, M. T.; van Lent, P. L. *Rheumatology* **2000**, *39*, 870.
(147) Signore, A.; Chianelli, M.; Toscano, A.; Monetini, L.; Ronga, G.; Nimmon, C. C. *Nucl. Med. Commun.* **1992**, *13*, 713.
(148) Chianelli, M.; Signore, A.; Fritzberg, A. R.; Mather, S. J. *Nucl. Med. Biol.* **1997**, *24*, 579.
(149) Signore, A.; Beverley, P. C.; Parman, A.; Negri, M.; Pozzilli, P. *Exp. Clin. Endocrinol.* **1987**, *89*, 301.
(150) Signore, A.; Chianelli, M.; Annovazzi, A.; Bonanno, E.; Spagnoli, L. G.; Pozzilli, P. *J. Nucl. Med.* **2000**, *41*, 242.
(151) Signore, A.; Chianelli, M.; Annovazzi, A.; Rossi, M.; Maiuri, L.; Greco, M. *Eur. J. Nucl. Med.* **2000**, *27*, 18.
(152) Annovazzi, A.; Biancone, L.; Caviglia, R.; Chianelli, M.; Capriotti, G.; Mather, S. J. *Eur. J. Nucl. Med. Mol. Imaging* **2003**, *30*, 374.
(153) Signore, A.; Annovazzi, A.; Barone, R.; Bonanno, E.; D'Alessandria, C.; Chianelli, M. *J. Nucl. Med.* **2004**, *45*, 1647.
(154) Loose, D.; Signore, A.; Bonanno, E.; Vermeersch, H.; Dierckx, R.; Deron, P. *Cancer Biother. Radiopharm.* **2008**, *23*, 25.
(155) Loose, D.; Signore, A.; Staelens, L.; Bulcke, K. V.; Vermeersch, H.; Dierckx, R. A. *Eur. J. Nucl. Med. Mol. Imaging* **2008**, *35*, 281.
(156) Renard, V.; Staelens, L.; Signore, A.; Van Belle, S.; Dierckx, R. A.; Van De Wiele, C. *Q. J. Nucl. Med. Mol. Imaging* **2007**, *51*, 352.
(157) Annovazzi, A.; Bonanno, E.; Arca, M.; D'Alessandria, C.; Marcoccia, A.; Spagnoli, L. G. *Eur. J. Nucl. Med. Mol. Imaging* **2006**, *33*, 117.
(158) Signore, A.; Picarelli, A.; Annovazzi, A.; Britton, K. E.; Grossman, A. B.; Bonanno, E. *Nucl. Med. Commun.* **2003**, *24*, 305.
(159) Lucia, P.; Parisella, M. G.; Danese, C.; Bruno, F.; Manetti, L. L.; Capriotti, G. *J. Rheumatol.* **2004**, *31*, 1225.
(160) Hay, R. V.; Skinner, R. S.; Newman, O. C.; Kunkel, S. L.; Lyle, L. R.; Shapiro, B. *Nucl. Med. Commun.* **1997**, *18*, 367.
(161) Gratz, S.; Rennen, H. J.; Boermanm, O. C.; Oyenm, W. J.; Corstensm, F. H. *J. Nucl. Med.* **2001**, *42*, 917.
(162) Gratz, S.; Rennen, H. J.; Boerman, O. C.; Oyen, W. J.; Burma, P.; Corstens, F. H. *J. Nucl. Med.* **2001**, *42*, 1257.
(163) Gross, M. D.; Shapiro, B.; Skinner, R. S.; Shreve, P.; Fig, L. M.; Hay, R. V. *J. Nucl. Med.* **1996**, *37*, 25P.
(164) Laterveer, L.; Lindley, I. J. D.; Heemskerk, D. P. P. M.; Camps, J. A.; Pauwels, E. K.; Willemze, R. *Blood* **1996**, *87*, 781.

(165) Bleeker-Rovers, C. P.; Rennen, H. J.; Boerman, O. C.; Wymenga, A. B.; Visser, E. P.; Bakker, J. H.; van der Meer, J. W.; Corstens, F. H.; Oyen, W. J. *J. Nucl. Med.* **2007**, *48*, 337.
(166) Van der Laken, C. J.; Boerman, O. C.; Oyen, W. J. G.; Van de Ven, M. P. T.; Laverman, P.; Van der Meer, J. W. M.; Corstens, F. H. M. *Nucl. Med. Commun.* **1997**, *18*, 478.
(167) Annovazzi, A.; D'Alessandria, C.; Bonanno, E.; Mather, S. J.; Cornelissen, B.; Van de Wiele, C. *Eur. J. Nucl. Med. Mol. Imaging* **2006**, *33*, 474.
(168) Hartung, D.; Petrov, A.; Haider, N.; Fujimoto, S.; Blankenberg, F.; Fujimoto, A. *J. Nucl. Med.* **2007**, *48*, 1816.
(169) Blankenberg, F. G.; Tait, J. F.; Blankenberg, T. A.; Post, A. M.; Strauss, H. W. *Eur. J. Nucl. Med.* **2001**, *28*, 1384.
(170) Virgolini, I.; Kurtaran, A.; Leimer, M.; Smith-Jones, P.; Agis, H.; Angelberger, P. *J. Nucl. Med.* **1997**, *38*, 1475.
(171) Shatten, C.; Pateisky, N.; Vavra, N.; Ehrenbock, P.; Angelberger, P.; Sivolapenko, G.; Epenetos, A. *Lancet* **1991**, *337*, 395.
(172) Reilly, R. M.; Kiarash, R.; Sandhu, J.; Lee, Y. W.; Cameron, R. G.; Hendler, A.; Vallis, K.; Gariepy, J. *J. Nucl. Med.* **2000**, *41*, 903.
(173) Prats, P. A.; Duconge, J.; Valenzuela, C.; Berlanga, J.; Edrosa, C. R.; Fernandez-Sanchez, E. *Biopharm. Drug Dispos.* **2002**, *23*, 67.
(174) Dickson, K. M.; Bergeron, J. J.; Philip, A.; O'Connor-McCourt, M.; Warshawsky, H. *Calcif. Tissue Int.* **2001**, *68*, 304.
(175) Brouwers, A. H.; Laverman, P.; Boerman, O. C.; Oyen, W. J. G.; Barrett, J. A.; Harris, T. D. *Nucl. Med. Commun.* **2000**, *21*, 1043.
(176) Riou, L. M.; Ruiz, M.; Sullivan, G. W.; Linden, J.; Leong-Poi, H.; Lindner, J. R. *Circulation* **2002**, *106*, 592.
(177) van Eerd, J. E.; Broekema, M.; Harris, T. D.; Edwards, D. S.; Oyen, W. J.; Corstens, F. H. *J. Nucl. Med.* **2005**, *46*, 1546.
(178) Broekema, M.; van Eerd, J. J.; Oyen, W. J.; Corstens, F. H.; Liskamp, R. M.; Boerman, O. C. *J. Med. Chem.* **2005**, *48*, 6442.
(179) Van Eerd, J. E.; Oyen, W. J.; Harris, T. D.; van Eerd, J. E.; Oyen, W. J.; Harris, T. D. *J. Nucl. Med.* **2005**, *46*, 786.
(180) van Eerd, J. E.; Oyen, W. J.; Harris, T. D.; Rennen, H. J.; Edwards, D. S.; Liu, S. *J. Nucl. Med.* **2003**, *44*, 1087.
(181) van Eerd, J. E.; Laverman, P.; Oyen, W. J.; Harris, T. D.; Edwards, D. S.; Ellars, C. E. *J. Nucl. Med.* **2004**, *45*, 89.
(182) Hartwig, W.; Carter, E. A.; Jimenez, R. E.; Werner, J.; Fischman, A. J.; Fernandez-Del; Castillo, C.; Warshaw, A. L. *J. Appl. Physiol.* **1999**, *87*, 743.
(183) Edwards, D. S.; Liu, S.; Ziegler, M. C.; Harris, A. R.; Crocker, A. C.; Heminway, S. J.; Barrett, J. A.; Bridger, G. J.; Abrams, M. J.; Higgins, J. D. *Bioconjugate Chem.* **1999**, *10*, 884.
(184) Moyer, B. R.; Vallabhajosula, S.; Lister-James, J.; Bush, L. R.; Cyr, J. E.; Snow, D. A. *J. Nucl. Med.* **1996**, *37*, 673.
(185) Palestro, C. J.; Weiland, F. L.; Seabold, J. E.; Valdivia, S.; Tomas, M. B.; Moyer, B. R. *Nucl. Med. Commun.* **2001**, *22*, 695.
(186) Krause, S.; Rennen, H. J.; Boerman, O. C.; Baumann, S.; Cyr, J. E.; Manchanda, R. *Nucl. Med. Biol.* **2007**, *34*, 925.
(187) Oyen, W. J.; Boerman, O. C.; Brouwers, F. M.; Barrett, J. A.; Verheugt, F. W.; Ruiter, D. J.; Corstens, F. H.; van der Meer, J. W. *Eur. J. Nucl. Med.* **2000**, *27*, 392.
(188) Rusckowski, M.; Qu, T.; Pullman, J.; Marcel, R.; Ley, A. C.; Ladner, R. C.; Hnatowich, D. J. *J. Nucl. Med.* **2000**, *41*, 363.
(189) Hnatowich, D. J.; Qu, T.; Chang, F.; Ley, A. C.; Ladner, R. C.; Rusckowski, M. *J. Nucl. Med.* **1998**, *39*, 56.
(190) Qu, T.; Wang, Y.; Zhu, Z.; Rusckowski, M.; Hnatowich, D. J. *Nucl. Med. Commun.* **2001**, *22*, 203.
(191) Welling, M. M.; Paulusma-Annema, A.; Balter, H. S.; Pauwels, E. K.; Nibbering, P. H. *Eur. J. Nucl. Med.* **2000**, *27*, 292.
(192) Welling, M. M.; Nibbering, P. H.; Paulusma-Annema, A.; Hiemstra, P. S.; Pauwels, E. K.; Calame, W. *J. Nucl. Med.* **1999**, *40*, 2073.
(193) Akhtar, M. S.; Khan, M. E.; Khan., B.; Irfanullah, J.; Afzal, M. S.; Khan, M. A. *Eur. J. Nucl. Med. Mol. Imaging* **2008**, *35*, 1056.
(194) Welling, M. M.; Lupetti, A.; Balter, H. S.; Lanzzeri, S.; Souto, B.; Rey, A. M. *J. Nucl. Med.* **2001**, *42*, 788.
(195) Meléndez-Alafort, L.; Rodrìguez-Cortés, J.; Ferro-Flores, G.; Murphy, C. A.; Herrera-Rodrìguez, R.; Martìnez-Duncker, C. *Nucl. Med. Biol.* **2004**, *31*, 373.
(196) Britton, K. E.; Wareham, D. W.; Das, S. S.; Solanki, K. K.; Amaral, H.; Bhatnagar, A. *J. Clin. Pathol.* **2002**, *55*, 817.
(197) Welling, M. M.; Hiemstra, P. S.; van den Barselaar, M. T.; Paulusma-Annema, A.; Nibbering, P. H.; Pauwels, E. K. *J. Clin. Invest.* **1998**, *102*, 1583.
(198) McAfee, J. G.; Subramanian, G.; Gagne, G. *Semin. Nucl. Med.* **1984**, *14*, 83.
(199) Babich, J. W.; Graham, W.; Barrow, S. A.; Dragotakes, S. C.; Tompkins, R. G.; Rubin, R. H. *J. Nucl. Med.* **1993**, *34*, 2176.
(200) Rennen, H. J.; Oyen, W. J. G.; Cain, S. A.; Monk, P. N.; Corstens, F. H.; Boerman, O. C. *Nucl. Med. Biol.* **2003**, *30*, 267.
(201) Rusckowski, M.; Gupta, S.; Liu, G.; Dou, S.; Hnatowich, D. J. *J. Nucl. Med.* **2004**, *45*, 1201.
(202) Oh, S. J.; Ryu, J. S.; Shin, J. W.; Yoon, E. J.; Ha, H. J.; Cheon, J. H. *Appl. Radiat. Isot.* **2002**, *57*, 193.
(203) Hall, A. V.; Solanki, K. K.; Vinjamuri, S.; Britton, K. E.; Das, S. S. *J. Clin. Pathol.* **1998**, *51*, 215.
(204) Vinjamuri, S.; Hall, A. V.; Solanki, K. K.; Bomanji, J.; Siraj, Q.; O'Shaughnessy, E. *Lancet* **1996**, *347*, 233.
(205) Sarda, L.; Saleh-Mghir, A.; Peker, C.; Meulemans, A.; Cremieux, A. C.; Le Guludec, D. *J. Nucl. Med.* **2002**, *43*, 239.
(206) Dumarey, N.; Blocklet, D.; Appelboom, T.; Tant, L.; Schoutens, A. *Eur. J. Nucl. Med. Mol. Imaging* **2002**, *2*, 530.
(207) Langer, O.; Mitterhauser, M.; Brunner, M.; Zeitlinger, M.; Wadsak, W.; Mayer, B. X. *Nucl. Med. Biol* **2003**, *30*, 285.
(208) Singh, A. K.; Verma, J.; Bhatnagar, A.; Ali, A. *World J. Nucl. Med.* **2003**, *2*, 103.
(209) Martin-Comin, J.; Soroa, V.; Rabiller, G.; Galli, R.; Cuesta, L.; Roca, M. *Rev. Esp. Med. Nucl.* **2004**, *23*, 357.
(210) Singh, A. K.; Verma, J.; Bhatnagar, A.; Sen, S.; Bose, M. *World J. Nucl. Med.* **2003**, *2*, 292.
(211) Causse, J. E.; Pasqualini, R.; Cypriani, B.; Weil, R.; Van der Valk, R.; Bally, P. *Int. J. Appl. Radiat. Isot.* **1990**, *41*, 493.
(212) Lupetti, A.; Welling, M. M.; Mazz, U.; Nibbering, P. H.; Pauwels, E. K. J. *Eur. J. Nucl. Med.* **2002**, *29*, 674.
(213) Boothe, D. M.; Boeckh, A.; Boothe, H. W. *Am. J. Vet. Res.* **2009**, *70*, 16.
(214) Siaens, R. H.; Rennen, H. J.; Boerman, O. C.; Dierckx, R.; Slegers, G. *J. Nucl. Med.* **2004**, *45*, 2088.
(215) Shimpi, H. H.; Nair, N. *Indian J. Nucl. Med.* **2003**, *18*, 16.
(216) Benitez, A.; Roca, M.; Martin-Comin, J. *Q. J. Nucl. Med. Mol. Imaging* **2006**, *50*, 147.
(217) Motaleb, M. A. *J. Radioanal. Nucl. Chem.* **2007**, *272*, 95.
(218) Tewson, T. J.; Yang, D.; Wong, G.; Macy, D.; DeJesus, O. J.; Nickles, R. J. *Nucl. Med. Biol.* **1996**, *23*, 767.
(219) Livni, E.; Babich, J.; Alpert, N. M.; Liu, Y. Y.; Thom, E.; Cleeland, R. *Nucl. Med. Biol.* **1993**, *20*, 81.
(220) Babich, J. W.; Rubin, R. H.; Graham, W. A.; Wilkinson, R. A.; Vincent, J.; Fischman, A. J. *Nucl. Med. Biol.* **1996**, *23*, 995.
(221) Nijhof, M. W.; Oyen, W. J. G.; van Kampen, A.; Claessens, R. A.; van der Meer, J. W.; Corstens, F. H. M. *J. Nucl. Med.* **1997**, *38*, 1300.
(222) Ortapamuk, H.; Hosal, B.; Naldoken, S. *Ann. Nucl. Med* **2002**, *16*, 461.
(223) Oyen, W. J. G.; Claessens, R. A. M. J.; van der Meer, J. W. M.; Rubin, R. H.; Strauss, H. W.; Corstens, F. H. M. *Clin. Infect. Dis.* **1992**, *14*, 1110.
(224) Buscombe, J. R.; Oyen, W. J. G.; Grant, A.; Claessens, R. A. M. J.; van der Meer, J. W. M.; Corstens, F. H. M. *J. Nucl. Med.* **1993**, *34*, 1621.
(225) Mairal, L.; Lima, P. D.; Martin Comin, J.; Baliellas, C.; Xiol, X.; Roca, M. *Eur. J. Nucl. Med.* **1995**, *22*, 664.
(226) Beckers, C.; Jeukens, X.; Ribbens, C.; Andre, B.; Marcellis, S.; Leclercq, P. *Eur. J. Nucl. Med.* **2006**, *33*, 275.
(227) Gratz, S.; Dorner, J.; Fischer, U. *Eur. J. Nucl. Med. Mol. Imaging* **2002**, *29*, 516.
(228) Schmitz, A.; Risse, J. H.; Grunwald, F. *Eur. Spine. J.* **2001**, *10*, 534.
(229) Stumpe, K. D.; Zanetti, M.; Weishaupt, D. *AJR, Am. J. Roentgenol.* **2002**, *179*, 1151.
(230) Herholz, K. *Ann. Nucl. Med.* **2003**, *17*, 79.
(231) Sohn, M.; Jones, B.; Whiting, J. J. *J. Nucl. Med.* **1993**, *34*, 2135.
(232) Buscombe, J.; Miller, R.; Lui, D.; Ell, P. *Nucl. Med. Commun.* **1991**, *12*, 583.
(233) Seabold, J. E.; Nepola, J. V.; Conrad, G. R.; Marsh, J. L.; Montgomery, W. J.; Bricker, J. A. *Am. J. Roentgenol.* **1989**, *152*, 1021.
(234) McAfee, J. G.; Thakur, M. L. *J. Nucl. Med.* **1976**, *17*, 480.
(235) Peters, A. M.; Danpure, H. J.; Osman, S.; Hawker, R. J.; Henderson, B. L.; Hodgson, H. J. *Lancet* **1986**, *2*, 945.
(236) Peters, A. M. *Semin. Nucl. Med.* **1994**, *24*, 110.
(237) Datz, F. L. *Semin. Nucl. Med.* **1994**, *24*, 92.
(238) Papos, M.; Nagy, F.; Narai, G.; Rajtar, M.; Szantai, G.; Lang, J. *Dig. Dis. Sci.* **1996**, *41*, 412.
(239) De Schrijver, M.; Streule, K.; Senekowitsch, R.; Fridrich, R. *Nucl. Med. Commun.* **1987**, *8*, 895.
(240) Liberatore, M.; Clemente, M.; Turilli, A. P.; Zorzin, L.; Marini, M.; Di Rocco, E. *Eur. J. Nucl. Med.* **1992**, *19*, 853.
(241) Wheeler, J.; Slack, N.; Duncan, A.; Palmer, H.; Harvey, R. *Nucl. Med. Commun.* **1990**, *11*, 127.
(242) Diot, P.; Le Pape, A.; Nolibe, D.; Normier, G.; Binz, H.; Revillard, J. P.; Lasfargues, G.; Lavandier, M.; Lemarie, E. *Br. J. Int. Med.* **1992**, *49*, 359.
(243) Perin, F.; Pittet, J. C.; Hoffschir, D.; Normier, G.; Binz, H.; Le Pape, A. *Nucl. Med. Biol.* **1993**, *20*, 963.
(244) Miot-Noirault, E.; Perin, F.; Routledge, L. *Eur. J. Nucl. Med.* **1996**, *23*, 61.

(245) Edgren, M.; Westlin, J.; Kalkner, K.; Sundin, A.; Nilsson, S. *Cancer Biother. Radiopharm.* **1999**, *14*, 59.
(246) Vanhagen, P. M.; Krenning, E. P.; Reubi, J. C. *Eur. J. Nucl. Med.* **1994**, *21*, 497.
(247) Ten Bokum, A. M. C.; Rosmalen, J. G. M.; Hofland, L. J.; Krenning, E. P.; Van Hagen, P. M.; Breeman, W. A. P. *Nucl. Med. Commun.* **2002**, *23*, 1009.
(248) Virgolini, I.; Angelberger, P.; Li, S.; Yang, Q.; Kurtaran, A.; Raderer, M.; Neuhold, N.; Kaserer, K.; Leimer, M.; Peck-Radosavljevic, M.; Scheithauer, W.; Niederle, B.; Eichler, H.-G.; Valent, P. *Eur. J Nucl. Med.* **1996**, *23*, 1388.
(249) Vallabhajosula, S.; Moyer, B. R.; Lister-James, J.; McBride, B. J.; Lipszyc, H.; Lee, H.; Bastidas, D.; Dean, R. T. *J. Nucl. Med.* **1996**, *37*, 1016.
(250) Dalm, V. A. S. H.; Van Hagen, P. M.; Krenning, E. P. Q. *J. Nucl. Med.* **2003**, *47*, 270.
(251) Valero, M.; Boan, J. F.; Rodriguez-Spiteri, N.; Torre, W.; Richter, J. A. *Clin. Nucl. Med.* **2006**, *31*, 20.
(252) Oyen, W. J. G.; Boerman, O. C.; Claessens, R. A. M. J.; van der Meer, J. W. M.; Corstens, F. H. M. *Nucl. Med. Commun.* **1994**, *15*, 289.
(253) Boerman, O. C.; Storm, G.; Oyen, W. J. G. *J. Nucl. Med.* **1995**, *36*, 1639.
(254) Oyen, W. J. G.; Boerman, O. C.; Storm, G. *J. Nucl. Med.* **1996**, *37*, 1392.
(255) Oyen, W. J. G.; Boerman, O. C.; Dams, E. T. M. *J. Nucl. Med.* **1997**, *38*, 1596.
(256) Dams, E. T. M.; Oyen, W. J. G.; Boerman, O. C. *J. Nucl. Med.* **1998**, *39*, 2172.
(257) Dams, E. T. M.; Nijhof, M. W.; Oyen, W. J. G. *J. Nucl. Med.* **2000**, *41*, 896.
(258) Dams, E. T. M.; Oyen, W. J. G.; Boerman, O. C. *J. Nucl. Med.* **2000**, *41*, 622.
(259) Brouwers, A. H.; De Jong, D. J.; Dams, E. T. M. *J. Drug. Targeting* **2000**, *8*, 225.
(260) Rusckowski, M.; Paganelli, G.; Hnatowich, D. J.; Magnani, P.; Virzi, F.; Fogarasi, M.; DiLeo, C.; Sudati, F.; Fazio, F. *J. Nucl. Med.* **1996**, *37*, 1655.
(261) Samuel, A.; Paganelli, G.; Chiesa, R.; Sudati, F.; Calvitto, M.; Melissano, G.; Grossi, A.; Fazio, F. *J. Nucl. Med.* **1996**, *37*, 55.
(262) Lazzeri, E.; Manca, M.; Molea, N.; Marchetti, S.; Consoli, V.; Bodei, L.; Bianchi, R.; Chinol, M.; Paganelli, G.; Mariani, G. *Eur. J. Nucl. Med.* **1999**, *26*, 606.
(263) Lazzeri, E.; Pauwels, E. K.; Erba, P. A.; Volterrani, D.; Manca, M.; Bodei, L.; Trippi, D.; Bottoni, A.; Cristofani, R.; Consoli, V.; Palestro, C. J.; Mariani, G. *Eur. J. Nucl. Med. Mol. Imaging* **2004**, *31*, 1505.
(264) Buursma, A. R.; Rutgers, V.; Hospers, G. A.; Mulder, N. H.; Vaalburg, W.; de Vries, E. F. *Nucl. Med. Commun.* **2006**, *27*, 25.
(265) Bennett, J. J.; Tjuvajev, J.; Johnson, P.; Doubrovin, M.; Akhurst, T.; Malholtra, S. *Nat. Med.* **2001**, *7*, 859.
(266) Buursma, A. R.; De Vries, E. F. J.; Garssen, J.; Kegler, D.; van Waarde, A.; Schirm, J. *J. Virol.* **2005**, *79*, 7721.
(267) Doorduin, J.; De Vries, E. F. J.; Dierckx, R. A.; Klein, H. C. *J. Labelled Compd. Radiopharm.* **2007**, *50*, S60.
(268) Cagnin, A.; Myers, R.; Gunn, R. N.; Lawrence, A. D.; Stevens, T.; Kreutzberg, G. W.; Jones, T.; Banati, R. B. *Brain* **2001**, *124*, 2014.
(269) Banati, R. B.; Goerres, G. W.; Myers, R.; Gunn, R. N.; Turkheimer, F. E.; Kreutzberg, G. W.; Brooks, D. J.; Jones, T.; Duncan, J. S. *Neurology* **1999**, *53*, 2199.
(270) Hammoud, D. A.; Endres, C. J.; Chander, A. R.; Guilarte, T. R.; Wong, D. F.; Sacktor, N. C.; McArthur, J. C.; Pomper, M. G. *J. Neurovirol.* **2005**, *11*, 346.
(271) Bosslet, K.; Auerbach, B.; Hoffken, H.; Joseph, K. *Nucl. Med.* **1989**, *28*, 149–59.
(272) Becker, W.; Dolkemeyer, U.; Gramatzki, M. *Eur. J. Nucl. Med.* **1993**, *20*, 1078.
(273) Meller, J.; Ivancevic, V.; Conrad, M. *J. Nucl. Med.* **1998**, *39*, 1248.
(274) Palestro, C. J.; Caprioli, R.; Love, C. J. *Foot Ankle Surg.* **2003**, *2*, 2.
(275) Gratz, S.; Behr, T.; Herrmann, A.; Dresing, K.; Tarditi, L.; Franceschini, R. *Eur. J. Nucl. Med.* **1998**, *25*, 386.
(276) Delcourt, A.; Huglo, D.; Prangere, T. *Diabetes Metab.* **2005**, *31*, 125.
(277) Morguet, A. J.; Dieter, M.; Ivancevic, V. *J. Am. Coll. Cardiol.* **1994**, *23*, 1171.
(278) Fayad, Z. A.; Amirbekian, V.; Toussaint, J. F.; Fuster, V. *Eur. J. Nucl. Med. Mol. Imaging* **2006**, *33*, 111.
(279) Signore, A.; Capriotti, G.; Scopinaro, F.; Bonanno, E.; Modesti, A. *Trends Immunol.* **2003**, *24*, 395.
(280) Signore, A.; Parisella, M. G.; Conti, F.; Chianelli, M.; Spinelli, F. R.; Borseti, G.; D'Ignazio, L.; Fiore Melacrinis, S.; Mather, S. J. *Eur. J. Nucl. Med.* **2000**, *27*, 925.
(281) Barone, R.; Procaccini, E.; Chianelli, M.; Annovazzi, A.; Fiore, V.; Hawa, M.; Nardi, G.; Ronga, Pozzilli, P.; Signore, A. *Eur. J. Nucl. Med.* **1998**, *25*, 503.
(282) Elkind, M. S.; Rundek, T.; Sciacca, R. R. *Atherosclerosis* **2005**, *180*, 181.
(283) van der Laken, C. J.; Boerman, O. C.; Oyen, W. J. *Eur. J. Nucl. Med.* **1995**, *22*, 1249.
(284) Rennen, H. J.; Boerman, O. C.; Oyen, W. J.; Corstens, F. H. *J. Nucl. Med.* **2003**, *44*, 1502.
(285) Rennen, H. J.; Boerman, O. C.; Oyen, W. J.; van der Meer, J. W.; Corstens, F. H. *J. Nucl. Med.* **2001**, *42*, 117.
(286) van der Laken, C. J.; Boerman, O. C.; Oyen, W. J.; van de Ven, M. T.; van der Meer, J. W.; Corstens, F. H. *J. Nucl. Med.* **2000**, *41*, 463.
(287) Ohtsuki, K.; Hayase, M.; Akashi, K.; Kopiwoda, S.; Strauss, H. W. *Circulation* **2001**, *104*, 203.
(288) Postema, P. T. E.; Wijnggaarde, R.; Vandenbosch, W. A.; Koij, P. P. M.; Oei, H. Y.; Hennemann, G.; Lamberts, S. W. J.; Krenning, E. P. *J. Nucl. Med.* **1995**, *95*, 203P.
(289) Diaz, M.; Bokisch, A.; Kahaly, G.; Hahn, K. *Eur. J. Nucl. Med.* **1993**, *20*, 844.
(290) Eberhardt, J. U.; Oberwohrmann, S.; Clausen, M.; Schulte, H.; Epe, B.; Henze, E. *Eur. J. Nucl. Med.* **1993**, *20*, 844.
(291) Bohuslavizki, K. H.; Oberw6rhmann, S.; Brenner, W.; Eberhardt, J. U.; Monig, H.; Clasen, M. *Nucl. Med. Commun.* **1995**, *16*, 912.
(292) Bahn, R.; Heufelder, A. *N. Engl. J. Med.* **1993**, *329*, 1468.
(293) Hurley, J. *J. Nucl. Med.* **1994**, *35*, 918.
(294) Krassas, G. E.; Dumas, A.; Pontikides, N.; Kaltsas, T. *Clin. Endocrinol.* **1995**, *42*, 571.
(295) Nocaudie, M.; Bailliez, A.; Itti, E.; Bauters, C.; Wemeau, J. L.; Marchandise, X. *Eur. J. Nucl. Med.* **1999**, *26*, 511.
(296) Solanki, K. K.; Mather, S. J.; Janabi, M. A.; Britton, K. E. *Nucl. Med. Commun.* **1988**, *9*, 753.
(297) Anderson, V. E.; Osheroff, N. *Curr. Pharm. Des.* **2001**, *7*, 337.
(298) Pan, X. S.; Yague, G.; Fisher, L. M. *Antimicrob. Agents Chemother.* **2001**, *45*, 3140.
(299) de Winter, F.; Gemmel, F.; Van Laere, K. *Eur. J. Nucl. Med. Mol. Imaging* **2004**, *31*, 233.
(300) Gemmel, F.; de Winter, F.; Van Laere, K. *Nucl. Med. Commun.* **2004**, *25*, 277.
(301) Sonmezoglu, K.; Sonmezoglu, M.; Halac, M. *J. Nucl. Med.* **2001**, *42*, 567.
(302) Fischman, A. J.; Babich, J. W.; Alpert, N. M.; Vincent, J.; Wilkinson, R. A.; Callahan, R. J. *Clin. Microbiol. Infect.* **1997**, *3*, 63.
(303) Fischman, A. J.; Livni, E.; Babich, J.; Alpert, N. M.; Liu, Y. Y.; Thom, E. *Antimicrob. Agents Chemother.* **1992**, *36*, 2286.
(304) Palestro, C. J. *Semin. Nucl. Med.* **1994**, *24*, 128.
(305) Knockaert, D. C.; Mortelmans, L. A.; De Roo, M. C. *Clin. Infect. Dis.* **1994**, *18*, 601.
(306) Perkins, P. J. *AJR, Am. J. Roentgenol.* **1981**, *136*, 1016.
(307) Bekerman, C.; Hoffer, P. B.; Bitran, J. D. *Semin. Nucl. Med.* **1984**, *14*, 296.
(308) Rizzello, A.; Di Pierro, D.; Lodi, F.; Trespidi, S.; Cicoria, G.; Pancaldi, D.; Nanni, C.; Marengo, M.; Marzola, M. C.; Al-Nahhas, A.; Rubello, D.; Boschi, S. *Nucl. Med. Commun.* **2009**, *30*, 542.
(309) Syrjala, M. T.; Valtonen, V.; Liewendahl, K. *J. Nucl. Med.* **1987**, *28*, 155.
(310) MacSweeney, J. E.; Peters, A. M.; Lavender, J. P. *Clin. Radiol.* **1990**, *42*, 414.
(311) Kjaer, A.; Lebech, A. M. *J. Nucl. Med.* **2002**, *43*, 140.
(312) Keenan, A. M.; Tindel, N. L.; Alavi, A. *Arch. Intern. Med.* **1989**, *149*, 2262.
(313) Larcos, G.; Brown, M. L.; Sutton, R. *AJR, Am. J. Roentgenol.* **1991**, *157*, 527.
(314) Harvey, J.; Cohen, M. M. *J. Foot Ankle Surg.* **1997**, *36*, 209.
(315) Alazraki, N.; Dries, D.; Datz, F. *J. Nucl. Med.* **1985**, *26*, 711.
(316) Poirier, J. Y.; Garin, E.; Derrien, C. *Diabetes. Metab.* **2002**, *28*, 485.
(317) Johnson, J. E.; Kennedy, E. J.; Shereff, M. J. *Foot Ankle Int.* **1996**, *17*, 10.
(318) Blume, P. A.; Dey, H. M.; Dailey, L. J. *J. Foot Ankle Surg.* **1997**, *36*, 120.
(319) Newman, L. G.; Waller, J.; Palestro, C. J. *J. Am. Med. Assoc.* **1991**, *266*, 1246.
(320) Wiseman, J.; Rouleau, J.; Rigo, P.; Strauss, H. W.; Pitt, B. *Radiology* **1976**, *120*, 135.
(321) Cerqueira, M. D.; Jacobson, A. F. *J. Nucl. Med.* **1989**, *30*, 703.
(322) Erba, P. A.; Lazzeri, E.; Sollini, M. *J. Nucl. Med.* **2008**, *49*, 133P.
(323) Seabold, J. E. *Nuclear Medicine in Clinical Diagnosis and Treatment*, 2nd ed.; Churchill Livingstone: Edinburgh, 1999; p 159.
(324) Bar-Shalom, R.; Yefremov, N.; Guralnik, L. *J. Nucl. Med.* **2006**, *47*, 587.
(325) Remedios, D.; Valabhji, J.; Oelbaum, R. *Clin. Radiol.* **1998**, *53*, 120.
(326) Kalliokoski, T.; Simell, O.; Haarparanta, M.; Viljanen, T.; Solin, O.; Knuuti, J.; Nuutila, P. *Diabetes Res. Clin. Pract.* **2005**, *70*, 217.
(327) Federici, L.; Blondet, C.; Imperiale, A. *Int. J. Clin. Pract.* **2008**, *64*, 55.

(328) Meller, J.; Altenvoerde, G.; Munzel, U. *Eur. J. Nucl. Med.* **2000**, *27*, 1617.
(329) Blockmans, D.; Knockaert, D.; Maes, A. *Clin. Infect. Dis.* **2001**, *32*, 191.
(330) Cascini, G. L.; De Palma, D.; Matteucci, F. *Nucl. Med. Commun.* **2006**, *27*, 213.
(331) Bleeker-Rovers, C. P.; Vos, F. J.; Mudde, A. H. *Eur. J. Nucl. Med. Mol. Imaging* **2007**, *34*, 694.
(332) Lorenzen, J.; Buchert, R.; Bohuslavizki, K. H. *Nucl. Med. Commun.* **2001**, *22*, 779.
(333) Bleeker-Rovers, C. P.; de Kleijn, E. M.; Corstens, F. H. *Eur. J. Nucl. Med. Mol. Imaging* **2004**, *31*, 29.
(334) Buysschaert, I.; Vanderschueren, S.; Blockmans, D. *Eur. J. Intern. Med.* **2004**, *15*, 151.
(335) Devillers, A.; Moissan, A.; Hennion, F. *Eur. J. Nucl. Med.* **1998**, *25*, 132.
(336) Keidar, Z.; Militianu, D.; Melamed, E. *J. Nucl. Med.* **2005**, *46*, 444.
(337) Schwegler, B.; Stumpe, K. D.; Weishaupt, D. J. *Intern. Med.* **2008**, *263*, 99.
(338) Basu, S.; Chryssikos, T.; Houseni, M. *Nucl. Med. Commun.* **2007**, *28*, 465.
(339) Hopfner, S.; Krolak, C.; Kessler, S. *Foot Ankle Int.* **2004**, *25*, 890.
(340) Stumpe, K. D.; Dazzi, H.; Shaffner, A.; Von Schulthess, G. H. *Eur. J. Nucl. Med.* **2000**, *27*, 822.
(341) Krupnick, A. S.; Lombardi, J. V.; Engels, F. H.; Zhuang, H.; Alavi, A.; Carpenter, J. P. *Vasc. Endovascular Surg.* **2003**, *37*, 363.
(342) Chacko, T. K.; Zhuang, H.; Nakhoda, K. Z.; Moussavian, B.; Alavi, A. *Nucl. Med. Commun.* **2003**, *24*, 615.
(343) Keidar, Z.; Engel, A.; Nitecki, S.; Bar Shalom, R.; Hoffman, A.; Israel, O. *Mol. Imaging Biol.* **2003**, *5*, 23.
(344) Stàdler, P.; Belohla'vek, O.; Spacek, M.; Micha'lek, P. *J. Vasc. Surg.* **2004**, *40*, 1246.
(345) Fukuchi, K.; Ishida, Y.; Higashi, M. *J. Vasc. Surg.* **2005**, *42*, 919.
(346) Jaruskova, M.; Belohlavek, O. *Eur. J. Nucl. Med. Mol. Imaging* **2006**, *33*, 913.
(347) Tsunekawa, T.; Ogino, H.; Minatoya, K.; Matsuda, H.; Sasaki, H.; Fukuchi, K. *Eur. J. Vasc. Endovasc. Surg.* **2007**, *33*, 187.
(348) Tegler, G.; Sorensen, J.; Bjorck, M.; Savitcheva, I.; Wanhainen, A. *J. Vasc. Surg.* **2007**, *45*, 828.
(349) Keidar, Z.; Engel, A.; Hoffman, A. *J. Nucl. Med.* **2007**, *48*, 1230.
(350) Lauwers, P.; Van den Broeck, S.; Carp, L.; Henriks, J.; Van Schil, P.; Blockx, P. *Angiology* **2007**, *58*, 717.
(351) Wasslius, J.; Malmstedt, J.; Kalin, B.; Larsson, S.; Sundin, A.; Hedin, U. *J. Nucl. Med.* **2008**, *49*, 1601.
(352) Marion, M. D.; Swanson, M. K.; Spellman, J.; Spieth, M. E. *J. Vasc. Surg.* **2009**, *50*, 907.
(353) Spacek, M.; Belohlavek, O.; Votrubova, J.; Sebesta, P.; Stadler, P. *Eur. J. Nucl. Med. Mol. Imaging* **2009**, *36*, 850.
(354) Gardet, E.; Addas, R.; Monteil, J.; Le Guyader, A. *Interact. Cardiovasc. Thorac. Surg.* **2010**, *10*, 142.
(355) Burroni, L.; D'Alessandria, C.; Signore, A. *J. Nucl. Med.* **2007**, *48*, 1227.
(356) Grafton, S. T. *Adv. Neurol.* **2000**, *83*, 87.
(357) Lee, B. Y.; Newberg, A. B.; Liebeskind, D. S.; Kung, J.; Alavi, A. *Clin. Nucl. Med.* **2004**, *29*, 620.
(358) Cagnin, A.; Brooks, D. J.; Kennedy, A. M.; Gunn, R. N.; Myers, R.; Turkheimer, F. E.; Jones, T.; Banati, R. B. *Lancet* **2001**, *358*, 461.
(359) Cagnin, A.; Rossor, M.; Sampson, E. L.; Mackinnon, T.; Banati, R. B. *Ann. Neurol.* **2004**, *56*, 894.
(360) Banati, R. B.; Newcombe, J.; Gunn, R. N.; Cagnin, A.; Turkheimer, F.; Heppner, F.; Price, G.; Wegner, F.; Giovannoni, G.; Miller, D. H.; Perkin, G. D.; Smith, T.; Hewson, A. K.; Bydder, G.; Kreutzberg, G. W.; Jones, T.; Cuzner, M. L.; Myers, R. *Brain* **2000**, *123*, 2321.
(361) Debruyne, J. C.; Versijpt, J.; Van Laere, K. J.; De Vos, F.; Keppens, J.; Strijckmans, K.; Achten, E.; Slegers, G.; Dierckx, R. A.; Korf, J.; De Reuck, J. L. *Eur. J. Neurol.* **2003**, *10*, 257.
(362) Gerhard, A.; Schwarz, J.; Myers, R.; Wise, R.; Banati, R. B. *Neuroimage* **2005**, *24*, 591.
(363) Capriotti, G.; Chianelli, M.; Signore, A. *Nucl. Med. Commun.* **2006**, *27*, 757.
(364) Annovazzi, A.; Bagni, B.; Burroni, L.; D'Alessandria, C.; Signore, A. *Nucl. Med. Commun.* **2005**, *26*, 657.
(365) Prandini, N.; Lazzeri, E.; Rossi, B.; Erba, P.; Parisella, M. G.; Signore, A. *Nucl. Med. Commun.* **2006**, *27*, 633.

CR900351R